

Founded 1925

Incorporated  
by Royal Charter 1961

*"To promote the advancement  
of radio, electronics and kindred  
subjects by the exchange of  
information in these branches  
of engineering."*

VOLUME 41 No. 2

FEBRUARY 1971

# THE RADIO AND ELECTRONIC ENGINEER

The Journal of the Institution of Electronic and Radio Engineers

## More Value by Design

'DESIGN' is a term which tends to have two connotations: to some there is only a narrower meaning associated solely with external appearance but this is by no means all the story. 'Design' is the whole process of the evolution of a component or piece of equipment, from ensuring that it can be made efficiently and economically for its purpose right through to achieving a pleasing appearance in the finished product. This latter point is obviously highly important where consumer appeal is concerned, but in other applications a well thought-out exterior design which combines conveniently and logically placed controls with an aesthetically pleasing layout will give that extra 'edge' against competitive models. All this is nowadays becoming well understood, in theory at least, but is it really implemented?

An exhibition held recently at The Design Centre in London and having the theme of 'More Value by Design' was organized by the Council of Industrial Design in collaboration with the Department of Trade and Industry and the Council of Engineering Institutions. Its aim was to show the economic importance of engineering design to management, designers, educationists and students concerned with the engineering industries and twenty case histories showing a product in 1960 and its often strikingly improved counterpart of 1970 illustrated the main theme. Several of these were drawn from the electronics industry, for example automatic flight control equipment, a new telephone and a printed wiring type of rotary switch. Supporting these presentations of complete designs were exhibits showing the salient properties and advantages of new materials and processes: carbon fibre, filled p.t.f.e. and superplastic metals, and cold forging, electromagnetic forming and electron-beam welding, to mention just a few.

Some of the improved designs shown took advantage of these new materials and processes but this in itself is not enough as was pointed out by the Secretary of State for Trade and Industry, Mr. John Davies who said, in opening the exhibition:

'Certainly one of the most notable transformations that have been taking place in industry has been the progressive integration of a series of disparate activities into a single continuous flow. Much is said about industrial restructuring but the emphasis is given perhaps excessively to the merger of corporate entities rather than to the linkage and co-ordination of related industrial processes. Even today there is still some hesitation to accept that manufacture, marketing and distribution are simply parts of a single stream of operations that concerns the presentation of the product to the customer.

'Even less is there widespread acceptance that the processes of research, development and design are similarly part of the same cohesive pattern. Research and design are seen as creative activities where the discipline of such tight relationships with the more perpetual elements of the industrial process could only be regarded as hampering. But such is really not the case. Imagination flourishes in a close association with the understanding of matching people's needs rather than in isolation from them.

'It seems to me that present developments in the professional attitudes to these problems correctly take the point of these observations and seek to lead industry into a better understanding of these relationships. The convergence of sophisticated thinking in organizations like the Council of Industrial Design and the Council of Engineering Institutions is unmistakable. To the layman they approach the problem of identifying the desirable finished article from opposite points of view but their own experienced consideration makes it clearer that those points of view are by no means opposite but at least parallel and perhaps even identical.'

The statement that 'design is efficiency, reliability, value, innovation, convenience, appearance' with which Mr. Davies concluded, provides all designers with a set of aims which can hardly be bettered.

F.W.S.

## INSTITUTION NOTICES

### Clerk Maxwell Memorial Lecture

The Seventh Clerk Maxwell Memorial Lecture will be given by Professor H. M. Barlow, Ph.D., F.R.S., C.Eng., F.I.E.E., on Tuesday, 9th March 1971, at 6.30 p.m. Professor Barlow has taken as the title of his lecture 'Guided Electromagnetic Waves' and appropriately, in view of his long association with the Department of Electronic and Electrical Engineering at University College London, the lecture is being given in the College's Engineering Lecture Theatre. Tickets will be necessary and may be obtained on application to the Institution either by post or by telephone (01-637 2771, Ext. 20).

#### SYNOPSIS OF THE LECTURE

*Highlights of Clerk Maxwell's Life and Work.* His ability to see beyond mathematical symbols to the wider consequences of the analysis. His intuitive understanding of physical realities. The importance of the paper 'The Dynamical Theory of the Electromagnetic Field'.

*Guided Waves.* Transverse spread deliberately restricted as in hollow tubular waveguides or by an evanescent field distribution. Maxwell's equations provide a means of solving these conditions.

*Requirements for Transmission of Power and Modes of Operation.* Faraday's concept of 'lines of force' lead to Maxwell's equations.

*Twin-Wire Lines and Coaxial Cables as Waveguides.* Lumped circuit vs. field distribution approach. Use of stratified dielectrics. The effect of surface impedance and how it may be exploited in the single-wire transmission line.

*Surface Waveguides.* Ways of reducing effect of outside obstacles. Problem of bends. The alternative of a dielectric rod or fibre.

*Waveguides Employing Transverse Standing Waves.* The low-loss guide for millimetre waves for long-distance communications and the problem of suppressing unwanted modes. The possibilities of using large diameter waveguides to transmit electric power with low losses. Waveguide applications for continuous signalling to trains in motion.

### Industrial Relations and the Chartered Engineer

The Council of Engineering Institutions is pressing for amendments to the British Government's Industrial Relations Bill. At present there is no one body which comes anywhere near representing the large number of professional engineers on industrial relations other than C.E.I., which, with its fifteen member Institutions (the latest addition, the Institute of Fuel, was admitted last month), can speak on behalf of some 300,000 members on the rolls of the C.E.I. Constituent Members.

Chartered Engineers are employed in many different industries and in some cases they are already represented by trade unions appropriate to their industry. Nevertheless, many have fears about the present structure and the extent to which it meets their needs. The C.E.I. set up a working party last Autumn to consider the implications of the proposed legislation for Chartered Engineers, to consult with its Constituent Members and to advise both Government and the Institutions on the best course of action for the profession. This action was referred to in the January 1971 issue of the *Journal* (page S.2) which gave extracts from the Bill.

Discussions clearly indicate that professional engineers wish to see the Industrial Relations Bill amended so that they are properly catered for, in particular that:

when Chartered Engineers are involved in collective bargaining they have separate representation to their satisfaction in any Agency shop arrangement;

there be a medium within the context of the Bill to enable the profession as a whole to be represented and that it can establish its requirements to the appropriate statutory agencies;

there be satisfactory provision in the Bill for the category of worker, as exemplified by a Chartered Engineer, who has special obligations in the public interest which are material to his employment.

C.E.I. has a federal function to represent the profession, and already does so to Parliament and the Government. Consideration is therefore being given as to how this role can be best extended within the framework of the proposed legislation. Meanwhile discussions are continuing with the Department of Employment as well as with other professional bodies and Members of Parliament.

### National Electronics Review

This bi-monthly review of progress in electronics, which is published by the National Electronics Council, contains articles of interest to manufacturers, research workers and users of electronic equipment. Members of the I.E.R.E. may subscribe to the *National Electronics Review* at a reduced price of £2.00 per year (6 issues). An order form is contained in the advertisement section at the back of this issue.

### Index to Volume 40

The index to Volume 40 (July-December 1970) of *The Radio and Electronic Engineer* is being sent out with this issue.

Members who wish to have their issues bound by the Institution should send them securely wrapped, together with the Index and a remittance of £1.50, to the Publications Department, I.E.R.E., 8-9 Bedford Square, London, WC1B 3RG.

### Changes of Address

The offices and Secretariat of the Electronic Components Board are now at Carrier House, Warwick Row, London S.W.1 (Telephone 01-828 7411). This change of address also applies to the Constituent Associations of the E.C.B. and other organizations for which the E.C.B. provides accommodation, including the British Radio Valve Manufacturers Association (B.V.A.), the Electronic Valve & Semiconductor Manufacturers Association (V.A.S.C.A.), the Radio & Electronic Component Manufacturers Federation (R.E.C.M.F.) and the Conference of the Electronics Industry (C.L.I.).

The new address of the Electronic Engineering Association is Leicester House, 8 Leicester Square, London WC2H 7BN (Telephone 01-437 0678). The E.E.A. is, therefore, now housed in the same building as the British Electrical and Allied Manufacturers Association (B.E.A.M.A.). This physical closeness will facilitate co-operation between the two Associations in matters of common interest.

# Frequency Domain Approach to Automatic Testing of Control Systems

By

**Professor D. R. TOWILL,**

M.Sc., C.Eng., M.I.Mech.E.,  
F.I.Prod.E., F.I.E.R.E.†

and

**P. A. PAYNE,**

(Graduate) †

*Reprinted from the Proceedings of the Conference on Automatic Test Systems held in Birmingham from 14th to 17th April, 1970.*

The system user must be satisfied that frequency domain data adequately measures the quality of his system in all the performance aspects of interest. This involves the interpretation of transfer functions other than system output/input, and the acquisition of data over a wide frequency band ranging from a few percent of bandwidth to several multiples of bandwidth, the latter for the detection of secondary resonances. However, only a few spot frequencies need be chosen to ensure that system response to actual operational signals is adequate. Careful selection will also maximize the diagnostic potential of the measurements. In noisy systems the measurement time for adequate confidence in gain and phase observations must be established before the test routine can be automated.

## Principal Symbols

$\theta_i$	system input (command variable)
$\theta_o$	system output (controlled variable)
$E \equiv \theta_i - \theta_o$	system error
$\omega_B$	system bandwidth (highest frequency at which amplitude ratio is $1/\sqrt{2}$ )
$M_p$	peak amplitude ratio of system steady state frequency response
$N$	noise signal
$u$	load disturbance signal
$\omega$	excitation frequency

## 1. Introduction

The frequency domain evaluation of system dynamic performance is well established, and the use of a template within which system frequency response must lie is one recommended test for U.S. Air Force equipment.<sup>1</sup> Modern methods for determining frequency response are shown in Fig. 1, the applications quoted are wide ranging, and include estimation of aircraft and milling machine dynamics. Of the methods shown, only the direct use of sine waves as the input stimulus is at present practicable without a computer being made available for data processing. In contrast, a digital transfer function analyser (t.f.a.) can be readily incorporated in semi- or fully-automatic test schemes.

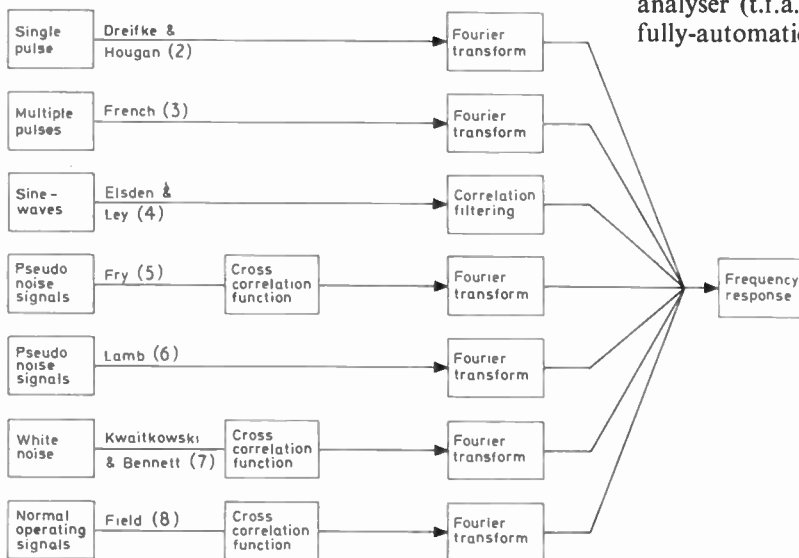


**Fig. 1.** Various methods of obtaining system frequency response.

$\omega_p$	frequency at which $M_p$ occurs
$\zeta$	damping ratio of secondary resonance
$K$	system gain
$T, nT$	time constants
$\omega_z$	positive breakpoint on system open-loop Bode plot
$\omega_{p1}, \omega_{p2}$	negative breakpoint on system open-loop Bode plot
$a$	network variable
$V_i$	voltage command variable
$V_o$	voltage controlled variable

Choice of test stimulus in manual and semi-automatic test procedures is influenced by cost, historical developments within a particular organization, skill levels of available personnel, and often, according to Lees,<sup>9</sup> prejudice. There have been many recent significant developments in dynamic test equipment,<sup>10</sup> and the frequent availability of a digital computer as stimulus and

† Dynamic Analysis Group, Department of Mechanical Engineering and Engineering Production, University of Wales Institute of Science and Technology, Cathays Park, Cardiff CF1 3NU.

data processor means that system users are now offered a wider choice of test domains. It follows that whereas in the past frequency domain techniques have enjoyed vast popularity due to relative ease of understanding and lack of adequate competition, we must now evaluate absolutely the frequency response as a dynamic test technique.

During the development stage of a system it is frequently necessary to provide detailed plots of system behaviour, copies of which may then travel as a master record of a 'good' response. Subsequently, for reasons of cost and time effectiveness, normal production, acceptance, and periodic maintenance tests are based on a relatively small number of frequencies. It is the purpose of this paper to consider the case of feedback control systems tested in closed loop under workshop or similar conditions, and to answer the following questions:

- (1) Does the steady-state frequency response of a system adequately predict the ability of the system to work effectively under operational conditions?
- (2) Which transfer functions are important, and over what frequency range?
- (3) At how many frequencies must the system be tested?
- (4) If the system is proved faulty, can the measurements indicate the nature of the fault?
- (5) At each frequency, how many times must each measurement be repeated in order to give adequate confidence to decisions?
- (6) For any given frequency, do the measurements vary according to the time at which they are observed?

The first four problems are solved by considering fundamental frequency domain properties of feedback control systems, whilst guidance on the last two problems is illustrated by results obtained during field experiments.

## 2. Function of a Feedback Control System

In general, the function of a control system is to follow a command signal ( $\theta_i$ ) with low dynamic and steady-state errors, and to reject unwanted noise signals ( $N$ ), and unwanted disturbances ( $u$ ).<sup>11</sup> One of the reasons for using feedback is to achieve adequate performance in the face of wide changes in load dynamics,<sup>12</sup> and if load dynamics change in the operational mode, these changes must either be simulated in the test mode or adequate allowance made by reducing test tolerances. At the design stage the designer interprets the specification into

a convenient synthesis domain and arrives at a bread-board model. Subsequently the system is tested operationally and the user, with or without the cognizance of the manufacturer, then selects a test procedure which correlates reasonably with operational performance. Too frequently, the method of test is thought to be of no concern to the system designer, but using the approach to be outlined in the next section, frequency domain test schedules can be laid down by the system designer in parallel with his system design activities.

## 3 Relationship between System Frequency Response and Operational Performance

In Fig. 2, a typical system Bode plot  $|\theta_o/E|$  is shown. It matters not whether the system is unity feedback;  $E$  is the system error,  $(\theta_i - \theta_o)$ . If we divide the frequency domain into three regions, with arbitrary boundaries ( $\pm 15$  dB suggested by Chen<sup>13</sup>, subsequently refined by Towill<sup>14</sup>), we may say;

(a) *Very Low Frequencies* ( $|\theta_o/E| > 15$ dB)

(i) The system follows very accurately,  $\theta_o \simeq \theta_i$ , and hence  $E/\theta_i \simeq E/\theta_o$ . Steady-state errors, i.e. tracking errors in following operational inputs are readily expressed as minimum gains of  $|E/\theta_i|$  at selected low frequencies.<sup>15</sup>

(ii) The shape of  $|\theta_o/E|$  in the low frequency region determines the settling times in following operational inputs. Each positive break-point will introduce a system dipole near the origin which will have a relatively slow decay,<sup>16</sup> and each dipole will have a residue related to the  $|\theta_o/E|$  gain at the break frequency. For example, a positive break-point occurring when the gain is +26 dB will contribute about 5% to the unit step response.<sup>14</sup>

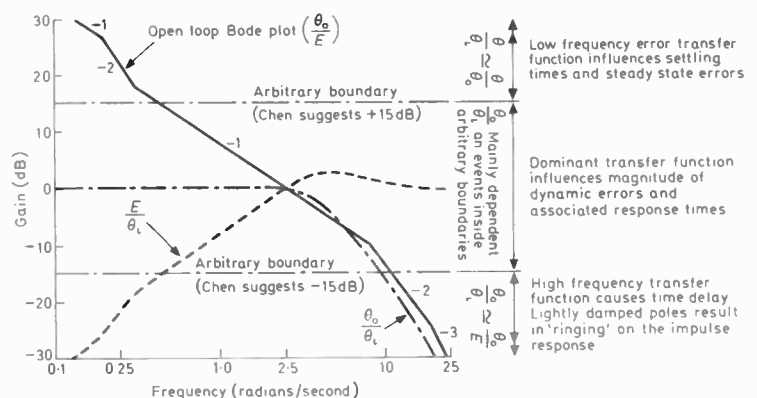
(b) *Very High Frequencies* ( $|\theta_o/E| < -15$ dB)

(i) The system follows very badly, and  $\theta_i \simeq E$ , hence the system response is approximately equal to  $|\theta_o/E|$ . Furthermore, real system poles resulting from the real open-loop poles in this region are approximately equal to the open-loop poles.<sup>13</sup>

(ii) The effect of these far-off real system poles is to introduce a time delay in the response of the system to operational inputs without altering peak errors to any great extent.<sup>17</sup>

(iii) The behaviour of  $|\theta_o/E|$  at high frequencies is a direct measure of noise rejection at these frequencies and extra lags may be introduced for this purpose.<sup>18</sup>

Fig. 2. Frequency domain influences on system dynamic response.



(iv) High frequency open-loop poles result in system poles of similar damping and frequency. If these poles are lightly damped, a significant ringing mode appears in response to impulsive stimuli whether these result from command signals, noise, or disturbances. Whilst these secondary modes are considerably attenuated every time the stimulus is integrated,<sup>17</sup> it is clear that if the modes are much excited in practice, then modal characteristics must be established and tolerated.

(c) *Intermediate Frequencies* ( $15\text{dB} > |\theta_o/E| > -15\text{dB}$ )

(i) A dominant transfer function is readily derived from the Bode plot in this region, and recent developments show that realistic accuracy in predicting dynamic errors may be expected.<sup>19</sup>

(ii) Dynamic errors are dependent on the shape of the dominant transfer function frequency response and the system bandwidth. Dynamic errors correlate well with bandwidth for a typical family of systems.<sup>20</sup>

(iii) Transmission of mid-frequency noise is very much affected by the dominant transfer function frequency response.

(iv) Saturation tendencies are related to the dominant system transfer function.<sup>21</sup>

Thus a division of frequency domain influences originally developed for system synthesis is found to provide a useful basis for relating fundamental system functions to frequency domain regions in which the adequacy of a particular function is observable. This division is also helpful in measuring load disturbance rejection because it is often found by algebraic manipulation that  $\theta_o/u(s)$  is simply related to  $\theta_o/E(s)$  and  $\theta_o/\theta_i(s)$  at particular frequencies. Then constraints on  $\theta_o/u(s)$  can be translated as additional constraints on  $\theta_o/E(s)$  and  $\theta_o/\theta_i(s)$ .

4. **Following the Command Signal,  $\theta_i$**

In reference 15,  $|E/\theta_i|$  is shown to be important at frequencies as low as  $0.01 \omega_B$ . At this frequency,  $\theta_o$  is so nearly equal to  $\theta_i$  as to be indistinguishable, and hence the only realistic check is to monitor  $|\theta_o/E|$  when  $|E|$  has some chosen value. It follows that if accurate command signal following is to be established,  $E$  must be monitored directly, unless the low-frequency integrations are obtained using operational amplifiers. In the latter case, the slope of  $|\theta_o/E|$  in the  $+15\text{ dB}$  region may be sufficient to establish tracking accuracy, and this slope may be related empirically to a single measurement of  $\theta_o/\theta_i(s)$  at a frequency of about  $0.2 \omega_B$ . Since settling times are affected by positive break-points in the high  $|\theta_o/E|$  region, if passive networks are used at low frequency, either we must measure  $|\theta_o/E|$  at a number of frequencies (to guarantee dynamic error time constants and residues), or measure at one frequency and set the gain limit high enough to guarantee that the residues are low whatever the time constants may be.

5. **Checking the Dominant Transfer Function**

Figure 3 shows the frequency responses for a family of dominant transfer functions (in the sense defined in Sect. 3). These transfer functions relate to an electro-hydraulic servomechanism, have been established from manufacturers' test data,<sup>24</sup> and all the responses satisfy the operational requirements as agreed by the user after full-scale trials. Common frequency domain performance criteria corresponding to these operational requirements are shown in Fig. 4, whilst time domain performance criteria are shown in Fig. 5. The constraints on dynamic errors effectively imposed by bandwidth variations of  $1.33 : 1$  and  $M_p$  varying from  $1.25$  to  $1.60$  are thus readily observed. With the exception of the time to peak

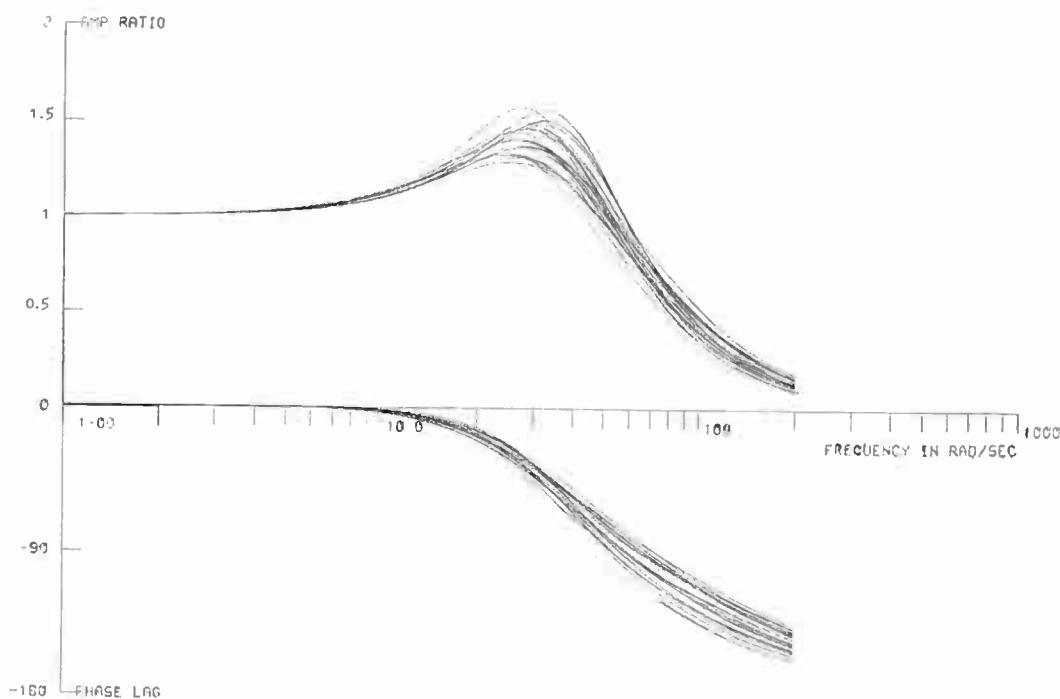


Fig. 3. Dominant transfer function frequency responses meeting operational requirements.

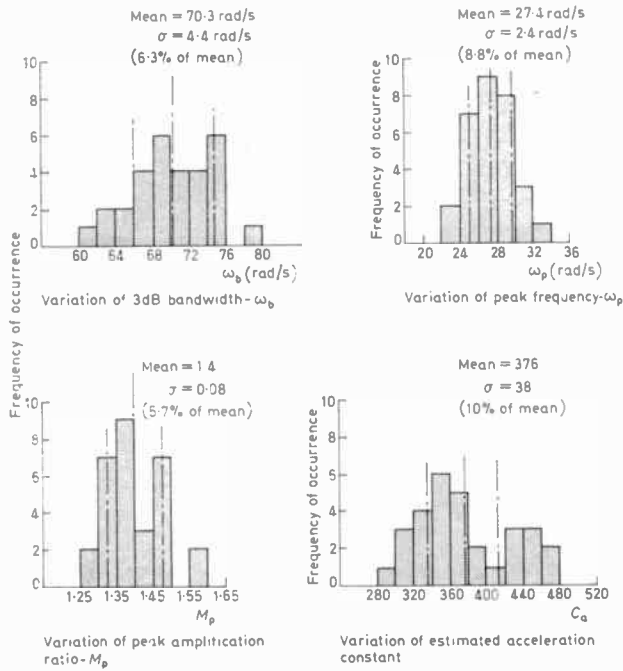


Fig. 4. Frequency response constraints imposed by frequency domain patterns of Fig. 3.

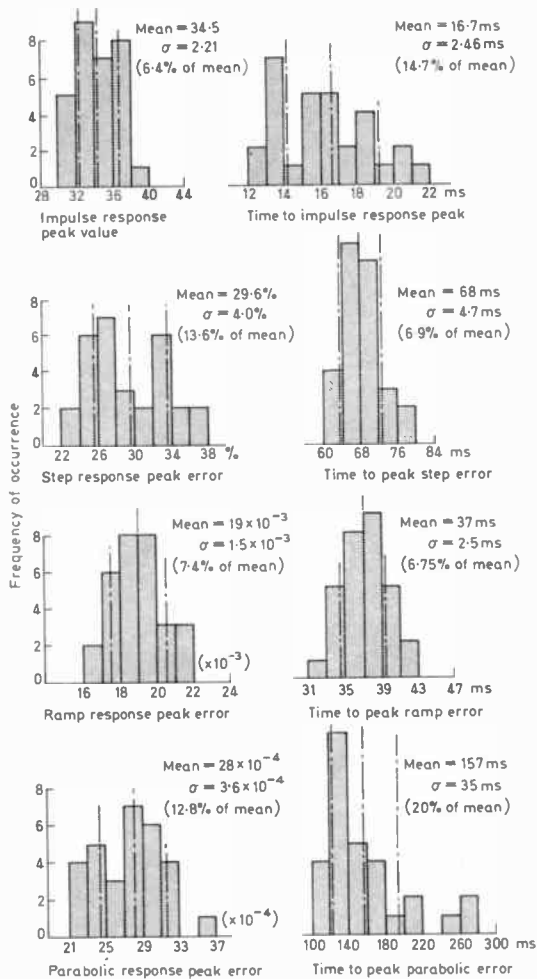


Fig. 5. Transient response constraints imposed by frequency domain patterns of Fig. 3.

parabolic error, all standard deviations of dynamic error are less than 15%, and most are less than 10% of the mean. Far-off system poles will delay the times shown by amounts readily deduced from reference 17, large changes in these poles only affecting these peak times by a small amount.

The frequency responses shown in Fig. 3, whilst referring to a specific electro-hydraulic servo are typical in shape and content to responses for a wide variety of physical systems, including satellite trackers and gun mountings.<sup>20</sup> At how many frequencies should we measure in order to have a reasonable level of confidence in constraining dynamic errors? To answer this question we need to generate a range of unacceptable systems, since then we can identify the frequencies at which the unwanted systems are most easily recognized. Figures 6 and 7 show the amplitude ratios and phase lags associated with some unsatisfactory systems chosen by analysing the production test data to isolate dominant transfer functions with coefficient combinations foreign to acceptable systems. These responses are found to fail operational requirements and are recognizable either by too high a peak amplification ratio ( $M_p$ ), or too low or too high bandwidth ( $\omega_B$ ). Acceptable responses in Fig. 3 may be used to indicate trial tolerances on amplitude and phase at any discrete frequency. Analyses based on the number of cases failing either gate show that suitable decisions may be made at  $\omega = 18, 50,$  and  $100$  rad/s. Table 1 shows the associated failure patterns and indicates that considerable redundancy has been built into the test procedure, thus increasing the chances of detecting freak combinations of circumstances not covered in the analysis. Additionally, there is considerable scope for gate width reduction before failure of good systems is likely to occur. Where the physical system is of high order, there will be some effect on the frequency response in the mid-frequency range, and it is sufficient to consider the contributions of the high order terms constant and adjust the gates on this basis. This procedure is justified statistically because such large changes are required in the higher terms in order to reflect greatly on any measurements made in the mid-frequency range. For the electro-hydraulic servo shown, the effect of the high-order terms is to increase the mid-tolerance phase lags by  $0^\circ, 5^\circ,$  and  $20^\circ$  at  $18, 50,$  and  $100$  rad/s respectively, whilst the amplitude mid-tolerance value is not significantly affected at any of the chosen frequencies. Since the phase lag at  $18$  rad/s is highly sensitive to the gain of  $\theta_0/E$  in the  $+15$  dB region,<sup>22</sup> with this particular system design the phase gate at this frequency provides enough constraint on the tracking errors to avoid tolerancing of  $E/\theta$ , directly.

6. Noise Rejection

Many systems operate under conditions where noise appears at the system input, the total signal seen by the system being  $\theta_i(t) + N(t)$ . Usually the frequency range of the noise is known sufficiently well to express noise rejection as a desired rate of cut-off<sup>18</sup> for measurement under test conditions where the noise is not present. Since rate of cut-off is roughly proportional to phase lag ( $-10$  dB/decade per  $45^\circ$  phase lag), it is usually sufficient

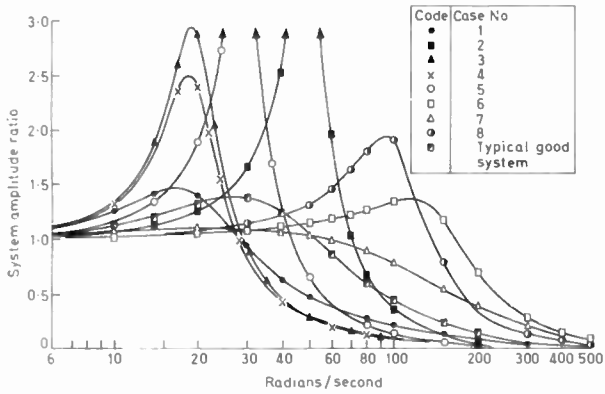


Fig. 6. Unsatisfactory amplitude ratios associated with dominant system transfer functions.

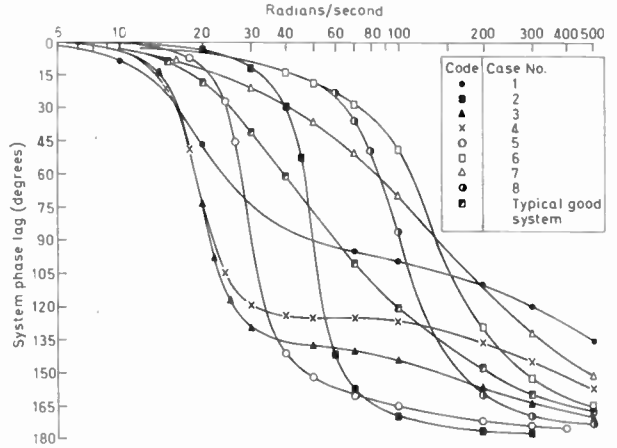


Fig. 7. Unsatisfactory phase lags associated with dominant system transfer functions.

to measure phase lag at one or two frequencies well beyond bandwidth. Whilst noise rejection is adequate if the phase lags are greater than some accepted minimum, a maximum expected value of phase lag at high frequency can form a gate, failure at which can lead to useful diagnostic information, as outlined in Section 8.

Where systems are tested under noisy conditions, measurement repeatability may be used as a measure of noise rejection, since variance is inversely proportional to the usefulness of an individual measurement.<sup>23</sup> The variance itself is then estimated in the test procedure and tolerated empirically.

7. Secondary Mode Identification

The problem of secondary resonances has already been discussed in Section 3. If such resonances can exist in a system, and can be excited operationally then they must be identified and hence constrained by the test procedure. Figure 8 shows the complete frequency responses for the family of electro-hydraulic servo-mechanisms whose dominant transfer functions were studied in Fig. 3. The secondary resonances (due to oil compressibility) are clearly observable, the damping ratios varying between 0.15 and 0.05. Although a damping ratio of 0.05 is low, further reduction would be

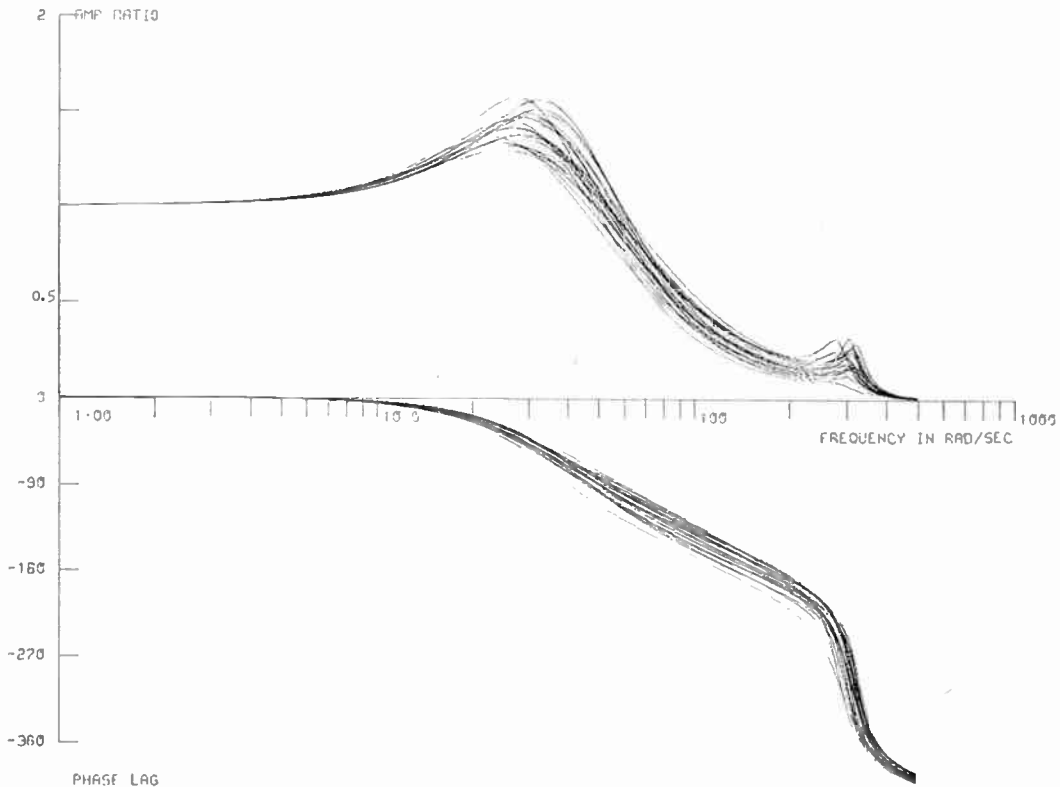


Fig. 8. Wider range frequency responses of electro-hydraulic servomechanism meeting operational requirements.

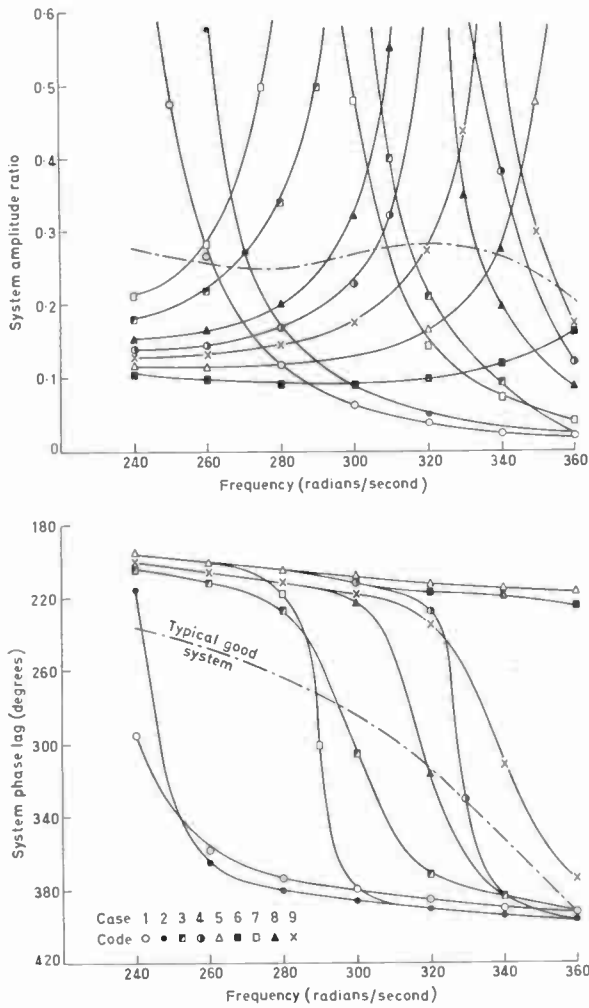


Fig. 9. Some unsatisfactory secondary modes.

catastrophic. In some systems with mechanical drives, the natural frequency of secondary resonances may stay reasonably constant over the working life of the system despite significant changes in secondary mode damping. Unfortunately, in hydraulic drives, the frequency may also change, due to entrainment of air in the oil, and due to oil temperature, hence any identification procedure must allow for changes in frequency when establishing damping ratio. Figure 9 shows the frequency responses corresponding to systems with secondary damping ratio less than 0.05, and with natural frequency varying from 240 to 390 rad/s, which is a wider range than that measured experimentally.<sup>24</sup> Table 2 shows the failure pattern for amplitude ratio and phase corresponding to gates set at discrete frequencies so as to pass all the operationally acceptable systems of Fig. 8. It can be seen that phase is a much more reliable measure than gain, the rejection factor being increased by greater than 4. If measurements are made at  $\omega = 260, 300,$  and  $340$  rad/s, each system fails at least twice, but there is clearly not the degree of redundancy built into this test as built into the dominant transfer function test of Table 1. Nevertheless, such secondary modes are checkable using three spot frequencies, phase measurements offering the greatest chance of failing bad systems.

The normalized phase slope (n.p.s.) technique<sup>25</sup> has also been applied to these systems. If the damping ratio is less than 0.05, the modulus of the normalized phase slope must be at least 20 at the resonant frequency. Is there a realistic chance of detecting such a resonance from spot frequency measurements, as distinct from a probing algorithm which will 'home' on to the resonant frequency? Computing n.p.s. at 10 rad/s intervals from  $\omega = 240$  to  $\omega = 390$  rad/s results in one measurement for each system being greater than 20. Due to the narrow peak of the n.p.s. curve, for such a spread in resonant frequencies, it is not realistic to measure at less than the sixteen spot frequencies chosen, and even this number may prove optimistic. However, if the resonant frequency is located, n.p.s. does give a ready estimate of  $\zeta$ , but clearly a homing algorithm should be built into the test procedure.

### 8. Fault Diagnosis

Figure 2 is a convenient starting point for a study of fault diagnosis, where such faults may be expressed in terms of frequency domain behaviour. Such an approach allows physical reasoning to reduce test procedure 'debugging' and simplifies software by indicating major failure patterns, these latter to be supplemented by simulated faults on real systems or analogue models. A basic philosophy is shown in Fig. 10, more complex phenomena can be understood by using the faults shown as elemental building blocks. The effect of faults occurring at high or low frequencies only are readily observable from the plot of  $|0_o/E|$ ,<sup>26</sup> whilst changes in the intermediate frequency range are readily catalogued by using the coefficient plane technique.<sup>27</sup> The latter technique is particularly useful when the system has minor feedback loops contributing to  $0_o/E$ . Since the fault conditions are related to the frequency measurements made in the go/no-go test phase, the frequencies at which the system fails aid initial diagnosis.

### 9. The Need for Adequate Access Points

The requirements for monitoring system error ( $E$ ) in order that the user be satisfied that tracking errors are satisfactorily small has already been emphasized, and it follows that suitable access points must be made available by system manufacturers.<sup>28</sup> Furthermore, the fault diagnosis chart of Fig. 10 shows that identification of faults is greatly assisted by the availability of direct measurements of  $E$ . It is also self-evident that unless further access points are provided, no source of gain change can be identified. Typically, seven major access points have been made available for fault diagnosis in a complex system,<sup>29</sup> and the relative advantages of monitoring many access points at a few frequencies and of monitoring few access points at many frequencies is a topic worthy of further study.<sup>30</sup>

### 10. Experimental Environment

Whilst the first four problems outlined in Section 1 can be solved by considering the general properties of systems, the last two problems can only be discussed by reference to specific environments. The electro-hydraulic servomechanisms discussed previously have been field

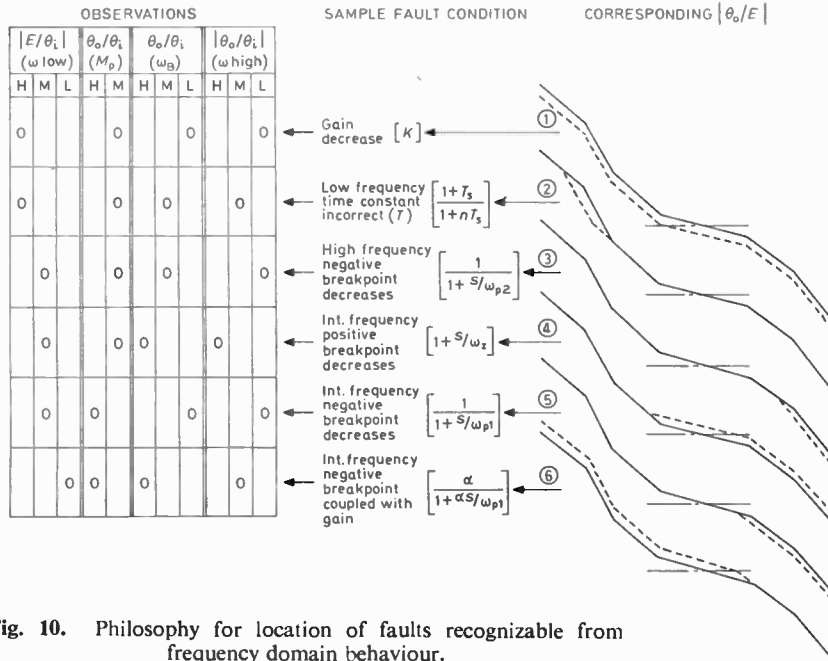


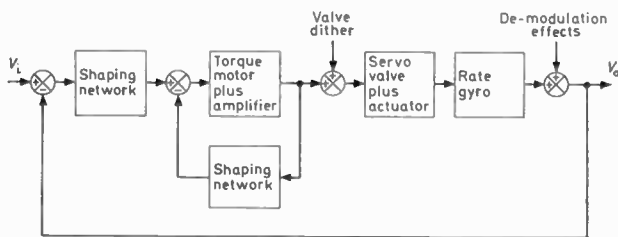
Fig. 10. Philosophy for location of faults recognizable from frequency domain behaviour.

tested under realistic workshop conditions; a typical output trace is shown in Fig. 11, and clearly illustrates the type of measurement problem so frequently met in the field. All the noise shown is generated within the servomechanism itself, when operating in anger there will be additional noise superimposed on the command signal. The inherent noise levels within servomechanisms have been found to vary considerably, for example, in twenty electro-hydraulic servomechanisms acceptable to the user, the noise level was found to vary from 0.10 V r.m.s. to 10.0 V r.m.s., with an average of 3.7 V r.m.s. This variation in noise level is sufficient to cause changes in signal/noise ratios of 10 : 1 to 1 : 10, and clearly if the systems really are acceptable to the user, the test procedure must cope with this magnitude of variation.

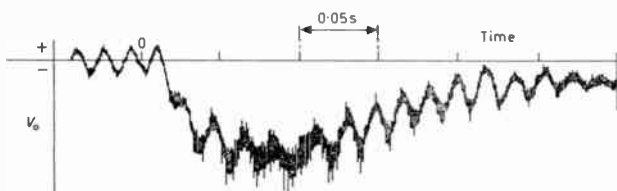
11. Effect of Non-linearities

Practical systems are non-linear for very small and very large stimuli. It is frequently possible to test systems under reasonably linear conditions such that the user has adequate confidence in the system under a much wider range of inputs, and this is true of the electro-hydraulic servomechanism as shown in Fig. 12, where phase and amplitude ratio are seen to vary little for a range of error amplitudes. At a frequency of 2 Hz there is a significant reduction in gain as  $|\text{error}|$  is increased, but this is thought to result from the interface equipment and the method of test, which effectively interjects a high-pass filter in series with the system.

There are exceptions in which the system under test is too non-linear to attach much significance to linear concepts, even if the system was hoped to be linear by the designer. One such system is described in reference 31, where for any input amplitude a quasi-linear curve fit may be found, but the resulting transfer function varies considerably even for small changes in input level. This



(a) Block diagram of electro-hydraulic servomechanism.



(b) Typical output trace.

Fig. 11. Noisy servomechanism used for experimental work.

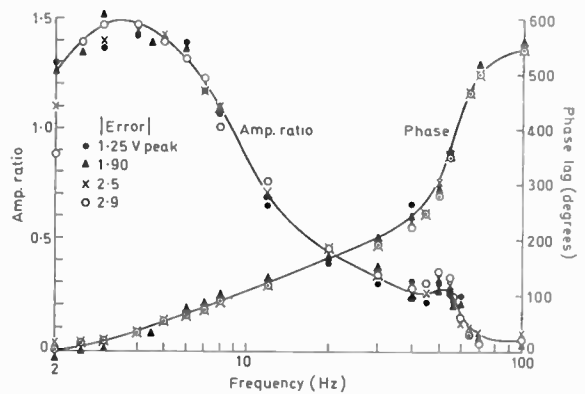


Fig. 12. Experimental frequency responses for constant value of  $|\text{error}|$ .

means that many more empirical relationships between test results and operational effectiveness must be established at the development stage before test conditions and tolerances are finalized.

**12. System Drift**

The user must know whether the performance of his system will drift with time. If large drifts are expected, this must be accounted for in the tolerancing procedure. As shown in Fig. 13, for the electro-hydraulic servo studied, at low frequency, (2 Hz) the drift range is 2 V ( $\pm 6\%$ ) and 4°, whilst at medium frequency (12 Hz) the drift range is 1 V ( $\pm 5\%$ ) and 5°. These drifts are less than the proposed gates of Section 5, and may be neglected at medium frequency, since good systems lie well within the tolerance gates chosen. At low frequencies drift of this magnitude need not affect confidence in the go/no-go decisions for the dominant transfer function since we can increase the lowest test frequency until the maximum recorded drift is no greater than the difference between the boundaries of good systems (Fig. 3) and the actual gates set (Table 1). But in moving away from 18 rad/s, we no longer constrain  $|E/\theta_1|$  in the 15 dB gain region, hence providing yet another argument for provision of access points which will permit  $E$  to be measured directly.

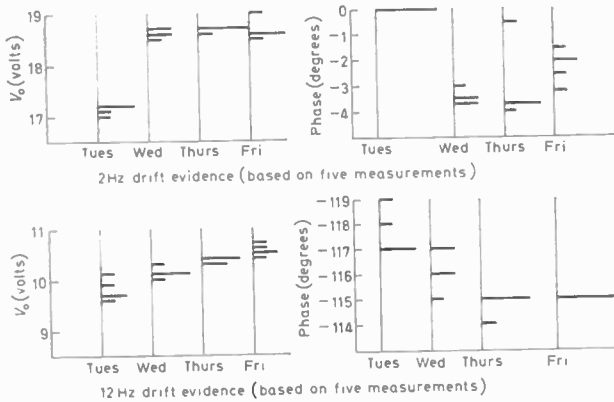


Fig. 13. Drift observed during 25 hours total running time.

**Table 1**

Failure patterns for dominant transfer functions

Case	$\omega$ rad/s				
	$M_p$	$\omega_B$	18	50	100
			Ph. G.	Ph. G.	Ph. G.
1	M	L	F F - F - F		
2	H	M	F - - F F -		
3	H	L	F F F F - F		
4	H	L	F F F F - F		
5	H	L	- F F F F F		
6	M	H	- - F - F F		
7	M	H	- - F - F F		
8	H	H	- - F F F F		

Gates	$\omega$	Phase	Gain
	18	5°- 30°	1.10-1.5
	50	45°-115°	0.70-1.30
	100	90°-150°	0.25-0.60

**Table 2**

Failure patterns for secondary modes

Case	$\omega$ rad/s							
	240	260	280	300	320	340	360	
	Ph. G.	Ph. G.	Ph. G.	Ph. G.	Ph. G.	Ph. G.	Ph. G.	
1	F F F - F - F - F - F - - -							
2	- F F F F - F F F - F - - -							
3	- - - - - - - - F - F - - -							
4	F - F - F - F - F - F F F - - -							
5	F - F - F - F - F - F - F - F F							
6	F - F - F - F - F - F - F - F -							
7	F - F - F F F F F - F - - -							
8	- - F - F - F - F F F F - - -							
9	- - F - F - F - - - - F - - -							

**13. Measurement Variance**

Due to inherent noise within systems, gain and phase measurements are subject to variation in a random manner. For just one such system, if the noise is stationary, and the power spectrum known, the variance at any frequency may be estimated directly. In the field, as discussed in Section 11, enormous variations in noise, and hence in variance are to be expected, between different systems of the same type. Since variance is reduced by increasing measurement time, roughly in accordance with the 'central limit' theorem,<sup>32</sup> the test procedure must order measurements of the correct duration to be made. In a previous study<sup>31</sup> inherent noise was found to be wide-band; for the electro-hydraulic servomechanism under discussion, there is wideband noise but also discrete high frequency noise due to dither and demodulation effects. Part of a wide frequency range repeatability experiment is shown in Fig. 14. At low and medium frequencies variance due to noise is small, and averaging is not really necessary. As expected, at 59 Hz, in the region of the dither frequency, the variance is enormous, suggesting averaging over a long measurement time. Figure 15 shows the moving average of measurements recorded in the noisy region, and verifies that under field experimental conditions, the 'central limit' theorem is a reasonable guide to variance reduction. Since the transfer function analyser used in these experiments has provision for ten cycle integration, results for this measurement time were recorded and are also shown in Fig. 15. The reduction in variance is impressive, as expected, and ambiguities in phase quadrant are completely resolved, thus accounting for a much greater reduction in the variance of the phase lag at 59 Hz than would be expected from the 'central limit' theorem. Since in the 59 Hz region we are concerned with gates of about 60°, a standard deviation due to noise alone of 9° is obviously too large. If the measure-

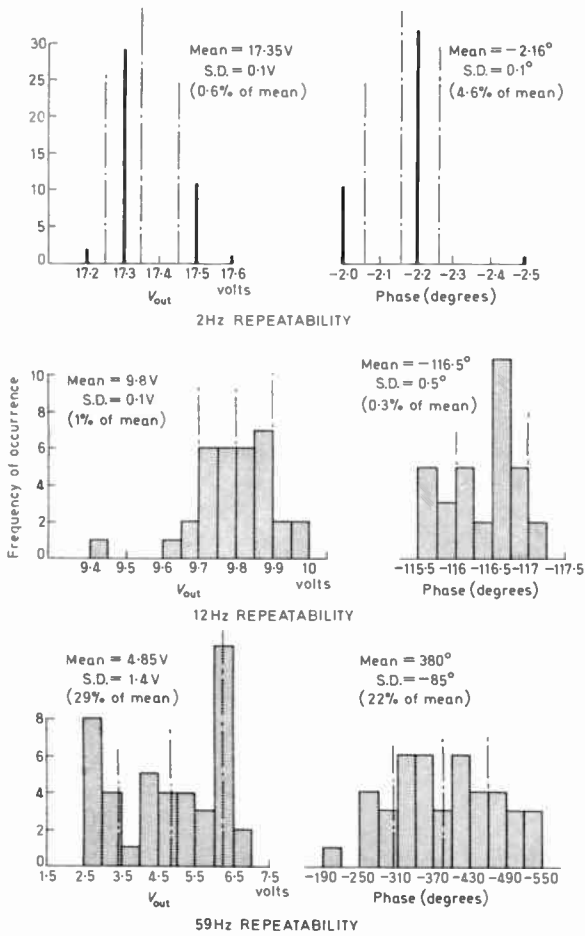


Fig. 14. Gain and phase repeatability with minimum integration time.

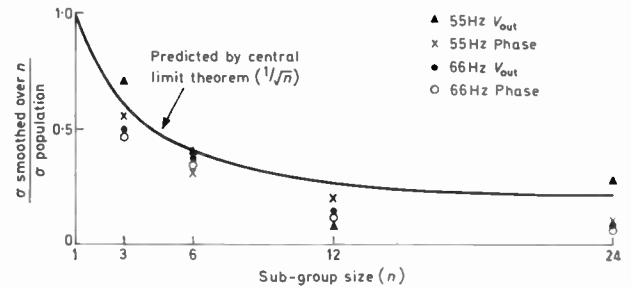
ment time is now increased to 100 cycles, the standard deviation due to noise is reduced to approximately 3%, and the chance of failing a good system due to measurement variability is then 0.40% compared with 5% if the integration is over ten cycles only. In some applications such as aboard ship, a large number of servomechanisms may be required to be computer-tested in rapid succession. If noise varies considerably from one servomechanism to another, an algorithm may be incorporated in the test procedure to estimate variance at specific frequencies as the measurement proceeds, the measurement time being truncated if a low variance is encountered, thus saving central computer time.

14. Conclusions

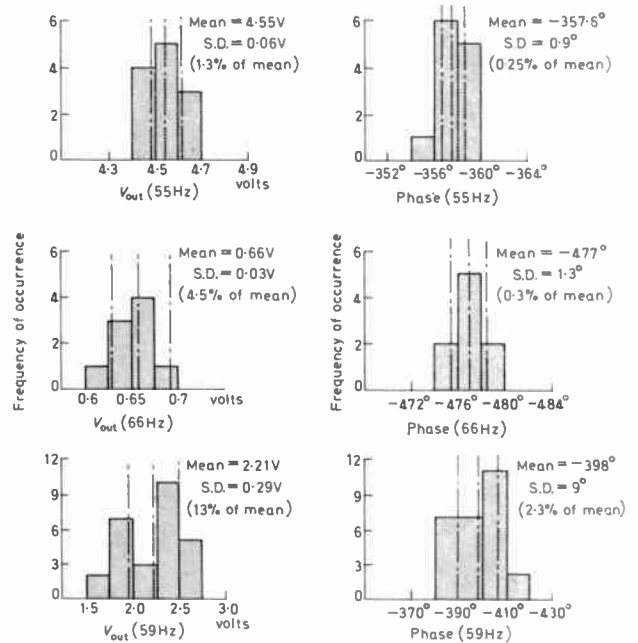
Operational requirements of many feedback control systems are readily translated into frequency domain tests. Dominant transfer functions, of prime importance in assessing dynamic errors, noise transmission, and saturated performance are readily constrained by setting gates on gain and phase at three intermediate frequencies. High-frequency noise rejection, and time delays to dynamic errors are both readily checked by measuring system phase lag at one or more high frequencies. If secondary modes are present, these are also constrained by measuring gain and phase at three high frequencies.

Tracking errors can only be readily established by monitoring system error at one or more very low frequencies. Some system failures can be diagnosed according to the pattern in which the go/no-go tests are failed. The need for careful consideration of access points at the design stage is highlighted firstly for monitoring system error, and secondly for the resolution of ambiguities in fault diagnosis.

Drift can be a problem at low frequency if an attempt is made to constrain tracking errors directly from an assessment of the dominant transfer function, an exercise frequently doomed to failure even in the absence of drift. Inherent noise is a problem, and our experience suggests that whereas averaging over ten cycles is adequate for testing in the presence of wideband noise, for testing at frequencies near a discrete noise source averaging over one hundred cycles may be more appropriate.



(a) Moving average of measurements recorded for 1 cycle integration time.



(b) Measurements recorded over 10 cycles.

Fig. 15. Reducing variance by increasing measurement time.

## 15. Acknowledgments

The authors acknowledge the active support of the Science Research Council and the Ministry of Technology. Helpful discussions took place with Mr. R. Levinge of the Solartron Electronic Group and with Mr. G. Griffiths, Department of Mathematics, U.W.I.S.T.

## 16. References

- Gibson J. E., Rekasius, Z. V., McVey, E. S., Sridhar, S. and Leedham, C. D., 'A set of standard specifications for linear automatic control systems', *Trans. Amer. Inst. Elect. Engrs*, **80**, pp. 65-77, 1961.
- Dreifke G. E. and Hougen, J. O., 'Experimental Determination of System Dynamics by Pulse Methods', 4th JAC Conference Proceedings, University of Minnesota, pp. 608-33, 1963.
- French, R. C., 'Transfer function measurement using fast pulses', *Electronic Engineering*, **38**, pp. 516-9, August 1966.
- Elsden, C. S. and Ley, A. J., 'A digital transfer function analyser based on pulse rate techniques', *Automatica*, **5**, No. 1, pp. 51-60, 1969.
- Fry, D. E., 'Use of Cross-correlation and Power Spectral Techniques for the Identification of Hunter Mk. 12 Dynamic Response', R.A.E. Tech. Report 69156, July 1969.
- Lamb, J. D., 'The Use of Pseudo Random Binary Signals for the Production of Dynamic Systems', Ph.D. Thesis, UWIST 1970.
- Kwaitkowski, A. W. and Bennett, F. E., 'Correlation Method of System Identification: Computer Programme and Experiment Design Considerations', Proceedings of the 7th International Machine Tool Design and Research Conference, Birmingham, 1966.
- Field, C. F., 'Cross-correlation and milling machine dynamics—a case study', *Int. J. Mach. Tool Design Res.*, **9**, pp. 81-96, 1969.
- Lees, S., 'Interpreting dynamic measurements of physical systems', *Trans. Amer. Soc. Mech. Engrs*, **80**, pp. 833-57, 1958.
- Holmes, J. S. (ed.), Proceedings of the Symposium on Servo Testing held at HMS *Collingwood* (subsequently published in the *Naval Electrical Review*).
- Towill, D. R., 'Transfer Function Techniques for Control Engineers', p. 17, (Iliffe, London, 1969).
- Horowitz, I., 'Fundamental theory of automatic linear feedback control systems', *I.R.E. Trans. on Automatic Control*, **AC-5**, pp. 5-19, 1959.
- Chen, Kan, 'Quick methods for estimating closed-loop poles of control systems', *Trans. A.I.E.E., (Applications and Industry)*, **76**, pp. 80-7, May 1957.
- Towill, D. R., 'Rapid synthesis technique for the duplicator class of feedback control systems', *Trans. Inst. Meas. Control*, **1**, No. 2, pp. T45-54, 1968.
- Chestnut, H. and Mayer, R. W., 'Servomechanisms and Regulating System Design', Vol. II, (John Wiley, New York, 1955), pp. 62-4.
- Biernson, G., 'Estimating transient responses from open loop frequency response', *Trans. A.I.E.E., (Applications and Industry)*, **75**, pp. 388-400, January 1956.
- Towill, D. R., Cooper, J. S. and Lamb, J. D., 'Dynamic analysis of fourth order feedback control systems', *Int. J. Control*, **10**, No. 2, pp. 121-46, August 1969.
- Gill, F. R., 'The Integrity of a Civil Blind Landing System with Particular Reference to the Azimuth Channel', R.A.E. Tech. Report, No. 65022, February 1965.
- Towill, D. R. and Mehdi, Z., 'Prediction of the Transient Response Sensitivity of High Order Linear Systems Using Low Order Models', University of Wales Institute of Science and Technology, DAG TN 29, May 1969.
- Brown, J. M., Towill, D. R. and Payne, P. A., 'Generalisation of Dynamic Error Constraints Imposed by Frequency Response Measurements', University of Wales Institute of Science and Technology, DAG TN 35, December 1970.
- Towill, D. R., 'Optimum transfer functions for feedback control systems with plant input saturation', *The Radio and Electronic Engineer*, **38**, No. 4, pp. 233-47, October 1969.
- Towill, D. R. and Baker, K. J., 'Use of Sensitivity Functions to Generate a Probabilistic Model for a Family of Rate Servos', University of Wales Institute of Science and Technology, DAG TN 31, September 1969.
- Bell, D. A., 'The recovery of information from noisy measurements', *Trans. Soc. Instrum. Tech.*, **18**, No. 2, pp. 89-102, June 1966.
- Payne, P. A., Towill, D. R. and Baker, K. J., 'Predicting servomechanism dynamic performance variation from limited production test data', *The Radio and Electronic Engineer*, **40**, No. 6, pp. 275-88, December 1970.
- Levinge, R. W., 'Measurement of resonances in high order transfer functions', *Trans. Inst. Meas. Control*, **2**, No. 3, pp. 102-5, March 1969.
- Chen, Kan, 'Analysis and design of feedback systems with gain and time constant variations', *I.R.E. Trans. on Automatic Control*, **AC-6**, pp. 73-9, 1961.
- Towill, D. R., 'Coefficient plane synthesis of zero velocity lag servomechanisms', *The Radio and Electronic Engineer*, **34**, No. 6, pp. 323-34, December 1967.
- Hayes, K. A., 'The Necessity for Test Points in Servomechanisms', Ministry of Technology Report REMC/28/FR, May 1969.
- Kirby, J. E. D., 'Final Report on the Evaluation of the Transfer Function Measurement Unit', Wayne Kerr Ltd., October 1968.
- Skwirzynski, J. K., 'The use of standard computer programmes for equipment diagnostic techniques', Proceedings of I.E.R.E. Convention on Electronics in the 1970s, (Symposium on Automatic Test Equipment), Cambridge, July 1968, (I.E.R.E. Conference Proceedings No. 12).
- Towill, D. R. and Lamb, J. D., 'Pseudo-random signals test non-linear servo' *Control Engineering*, **17**, No. 11, pp. 59-63, November 1970.
- Bowman, E. H. and Fetter, R. B., 'Analysis for Production Management', p. 157, (Richard D. Irwin, New York, 1957).

*Manuscript first received by the Institution on 8th January 1970 and in final form on 23rd September 1970. (Paper No. 1364/IC 39.)*

# Drift and Low Frequency Noise

By

**G. G. BLOODWORTH,**

M.A., D.U.S., Ph.D., C.Eng., F.I.E.R.E.†

and

**R. J. HAWKINS,**

B.Sc., Ph.D.†

To compare errors arising in a measuring instrument from drift and low frequency ( $1/f$ ) noise, the behaviour of the latter in the time domain is calculated. The standard deviation is expressed in terms of the cut-off frequency and integration time of the instrument, and the frequency index of the noise, which can be measured at audio frequencies. Optimum values of these quantities are discussed. The theory is illustrated by reference to measurements on m.o.s. transistors which indicate that current noise may sometimes be the main cause of 'drift' for periods between a day and a year.

## 1. Introduction

Measurements of current noise at very low frequencies have shown that the  $1/f$  spectrum observed at audio frequencies extends downwards apparently without limit. In m.o.s. transistors, for example, the spectrum has been analysed<sup>1</sup> down to  $5 \times 10^{-5}$  Hz and theoretical considerations<sup>2</sup> suggest that it may well continue for many more decades. This means that current noise contributes to 'drift', and this contribution ought to be predictable from measurements at audio frequencies. The nature and extent of this predictability will be discussed here.

The term 'drift' is applied to slow current changes in electronic circuits caused by a variety of undesired physical changes. The concept is limited to the time domain because drift components are generally slow and aperiodic and therefore do not make a significant contribution to the output signal power at any frequency where band-pass filters are commonly used, say above 100 Hz. On the other hand, low frequency noise is normally characterized in the frequency domain because it is important at signal frequencies and the noise power is a fairly simple function of frequency. In almost all practical circuits the dominant component is  $1/f$  noise caused by conductivity fluctuations in a semiconductor or thermionic device. In band-pass amplifiers the noise power is still rising at the lowest signal frequency, say 100 Hz. Noise at lower frequencies may be conceptually transferred to the time domain and simply considered as indistinguishable from drift.

It is suggested that in fact drift and noise should be distinguished wherever possible because they have different physical causes and cures. As the extent to which this is possible depends on their different characteristics in the time domain, the main features of these characteristics will be compared below. In view of the diverse causes of drift no particular physical system will be considered in detail, and it will simply be assumed that there are various transient components decaying exponentially with a wide range of time constants and amplitudes. Attention will be mainly focused on the comparative shape in the time domain of the integrated effect of noise components with a  $1/f$  spectrum, and the error ('drift') of a measuring instrument subjected to such noise.

† Department of Electronics, University of Southampton.

## 2. Dependence of Error Caused by Current Noise on Integration Time and Instrument Bandwidth

Suppose the noise power spectral density has a dependence on angular frequency ( $\omega$ ) of the form

$$G(\omega) = g\omega^{-(1+\alpha)}$$

where  $g$  and  $\alpha$  are assumed to be constant over the frequency range of interest. It is unrealistic to consider only a simple  $1/f$  spectrum ( $\alpha = 0$ ), since published measurements<sup>2</sup> of current noise have given values of  $\alpha$  between  $-0.1$  and  $+0.4$ , and mainly concentrated around  $+0.1$  to  $+0.2$ . The significance of  $\alpha$  in the time domain will now be considered.

The most important statistical parameter is the variance of the fluctuations in a given bandwidth, which determines the signal/noise ratio for an instrument using that bandwidth. An instrument which receives noise for a time  $T$  does not respond to fluctuations with angular frequency  $\omega \ll 1/T$ . Also it will have a finite upper cut-off frequency  $\omega_m$ . Taking sharp cut-offs for simplicity, the total noise power  $v_n^2$  to which it responds is given approximately by the following expression. A more thorough analysis in the Appendix justifies this apparently crude approximation.

$$\begin{aligned} \overline{v_n^2} &= g \int_{1/T}^{\omega_m} \omega^{-(1+\alpha)} d\omega \\ &= \frac{g}{\alpha} (T^\alpha - \omega_m^{-\alpha}) \\ &= \frac{g}{\alpha} T^\alpha (1 - (T\omega_m)^{-\alpha}) \end{aligned} \quad \dots\dots(1)$$

The corresponding result for  $\alpha = 0$  is

$$\overline{v_n^2} = g \ln (T\omega_m) \quad \dots\dots(2)$$

The amplitude of the noise lies within  $\pm 2\sqrt{\overline{v_n^2}}$  of its mean value for 95% of the time, assuming that its distribution is Gaussian. Analysis<sup>1</sup> of low-frequency noise measurements on m.o.s. transistors has confirmed the validity of this assumption, which is consistent with all physical models for current noise.

Equation (2) for true  $1/f$  noise ( $\alpha = 0$ ) shows that the variance of the noise waveform depends simply on  $T\omega_m$ ; and for a given  $\omega_m$ , it increases logarithmically with  $T$ . The latter dependence has been reported by Brophy<sup>3</sup> for

1/f noise in a reverse-biased p-n junction, for sample lengths  $T$  in the range 10–1800 s. Brophy also reported that the variance of current noise measured in successive periods shows greater fluctuations than those found for thermal noise. The variance of the variance was found to be approximately 0.7% for the p-n junction, and 7% for a carbon resistor, independently of the sample length. These changes in variance increase slightly the probability of larger fluctuations occurring, but as this is a second-order effect it is ignored in the present contribution.

Referring to equation (2), we might attempt to improve the accuracy of an instrument whose output is fluctuating due to a noise component, by reducing  $\omega_m$ . This change would slow the response of the instrument when the d.c. input signal is applied, and it would be necessary to increase the integration time  $T$  to allow the instrument to settle down before the reading is taken. The transient error would decrease with a time constant  $1/\omega_m$ , assuming for simplicity that the instrument has just the single time-constant. For the same transient error  $\omega_m T$  would in fact have to be unaltered, and therefore the error due to current noise (with  $\alpha = 0$ ) would not change, and no advantage would be gained. If for a given  $\omega_m$  the integration time is unnecessarily prolonged beyond the period of the transient error, the drift error due to noise will increase logarithmically with  $T$ .

Using the general equation (1) for non-zero  $\alpha$ , values of  $\sqrt{\langle v_n^2 \rangle}$  for various values of  $\alpha$  and  $T$  are plotted in Fig. 1. We have taken the typical value of  $g = 1 \mu V^2$  for a m.o.s. transistor above pinch-off (referred to the gate voltage). For the full curves  $\omega_m = 1 \text{ rad/s}$ , for the dashed curves  $\omega_m T = 10$ , and each curve is labelled with the corresponding value of  $\alpha$ . For an instrument used to take a single d.c. measurement, a value of 10 for  $\omega_m T$  might allow it to settle to a reasonably steady reading of the signal.

It is apparent that for  $\alpha > 0$  the standard deviation of the noise increases quite rapidly with  $T$ . Thus, if  $T$  is increased, keeping  $\omega_m T$  constant as before, the error due to noise is only reduced if  $\alpha < 0$  (for example  $\alpha = -1$  for white noise). If  $\alpha > 0$ , which is usually the case for current noise, the error becomes progressively worse.

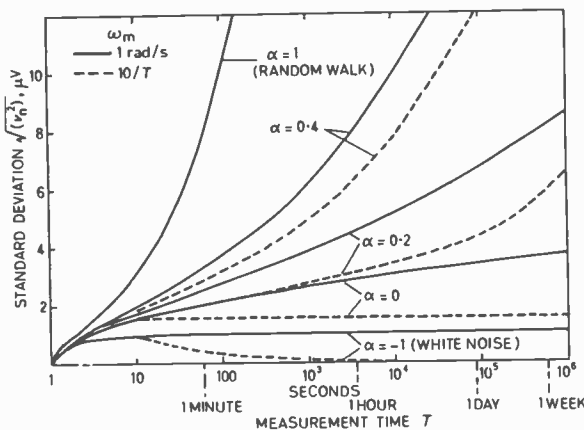


Fig. 1. Predicted response to noise of the form  $1/f^{1+\alpha}$  applied for a time  $T$  to a measuring instrument with a high-frequency cut-off at  $\omega_m$ .

Although for high positive values of  $\alpha$  the slope of each curve increases progressively on a logarithmic time scale, it decreases on a linear scale. For all values of  $\alpha$  reported for current noise the divergence is less than that of the well-known random-walk model applicable to diffusion processes, in which the spectral density is inversely proportional to the square of frequency (i.e.  $\alpha = +1$ ).

For a fixed noise power  $g$  at 1 rad/s, the standard deviation for extended periods of time increases rapidly with  $\alpha$ . A reasonably accurate knowledge of the frequency index is therefore important. A transistor operating point which gives a good noise figure at 1 Hz but a large value of  $\alpha$  may be far from the optimum point for a measurement extending over a week, if other bias conditions give smaller values of  $\alpha$ .

Values of  $\omega_m T$  larger than 10 are required if repeated measurements are to be taken without resetting the instrument. For example, daily measurements over a year would mean that  $T$  is a year and  $1/\omega_m$  would have to be less than a day so that the instrument could respond to daily signal changes. The best choice for  $\omega_m$  would depend on the relative values of transient errors (worse for smaller  $\omega_m$ ) and the noise contribution (worse for larger  $\omega_m$ ). The latter can be estimated from equation (1).

### 3. Comparison of Errors Caused by Current Noise and Exponential Drift Components

In addition to low-frequency noise, there is usually a systematic non-random drift in the operating point of a semiconductor device. In the m.o.s.t., for example, this is due mainly to ionic conduction and polarization in the gate insulator. There may also be a small drift due to the gradual filling of the oxide traps near the interface after bias voltages have been applied.<sup>4</sup> Some of our own measurements have shown that the drift rate can be of the order of 1 mV/s initially, but it decreases rapidly. After settling times of the order of days, we have observed in most cases that this drift component no longer dominates and the magnitude of the output is consistent with its being due primarily to random 1/f noise. Over longer periods, say a year, the drift will dominate again if it has a component which increases more than the standard deviation of the noise.

Shown in Fig. 2 is a simple theoretical example of drift produced by species of ions with different time constants, compared with current noise having a frequency index of 1.2 and the same magnitude at 1 rad/s as in Fig. 1. In this example, the faster decay has a magnitude  $V_1 = 100 \text{ mV}$ , and a time-constant  $\tau_1 = 10^4 \text{ s}$ . The change in voltage,  $V$ , from the initial conditions is assumed to be given by

$$V = V_1 [1 - \exp(-T/\tau_1)]$$

and is shown by the solid curve. The noise magnitude is represented by error bars of  $\pm 2$  standard deviations. The figure shows that voltage changes after one day are predominantly due to the random noise.

The broken curve (a) shows the additional effect of a possible second drift process with a magnitude

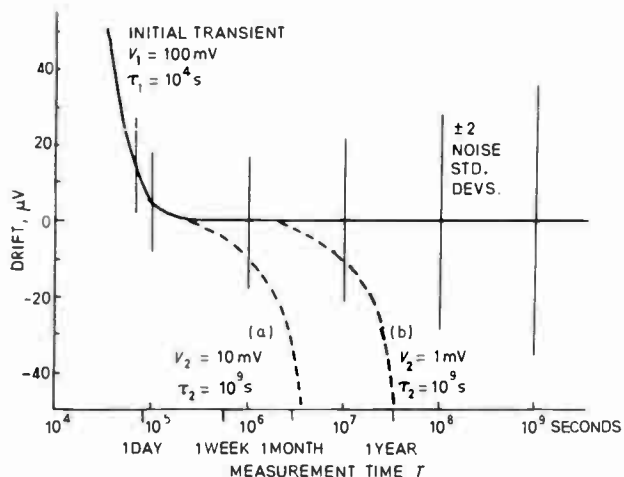


Fig. 2. Possible drift due to processes with time-constants  $\tau_1, \tau_2$  and magnitudes  $V_1, V_2$ , compared with current noise of the form  $1/f^{1.2}$

$V_2 = 10$  mV and a time-constant  $\tau_2 = 10^9$  s (about 30 years). For values of  $T \ll 10^9$  s this component gives a constant drift rate of  $10^{-11}$  V/s, and it will be seen that this predominates over the noise after about a month. The broken curve (b) shows a possible alternative component which has a smaller magnitude (or longer time-constant) by a factor of 10, and predominates over the noise after a year.

These simple examples accord with our own measurements on m.o.s. transistors up to  $10^6$  s, and suggest that  $1/f$  noise is important at least in medium-term operation of these devices. For operation over very long periods of time, say more than a year, slow drift components probably predominate. When the latter eventually approach their equilibrium states the noise will again predominate—if our descendants are still carefully preserving and observing the transistor concerned!

4. Conclusions

As the physical origins of current noise and drift are believed to be essentially separate in m.o.s. transistors and other semiconductor devices used in measuring instruments, it is important to know which is more significant in any particular application. Theoretical considerations, supported by some measurements, suggest that random noise may be the dominant factor for certain measuring times, for example roughly between a day and a year in the case of some m.o.s. transistors we have investigated.

The effect of random noise is predictable in the sense that the standard deviation for the period of the proposed operation can be calculated from simple rapid measurements of  $g$  and  $\alpha$  at audio frequencies. The simple analysis given above shows the sensitivity of this error to the value of  $\alpha$ . Our measurements on a few transistors have shown that  $\alpha$  can sometimes vary quite significantly over the frequency range  $10^{-4}$  to  $10^4$  Hz. Nevertheless, extrapolation from a.f. measurements gives an approximate value for  $\alpha$ , and hence for the standard deviation, and the latter indicates the error to be expected if there

is no other source of drift. When this is compared with the actual performance of the transistor in service, one can decide which problem to tackle—the noise or the drift.

5. Acknowledgments

This work arose from collaboration and stimulating discussions with staff at the U.K.A.E.A. Establishment at Winfrith. Financial support has been provided by the Science Research Council.

6. References

1. Mansour, I. R. M., Hawkins, R. J. and Bloodworth, G. G., 'Measurement of current noise in m.o.s. transistors from  $5 \times 10^{-5}$  to 1 Hz', *The Radio and Electronic Engineer*, 35, pp. 212-16, April 1968.
2. Bloodworth, G. G. and Hawkins, R. J., 'The physical basis of current noise', *The Radio and Electronic Engineer*, 38, pp. 17-22. July 1969.
3. Brophy, J. J., 'Low-frequency variance noise', *J. Appl. Phys.*, 41, pp. 2913-6, June 1970.
4. Lundström, I., Christensson, S. and Svensson, C., 'Hysteresis effects in m.o.s. transistors due to carrier trapping at the semiconductor-oxide interface', I.P.P.S.-I.E.E. Conference 'Physical Aspects of Noise in Electronic Devices', Nottingham, September 1968.
5. Bell, D. A., 'Electrical Noise' (Van Nostrand, New York, 1960).

7. Appendix: Low-frequency Cut-off of Noise owing to Finite Integration Time

The effect of noise on a system is to cause successive samples of its output to differ in an unpredictable way. Following Bell<sup>5</sup>, we first consider a single component of the noise of angular frequency  $\omega$  sampled at times  $t = s$  and  $(s+T)$ , and represented by the sine wave  $V \sin \omega t$ . The difference  $\Delta V$  between the samples is given by

$$\Delta V = V(\sin [\omega(s+T)] - \sin \omega s) = V(\sin \omega s(\cos \omega T - 1) + \cos \omega s \sin \omega T)$$

Since the noise components have random phase, we consider mean square values, averaged over all values of  $s$ , for the same values of  $\omega$  and  $T$ . Thus

$$\overline{\Delta V^2} = V^2(\overline{\sin^2 \omega s(\cos \omega T - 1)^2} + \overline{\cos^2 \omega s} \cdot \overline{\sin^2 \omega T} + \overline{\sin \omega s \cos \omega s(\cos \omega T - 1) \sin \omega T}) = V^2(1 - \cos \omega T) = 2V^2 \sin^2 \left(\frac{\omega T}{2}\right)$$

For  $\omega T \ll 1$ ,

$$\overline{\Delta V^2} \approx \frac{1}{2} V^2 \omega^2 T^2$$

Therefore the output power at angular frequencies below  $1/T$  is rapidly attenuated, although the current noise power ( $V^2$  in this example) may be inversely proportional to  $\omega$ . For  $\omega T > 1$ ,  $2 \sin^2 (\omega T/2)$  oscillates rapidly about the average value of unity. In view of this, it is reasonable to use the following approximation for  $\overline{\Delta V^2}/V^2$  to estimate the total effect of the finite integration time  $T$ :

$$\frac{\overline{\Delta V^2}}{V^2} = \begin{cases} \frac{1}{2} \omega^2 T^2, & \text{for } \omega T \leq \sqrt{2} \\ 1, & \text{for } \omega T \geq \sqrt{2} \end{cases}$$

This relation gives the response  $\overline{\Delta V^2}$  of the instrument in a time  $T$  to noise of variance  $V^2 = G(\omega) d\omega$  in any small bandwidth  $d\omega$ . The total response to current noise with frequency index  $(1+\alpha)$  is now given by integrating over all frequencies up to the cut-off frequency  $\omega_m$  of the instrument. The assumption of a sharp cut-off at  $\omega_m$  is clearly a minor approximation since the reduced response of the instrument is accentuated by the decrease in current noise power.

$$v_n^2 = \int_0^{\omega_m} \overline{\Delta V^2} = \frac{gT^2}{2} \int_0^{\omega_m} \omega^{1-\alpha} d\omega + g \int_0^{\omega_m} \frac{d\omega}{\sqrt{2}T \omega^{1+\alpha}}$$

$$= \frac{g}{2-\alpha} \left(\frac{T}{\sqrt{2}}\right)^\alpha + \frac{g}{\alpha} \left[ \left(\frac{T}{\sqrt{2}}\right)^\alpha - \frac{1}{\omega_m^\alpha} \right]$$

$$= \frac{g}{\alpha} \left[ \left(\frac{T}{\sqrt{2}}\right)^\alpha \cdot \frac{1}{1-\alpha/2} - \frac{1}{\omega_m^\alpha} \right]$$

Now  $\sqrt{2}^\alpha \approx 1 + \alpha(\sqrt{2}-1)$ , since  $|\alpha|$  is typically less than 0.4, and so  $\sqrt{2}^\alpha(1-\alpha/2)$  is close to unity (within a few per cent). Therefore

$$v_n^2 \approx \frac{g}{\alpha} T^\alpha (1 - (T\omega_m)^{-\alpha})$$

This result conforms with equation (1) obtained by assuming a sharp cut-off of the noise at  $\omega = 1/T$ .

*Manuscript first received by the Institution on 27th July 1970 and in final form on 20th October 1970. (Paper No. 1365/CC96.)*

© The Institution of Electronic and Radio Engineers, 1971

### STANDARD FREQUENCY TRANSMISSIONS—January 1971

(Communication from the National Physical Laboratory)

Jan. 1971	Deviation from nominal frequency in parts in 10 <sup>10</sup> (24-hour mean centred on 0300 UT)			Relative phase readings in microseconds N.P.L.—Station (Readings at 1500 UT)		Jan. 1971	Deviation from nominal frequency in parts in 10 <sup>10</sup> (24-hour mean centred on 0300 UT)			Relative phase readings in microseconds N.P.L.—Station (Readings at 1500 UT)	
	GBR 16 kHz	MSF 60 kHz	Droitwich 200 kHz	*GBR 16 kHz	†MSF 60 kHz		GBR 16 kHz	MSF 60 kHz	Droitwich 200 kHz	*GBR 16 kHz	†MSF 60 kHz
1	-299.7	-0.1	0	650	636.6	17	-300.0	-0.1	0	657	648.3
2	-300.1	-0.1	0	651	637.7	18	-300.2	-0.1	0	659	648.8
3	-300.1	-0.2	0	652	639.7	19	-300.0	-0.1	0	659	649.7
4	-300.2	-0.2	+0.1	654	640.0	20	-300.1	-0.1	0	660	650.4
5	-300.1	-0.1	0	655	641.3	21	-300.2	-0.2	-0.1	662	652.6
6	-300.1	0	0	656	643.6	22	-300.1	-0.2	-0.1	663	654.9
7	-300.0	-0.1	0	656	640.6	23	-300.1	-0.1	0	664	656.1
8	-300.1	-0.1	0	657	641.9	24	-300.1	-0.1	0	665	657.3
9	-300.0	0	+0.1	657	642.0	25	-299.9	0	0	664	657.8
10	-300.0	0	+0.1	657	641.9	26	-300.3	-0.1	0	667	658.7
11	-300.0	-0.1	+0.1	657	642.5	27	-299.6	0	0	663	658.8
12	-299.9	-0.1	+0.1	656	644.9	28	-300.1	-0.1	0	664	659.3
13	-300.0	0	+0.1	656	645.3	29	-300.2	0	0	666	659.5
14	-300.0	0	+0.1	656	645.3	30	-300.0	-0.2	0	666	661.4
15	-300.0	-0.1	0	656	646.3	31	-300.1	0	0	667	661.4
16	-300.1	-0.1	+0.1	657	647.5						

Note: The frequency offset for 1971 will be  $-300 \times 10^{-10}$ .

All measurements in terms of H.P. Caesium Standard No. 334, which agrees with the N.P.L. Caesium Standard to 1 part in 10<sup>11</sup>.

\* Relative to UTC Scale; (UTC<sub>NPL</sub> - Station) = + 500 at 1500 UT 31st December 1968.

† Relative to AT Scale; (AT<sub>NPL</sub> - Station) = + 468.6 at 1500 UT 31st December 1968.

# The Synthesis and Analysis of Active RC Ladder Networks using the Recurrent-Continuant Method

By

**Squadron Leader  
NORMAN R. S. NESBITT,**  
B.Sc., M.Sc.†

Given the polynomial in  $s$  which describes the reciprocal of the transfer function of the circuit to be synthesized, the recurrent determinant may be determined. The continuant determinant is evaluated by a logical sequence of operations on the recurrent determinant. The values of the elements of the continuant determine either the gains of the amplifiers in the circuit when the component values are specified or the component values when the amplifier gains are specified. The reverse procedure of producing the recurrent from the continuant is also described and from the recurrent the reciprocal of the transfer function of the network may be obtained.

## 1. Introduction

Synthesis and analysis procedures for active RC networks are described in this paper. The procedures form the basis of a computer program which is currently being written in *Algol 60* for use with a 4100 Elliott computer. The derivation of the recurrent from the transfer function and the continuant from the network is briefly described, a full treatment having been given elsewhere.<sup>1</sup>

The transformation from the recurrent to the continuant requires mathematical manipulations of the determinants and to avoid lengthy verbal explanations in the determinant description, two symbols are introduced. An arrow is used to indicate the two rows or columns which take part in an operation. The head of the arrow indicates which row or column is being operated upon. A ring encircling an element is used to indicate that the magnitude of that element is being changed to 1, 0, or  $-1$  by the operation. For example, the symbols in:

$$\begin{vmatrix} 1 & 1 & 0 & 1 \\ -1 & s & 0 & 0 \\ 0 & -1 & 1 & 0 \\ 0 & \textcircled{-1} & 0 & s \end{vmatrix} = \begin{vmatrix} 1 & 1 & 0 & 1 \\ -1 & s & 0 & 0 \\ 0 & -1 & 1 & 0 \\ 0 & 0 & -1 & s \end{vmatrix}$$

indicate that the third row is multiplied by a factor having the appropriate sign and added to the fourth row so as to reduce the second element in that row to zero.

The synthesis of low-pass filters only is considered since it has been shown that the other filter networks may be derived from these.<sup>2</sup>

To illustrate the procedures, the synthesis and analysis of a third order network is considered.

† Electronic Engineering Wing, Royal Air Force College, Cranwell, Lincolnshire.

## 2. Formation of the Recurrent

Consider the synthesis of a third-order network for which the reciprocal of its voltage transfer function is:

$$F(s) = a_3 s^3 + a_2 s^2 + a_1 s + a_0$$

The recurrent is a determinant whose value is  $F(s)$  and whose elements are determined directly from the expression for  $F(s)$ . In its simplest form, the recurrent is:

$$\begin{vmatrix} a_3 & a_2 & a_1 & a_0 \\ -1 & s & 0 & 0 \\ 0 & -1 & s & 0 \\ 0 & 0 & -1 & s \end{vmatrix}$$

This recurrent may be transformed into a continuant whose interpretation would lead to passive circuits containing both inductors and capacitors. For single reactance networks, the frequency dependent terms along the leading diagonal must be separated by non-frequency dependent elements. This is readily achieved by introducing the additional elements:

$$\begin{vmatrix} a_3 & a_2 & 0 & a_1 & 0 & a_0 \\ -1 & s & 0 & 0 & 0 & 0 \\ 0 & 0 & 1 & 0 & 0 & 0 \\ 0 & -1 & 0 & s & 0 & 0 \\ 0 & 0 & 0 & 0 & 1 & 0 \\ 0 & 0 & 0 & -1 & 0 & s \end{vmatrix}$$

The value of the determinant is not changed by this modification.

## 3. Transformation of Recurrent to Continuant

The particular example of a third-order binomial filter is considered for which:

$$F(s) = s^3 + 3s^2 + 3s + 1$$

The resultant ladder network is to contain the RC

components  $R_1, C_1, R_2, C_2, R_3, C_3$  having values of  $6\Omega, 5F, 4\Omega, 3F, 2\Omega,$  and  $1F$  respectively.

The modified continuant is:

$$\begin{vmatrix} 1 & 3 & 0 & 3 & 0 & 1 \\ -1 & s & 0 & 0 & 0 & 0 \\ 0 & 0 & 1 & 0 & 0 & 0 \\ 0 & -1 & 0 & s & 0 & 0 \\ 0 & 0 & 0 & 0 & 1 & 0 \\ 0 & 0 & 0 & -1 & 0 & s \end{vmatrix}$$

The first step in the transformation is to move the  $-1$  elements to positions just below the leading diagonal.

$$\begin{vmatrix} 1 & 3 & 0 & 3 & 0 & 1 \\ -1 & s & 0 & 0 & 0 & 0 \\ 0 & \textcircled{0} & 1 & 0 & 0 & 0 \\ 0 & -1 & 0 & s & 0 & 0 \\ 0 & 0 & 0 & \textcircled{0} & 1 & 0 \\ 0 & 0 & 0 & -1 & 0 & s \end{vmatrix} = \begin{vmatrix} 1 & 3 & 0 & 3 & 0 & 1 \\ -1 & s & 0 & 0 & 0 & 0 \\ 0 & -1 & 1 & 0 & 0 & 0 \\ 0 & \textcircled{-1} & 0 & s & 0 & 0 \\ 0 & 0 & 0 & -1 & 1 & 0 \\ 0 & 0 & 0 & \textcircled{-1} & 0 & s \end{vmatrix} = \begin{vmatrix} 1 & 3 & 0 & 3 & 0 & 1 \\ -1 & s & 0 & 0 & 0 & 0 \\ 0 & -1 & 1 & 0 & 0 & 0 \\ 0 & 0 & -1 & s & 0 & 0 \\ 0 & 0 & 0 & -1 & 1 & 0 \\ 0 & 0 & 0 & 0 & -1 & s \end{vmatrix}$$

The magnitudes of the elements of the leading diagonal are now adjusted to equal the desired values of the components.

Multiply column 1 by  $R_1$ , divide row 2 by  $R_1$ .

Multiply column 2 by  $C_1R_1$ , divide row 3 by  $C_1R_1$ .

Multiply column 3 by  $R_2C_1R_1$ , divide row 4 by this factor and continue until the penultimate column.

Having completed these steps, the determinant is now of the form:

$$\begin{vmatrix} 6 & 90 & 0 & 1080 & 0 & 1 \\ -1 & 5s & 0 & 0 & 0 & 0 \\ 0 & -1 & 4 & 0 & 0 & 0 \\ 0 & 0 & -1 & 3s & 0 & 0 \\ 0 & 0 & 0 & -1 & 2 & 0 \\ 0 & 0 & 0 & 0 & -1 & .00139s \end{vmatrix}$$

There now follows a repetitive cycle of four steps where each step may contain more than one operation.



Note that the final step of the last cycle is not performed.  
The last element in the first row is moved to the fifth row.

$$\begin{bmatrix} 6 & 1 & 0 & 0 & 0 & 1 \\ -1 & 5s & 1 & 0 & 0 & .4605s \\ 0 & -1 & 4 & 1 & 0 & 0 \\ 0 & 0 & -1 & 3s & 1 & .0222s \\ 0 & 0 & 0 & -1 & 2 & 0 \\ 0 & 0 & 0 & 0 & -1 & .00139s \end{bmatrix} = \begin{bmatrix} 6 & 1 & 0 & 0 & 0 & 0 \\ -1 & 5s & 1 & 0 & 0 & -4.54s \\ 0 & -1 & 4 & 1 & 0 & 0 \\ 0 & 0 & -1 & 3s & 1 & -2.98s \\ 0 & 0 & 0 & -1 & 2 & 1 \\ 0 & 0 & 0 & 0 & -1 & .00139s \end{bmatrix}$$

This final determinant is the continuant and because of the nature of the mathematical operations used in its derivation its value must equal the value of the recurrent, i.e.  $F(s)$ .

**4. Interpretation of the Continuant**

Nodal analysis of the circuit shown in Fig. 1 leads to the equations:

$$\begin{aligned} V_1 &= I_1 R_1 + V_2 \\ 0 &= -I_1 + sC_1 V_2 + I_2 && -A_1 sC_1 V_4 \\ 0 &= -V_2 + I_2 R_2 + V_3 \\ 0 &= -I_2 + sC_2 V_3 + I_3 && -A_2 sC_2 V_4 \\ 0 &= -V_3 + I_3 R_3 + V_4 \\ 0 &= -I_3 + (1 - A_3) sC_3 V_4 \end{aligned}$$

The matrix form of these equations is:

$$\begin{bmatrix} V_1 \\ 0 \\ 0 \\ 0 \\ 0 \\ 0 \end{bmatrix} = \begin{bmatrix} R_1 & 1 & 0 & 0 & 0 & 0 \\ -1 & sC_1 & 1 & 0 & 0 & -A_1 sC_1 \\ 0 & -1 & R_2 & 1 & 0 & 0 \\ 0 & 0 & -1 & sC_2 & 1 & -A_2 sC_2 \\ 0 & 0 & 0 & -1 & R_3 & 1 \\ 0 & 0 & 0 & 0 & -1 & (1 - A_3) sC_3 \end{bmatrix} \begin{bmatrix} I_1 \\ V_2 \\ I_2 \\ V_3 \\ I_3 \\ V_4 \end{bmatrix}$$

Solving this matrix equation gives:

$$\frac{V_1}{V_2} = F(s) = \begin{bmatrix} R_1 & 1 & 0 & 0 & 0 & 0 \\ -1 & sC_1 & 1 & 0 & 0 & -A_1 sC_1 \\ 0 & -1 & R_2 & 1 & 0 & 0 \\ 0 & 0 & -1 & sC_2 & 1 & -A_2 sC_2 \\ 0 & 0 & 0 & -1 & R_3 & 1 \\ 0 & 0 & 0 & 0 & -1 & (1 - A_3) sC_3 \end{bmatrix}$$

This determinant must therefore equal the continuant in value and it is of the same form. Thus comparison of their elements gives the values of the components in the network.

In the particular example of the binomial filter:

$$\begin{aligned} A_1 &= -(-4.54)/5 = 0.908 \\ A_2 &= -(-2.98)/3 = 0.993 \\ A_3 &= 1 - 0.00139 = 0.9986 \end{aligned}$$

The synthesized active circuit diagram is shown in Fig. 2. The 1F capacitor/ $A_3$  combination may be replaced by a single passive element of value 0.00139F but it was decided to preserve the symmetry of the circuit since this adjustment may be made at the end of the synthesis procedure.

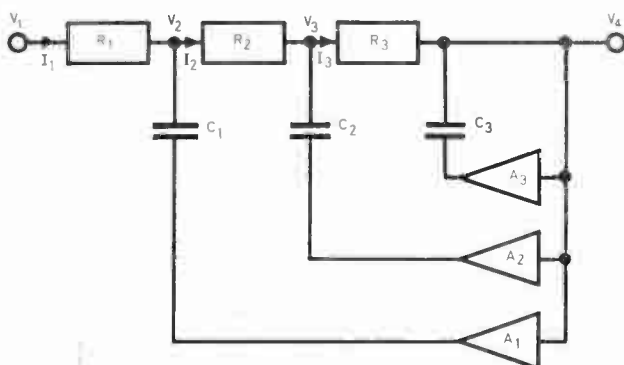


Fig. 1. Generalized third-order low-pass filter.

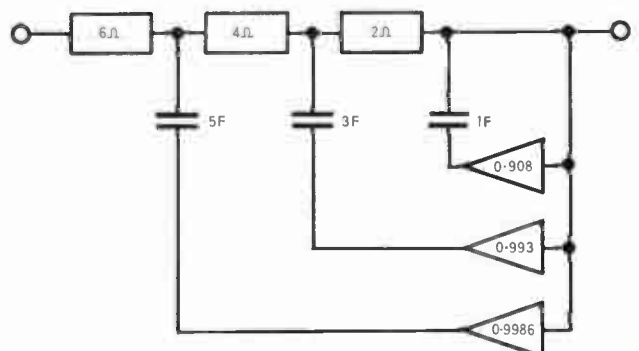


Fig. 2. Third-order binomial low-pass filter.

5. Transformation from Continuant to Recurrent

To illustrate this procedure, the gain of amplifier  $A_1$  is increased by 10%. The recurrent is now:

$$\begin{vmatrix} 6 & 1 & 0 & 0 & 0 & 0 \\ -1 & 5s & 1 & 0 & 0 & -4.994s \\ 0 & -1 & 4 & 1 & 0 & 0 \\ 0 & 0 & -1 & 3s & 1 & -2.98s \\ 0 & 0 & 0 & -1 & 2 & 1 \\ 0 & 0 & 0 & 0 & -1 & .00139s \end{vmatrix}$$

The element 1 in the 5th row, 6th column is moved to the first row.

$$\begin{vmatrix} 6 & 1 & 0 & 0 & 0 & 0 \\ -1 & 5s & 1 & 0 & 0 & -4.994s \\ 0 & -1 & 4 & 1 & 0 & 0 \\ 0 & 0 & -1 & 3s & 1 & -2.98s \\ 0 & 0 & 0 & -1 & 2 & \textcircled{1} \\ 0 & 0 & 0 & 0 & -1 & .00139s \end{vmatrix} = \begin{vmatrix} 6 & 1 & 0 & 0 & 0 & 1 \\ -1 & 5s & 1 & 0 & 0 & .0062s \\ 0 & -1 & 4 & 1 & 0 & 0 \\ 0 & 0 & -1 & 3s & 1 & .022s \\ 0 & 0 & 0 & -1 & 2 & 0 \\ 0 & 0 & 0 & 0 & -1 & .00139s \end{vmatrix}$$

A repetitive cycle consisting of four steps per cycle is performed.

1st cycle:

$$\begin{vmatrix} 6 & 1 & 0 & 0 & 0 & 1 \\ -1 & 5s & 1 & 0 & 0 & \textcircled{.0062s} \\ 0 & -1 & 4 & 1 & 0 & 0 \\ 0 & 0 & -1 & 3s & 1 & \textcircled{.022s} \\ 0 & 0 & 0 & -1 & 2 & 0 \\ 0 & 0 & 0 & 0 & -1 & .00139s \end{vmatrix} = \begin{vmatrix} 6 & 1 & 0 & 0 & 0 & 1 \\ -1 & 5s & 1 & 0 & \textcircled{4.46} & 0 \\ 0 & -1 & 4 & 1 & 0 & 0 \\ 0 & 0 & -1 & 3s & \textcircled{16.97} & 0 \\ 0 & 0 & 0 & -1 & 2 & 0 \\ 0 & 0 & 0 & 0 & -1 & .00139s \end{vmatrix}$$

$$\begin{aligned}
 &= \left[ \begin{array}{cccccc} 6 & 1 & 0 & 0 & 128.6 & 1 \\ -1 & 5s & 1 & 0 & 0 & 0 \\ 0 & -1 & 4 & 1 & 67.88 & 0 \\ 0 & 0 & -1 & 3s & 0 & 0 \\ 0 & 0 & 0 & -1 & 2 & 0 \\ 0 & 0 & 0 & 0 & -1 & .00139s \end{array} \right] = \left[ \begin{array}{cccccc} 6 & 1 & 0 & 64.29 & 0 & 1 \\ -1 & 5s & 1 & 0 & 0 & 0 \\ 0 & -1 & 4 & 34.94 & 0 & 0 \\ 0 & 0 & -1 & 3s & 0 & 0 \\ 0 & 0 & 0 & -1 & 2 & 0 \\ 0 & 0 & 0 & 0 & -1 & .00139s \end{array} \right]
 \end{aligned}$$

2nd cycle:

$$\begin{aligned}
 &= \left[ \begin{array}{cccccc} 6 & 1 & 0 & 99.24 & 0 & 1 \\ -1 & 5s & 1 & 174.7s & 0 & 0 \\ 0 & -1 & 4 & 0 & 0 & 0 \\ 0 & 0 & -1 & 3s & 0 & 0 \\ 0 & 0 & 0 & -1 & 2 & 0 \\ 0 & 0 & 0 & 0 & -1 & .00139s \end{array} \right] = \left[ \begin{array}{cccccc} 6 & 1 & 0 & 99.24 & 0 & 1 \\ -1 & 5s & 59.24 & 0 & 0 & 0 \\ 0 & -1 & 4 & 0 & 0 & 0 \\ 0 & 0 & -1 & 3s & 0 & 0 \\ 0 & 0 & 0 & -1 & 2 & 0 \\ 0 & 0 & 0 & 0 & -1 & .00139s \end{array} \right]
 \end{aligned}$$

$$\begin{aligned}
 &= \left[ \begin{array}{cccccc} 6 & 1 & 355.4 & 99.24 & 0 & 1 \\ -1 & 5s & 0 & 0 & 0 & 0 \\ 0 & -1 & 4 & 0 & 0 & 0 \\ 0 & 0 & -1 & 3s & 0 & 0 \\ 0 & 0 & 0 & -1 & 2 & 0 \\ 0 & 0 & 0 & 0 & -1 & .00139s \end{array} \right] = \left[ \begin{array}{cccccc} 6 & 89.86 & 0 & 99.24 & 0 & 1 \\ -1 & 5s & 0 & 0 & 0 & 0 \\ 0 & -1 & 4 & 0 & 0 & 0 \\ 0 & 0 & -1 & 3s & 0 & 0 \\ 0 & 0 & 0 & -1 & 2 & 0 \\ 0 & 0 & 0 & 0 & -1 & .00139s \end{array} \right]
 \end{aligned}$$

The last operation of the final cycle is not carried out.

The magnitudes of the elements in the leading diagonal are reduced to unity by repeatedly carrying out the sequence of dividing the  $n$ th row by the magnitude of the  $n$ th diagonal element and then multiplying the  $(n-1)$ th column by the same factor, starting with  $n = 6$  and finishing with  $n = 2$ .

$$\begin{vmatrix} 6 & 89.86 & 0 & 99.24 & 0 & 1 \\ -1 & 5s & 0 & 0 & 0 & 0 \\ 0 & -1 & 4 & 0 & 0 & 0 \\ 0 & 0 & -1 & 3s & 0 & 0 \\ 0 & 0 & 0 & -1 & 2 & 0 \\ 0 & 0 & 0 & 0 & -1 & .00139s \end{vmatrix} = \begin{vmatrix} 1.001 & 2.998 & 0 & .276 & 0 & 1 \\ -1 & s & 0 & 0 & 0 & 0 \\ 0 & -1 & 1 & 0 & 0 & 0 \\ 0 & 0 & -1 & s & 0 & 0 \\ 0 & 0 & 0 & -1 & 1 & 0 \\ 0 & 0 & 0 & 0 & -1 & s \end{vmatrix}$$

Finally to form the recurrent, the -1 elements are scattered by adding each odd column to its preceding column and then adding each odd row (except the first) to its following row.

$$\begin{vmatrix} 1.001 & 2.998 & 0 & .276 & 0 & 1 \\ -1 & s & 0 & 0 & 0 & 0 \\ 0 & \textcircled{-1} & 1 & 0 & 0 & 0 \\ 0 & 0 & -1 & s & 0 & 0 \\ 0 & 0 & 0 & \textcircled{-1} & 1 & 0 \\ 0 & 0 & 0 & 0 & -1 & s \end{vmatrix} = \begin{vmatrix} 1.001 & 2.998 & 0 & .276 & 0 & 1 \\ -1 & s & 0 & 0 & 0 & 0 \\ 0 & 0 & 1 & 0 & 0 & 0 \\ 0 & -1 & \textcircled{-1} & s & 0 & 0 \\ 0 & 0 & 0 & 0 & 1 & 0 \\ 0 & 0 & 0 & -1 & \textcircled{-1} & s \end{vmatrix}$$

$$= \begin{vmatrix} 1.001 & 2.998 & 0 & .276 & 0 & 1 \\ -1 & s & 0 & 0 & 0 & 0 \\ 0 & 0 & 1 & 0 & 0 & 0 \\ 0 & -1 & 0 & s & 0 & 0 \\ 0 & 0 & 0 & 0 & 1 & 0 \\ 0 & 0 & 0 & -1 & 0 & s \end{vmatrix}$$

The elements in row 1 of the recurrent indicate that the modified network has the reciprocal transfer function:

$$F(s) = 1.001s^3 + 2.998s^2 + 0.276s + 1$$

**6. Applications**

Although the examples in this paper were concerned with a 3rd-order filter, the principles of analysis and synthesis outlined above may readily be extended to any order of filter.

The following procedures have been written in *Algol 60*:

- RECCON, which carries out the recurrent to continuant transformation for any specified order of filter;
- CONREC, which performs the continuant to recurrent transformation;
- CONMAT, which lists the elements of the continuant;
- RECMAT, which lists the elements of the recurrent;
- CIRCUIT, which uses the elements of the continuant to draw the circuit diagram on a digital plotter.

The examples considered in this paper were also presented to the computer in the following way. The input data tape contained the order of the transfer function, the coefficients of the transfer function and the relative values of the *RC* components. A program was written to print out the reciprocal of the transfer function and to form the recurrent in an array. The procedures RECMAT, RECCON, CONMAT and CIRCUIT were called upon and the computer outputs confirmed the results obtained earlier.

The gain of one amplifier was increased 10% by multiplying by 1.1 the element in the second row, final column of the array storing the continuant. Procedures CONMAT, CIRCUIT, CONREC and RECMAT were called upon and the computer outputs agreed with the results already obtained. Finally the modified reciprocal transfer function was printed out from the elements of row 1 of the recurrent.

This test program indicates the main application of the recurrent-continuant synthesis and analysis technique. The logical nature of the procedures enables them to be performed rapidly and accurately by computer. The problem of synthesizing and then analysing the performance of a circuit when its component values vary becomes no more difficult for a tenth-order filter than for a first-order filter.

The program is to be extended in two ways. An optimization procedure is to be written which would allow the relative values of the components to be varied to obtain the greatest circuit stability. A second procedure is required to plot the frequency response of the desired circuit having optimum component values together with the frequency responses obtained when the components in the circuit are allowed to vary from their optimum values by specified amounts. It is hoped that the results of this work will be published later.

## 7. Acknowledgments

The author would like to thank Dr. G. G. Bloodworth and Mr. J. G. Holbrook of the University of Southampton for their assistance in this work and for checking the literal and technical accuracy of the manuscript.

## 8. References

1. Holbrook, James G., 'The recurrent-continuant method of transfer function synthesis', *The Radio and Electronic Engineer*, **38**, No. 2, pp. 73-9, August 1969.
2. Holbrook, James G., 'Laplace Transforms for Electronic Engineers', 2nd edn. (Pergamon, New York and London, 1966).

*Manuscript first received by the Institution on 22nd June 1970 and in revised form on 22nd September 1970. (Paper No. 1366/CC 97.)*

© The Institution of Electronic and Radio Engineers, 1971

# A Computer Controlled Test System for Digital Equipment

By

**C. CLARKE,**

B.Sc., C.Eng., M.I.E.E.†

*Reprinted from the Proceedings of the Conference on Automatic Test Systems held in Birmingham from 14th to 17th April 1970*

This paper describes the requirements of digital equipment testing and describes a test system, controlled by a digital computer, capable of testing a wide variety of digital equipment.

## 1. Introduction. Test Requirements

In order to clarify the description of the test system it is first necessary to define the term digital equipment, as understood in the paper, and the properties which require testing. For test purposes a digital equipment can be considered to have all input and output terminals that are accessible during testing, operating in a binary digital manner, that is with two possible voltage levels only. It is convenient to adopt the convention that the most positive voltage level is called one and the most negative level is called zero. The state of all input or output terminals at any one time can then be simply described by a multi-digit binary number, or pattern, each digit corresponding to a particular terminal.

### 1.1. Logic Function Tests

The main feature of digital testing is truth table checking, that is verification that the output binary pattern is correct for each of a succession of input patterns. The output terminals do not reach their correct state immediately the input pattern is changed. Dependent on the complexity of the unit under test, there is always a finite time before the correct output is obtained. The verification of this time delay is the basis of 'logic speed' testing. With many types of digital units the output pattern is unchanging after its initial settling time, however some devices such as pulse generators may have an output intentionally time-dependent; furthermore, some units may require a succession of input patterns to be applied in a predetermined time sequence before performance can be verified. A further property requiring checking in some cases is the tendency for incorrect output to occur transiently at a terminal where the output should not change state when the input pattern is changed.

### 1.2. Voltage Level Testing

To ensure full interchangeability of digital units, in addition to the properties already described, it is necessary to verify the electrical values of the signals at each input and output. Each input must behave correctly with limit values of voltage while the currents at either voltage level must be below the required maximum. Similarly, the voltages produced at each output must have satisfactory values at a defined maximum value of load.

### 1.3. Intermittent Fault Detection

In many applications of digital equipment intermittent faults of very short duration can have a serious effect on performance. To ensure a satisfactory freedom from

such faults it is necessary to repeat many times the complete cycle of tests on the unit, each test being defined as the verification of the response of the unit under test to a particular input pattern. It can be shown that, to obtain a given degree of confidence that intermittent faults of specified form are not present, the test cycle should be repeated for a time, which is inversely proportional to the percentage of the test cycle time for which the fault is detectable. Since any particular defect is only detectable by some of the tests in the complete cycle, it follows that the verification of correct functioning of a unit under test should be performed with the smallest number of tests which will check all performance features.

### 1.4. Diagnosis of Faults

The set of tests sufficient to verify correct performance is usually insufficient for satisfactory fault diagnosis, therefore additional tests are needed. For any given total test period the performance of unnecessary diagnostic tests will reduce the test assurance in respect of intermittent faults for the reasons already given. It follows that a testing system must have some decision making capability in order that diagnostic tests are performed only when required.

The required decision making capability in an automatic test system is most economically obtained by the use of a digital computer as a control device. At the same time, the core store of the computer provides a rapid access storage medium for test data, permitting the test cycle rate necessary for intermittent fault detection.

## 2. Test Machine Realization

### 2.1. System Hardware

Figure 1 is a simplified block diagram of the complete system hardware. The tape reader is used for feeding test data to the computer. The printer records fault

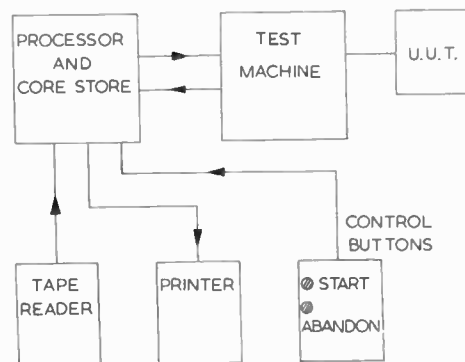


Fig. 1. System block diagram.

† Research Division, The Marconi Company Ltd., Chelmsford.

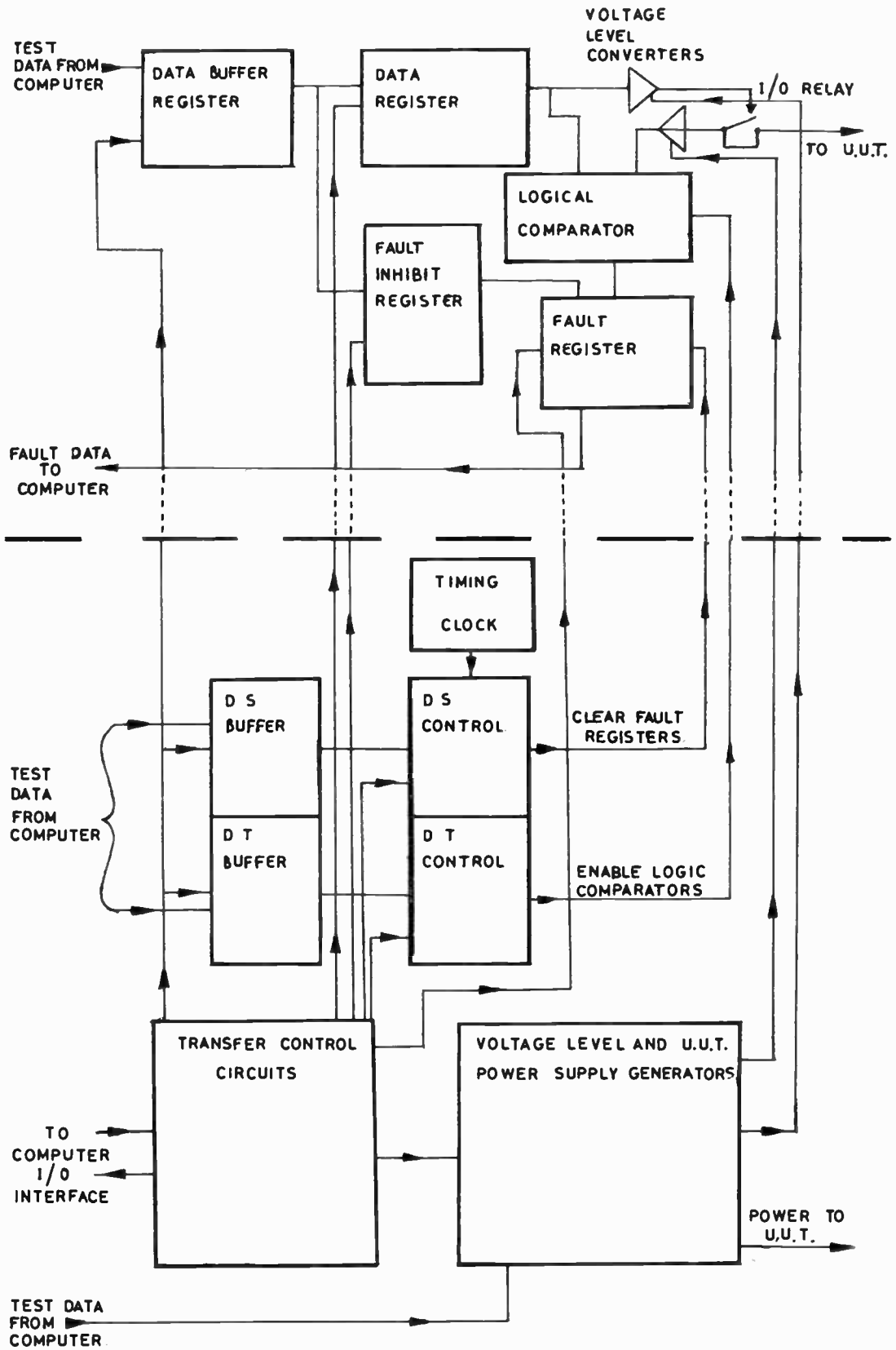


Fig. 2. Simplified block diagram of test machine.

data or tests passed. The control buttons allow the operator to initiate testing when a unit under test, hereafter abbreviated to u.u.t., is connected, or to cause any unit test sequence to be abandoned.

## 2.2. Test Equipment

Figure 2 is a simplified diagram of the test equipment which, under control from the computer, generates the stimuli required for the u.u.t. and verifies the responses.

Above the horizontal dotted line in Fig. 2 is the equipment repeated for each test channel of the machine, one channel being required for each tested terminal of the u.u.t. Below the dotted line is that part of the test machine common to all channels.

## 2.3. Basic Test Technique

Referring to Fig. 2, the data register which has one bit per channel, holds both the input and output binary patterns. A channel connected to an input terminal of the u.u.t. holds one bit of the input pattern whilst a channel connected to an output terminal holds one bit of the output pattern.

A channel connected to an input terminal of the u.u.t. has its input/output relay contacts closed, thus allowing the input pattern at voltage levels set by the voltage level converters to be applied to the u.u.t.

The u.u.t. terminal (either input or output) is connected permanently to a logical comparator whose other input is obtained from the corresponding bit of the data register. The comparator is a NOT EQUIVALENT circuit which provides a setting signal for the corresponding bit of the fault register whenever the state of the u.u.t. terminal differs from that of the data register bit. Each comparator is controlled by an enable/inhibit line whose function will be described later.

The fault register and comparator combination provides a means for detecting and storing fault data both for intermittent and continuous faults until the computer has been able to make the necessary fault records.

By combining the outputs from the fault register in one OR gate (not shown in Fig. 2), the computer may be interrupted on the occurrence of a faulty output on any channel. Whenever the computer responds to the interrupt and reads the state of the fault register, a record of all faults in that test is obtained. Compared with systems in which u.u.t. outputs are first read into the computer and then checked by software means, this technique permits an enormous increase in the percentage of test time available for fault detection. From the time that the test conditions are set up, until the next test is started, faults can be detected, whereas with direct transfer of output data, faults are only detectable if present during the actual transfer. Depending on the type of computer used, transfers may take as little as 50 nanoseconds, in a test duration, including the set-up time, of 100 microseconds or more.

## 2.4. Response Time Testing

To increase further the percentage of test time available for fault detection and to make response time measurement possible, the test data from the computer are

transferred to a buffer register, equal in length to the test data register. The buffer register permits data for a test to be assembled by the computer without the need to terminate the previous test. The test set-up time due to the test system is thus reduced, from the time for a number of computer output operations, to the time for transfer from the buffer to the data register.

Following transfer from the buffer to the data register the u.u.t. will require a finite time to respond to the new stimuli. During this period the comparator will in general give a fault indication even with a good u.u.t. It is therefore necessary to suppress fault indication for this period. It is also necessary to clear the fault register of previous faults, which will have already been recorded by the computer. Both operations are combined by holding the fault register in a clear state for the required period following the transfer between the data and buffer registers. The duration of the settling period, conveniently called DS, is generated by a programmable delay such as a timing clock and counter as indicated in Fig. 2.

It is frequently the case that the response time of the u.u.t. is not the same for each test. For this reason the data buffer register must be extended to include a section to hold the DS until it is required. Should the value of DS be zero on transfer to the data register the fault register will not be cleared at all. This feature is essential in order to test for the absence of spurious output pulses at output terminals whose state is not expected to change as a result of the input change.

## 2.5. Selective Test Inhibition

It is often the case that some output terminals of the u.u.t. will have different response times and some may produce trains of pulses. Since the same value of DS applies to all output terminals some outputs may change state quite correctly but result in a spurious fault indication. To prevent the occurrence of such spurious faults an inhibit register is provided (see Fig. 2). The inhibit register is of the same length as the data register, i.e. one bit per channel, and is arranged so that when any bit is set the corresponding bit of the fault register is held clear, thus excluding the connected output terminal of the u.u.t. from testing until the appropriate inhibit register bit is cleared.

The state of the inhibit register must be set before the initiation of a test by data transfer to the data register. Furthermore, the inhibit register should not change during a test. The inhibit register is therefore buffered by the same buffer register used for truth table data.

## 2.6. Transient Output Requirements

In order to test time dependent outputs from the u.u.t., it is necessary to be able to inhibit fault indications at a defined time after the start of a testing period without clearing the fault register. Therefore following the DS period we have the programmable duration of test period, conveniently called DT, during which an output from the comparator is able to set the corresponding fault register bit. The DT period is defined as lasting from the end of the DS period until it is terminated by its own timing counter (see Fig. 2). As in the case of

DS, the DT generator also requires its time data to be buffered.

There are two types of DT controlling data that may be output from the computer, namely 'continuous' and 'time'. One of the possible bit patterns in the DT register is allocated to the 'continuous' condition. All other patterns form digital representations of the DT period. The continuous mode of operation, which is used whenever possible, causes the DT period to be terminated only by the next DS period at the start of the next test. In this way the test cycle rate is maximized whilst still maintaining a high percentage of total time available for fault detection. In the 'time' mode of operation, the DT delay circuit alone determines the period during which fault information can be set into the fault register. Depending upon the programmed values of DS and DT, either the cycle rate of testing will be below that of which the computer is capable, or the percentage of time used for fault detection will be reduced. A defined time value for DT is only required, in conjunction with a suitable value for DS, when it is necessary to test an output with a time varying digital waveform.

### 2.7. Logic Voltage Levels

In order to cater for differing voltage levels in different types of u.u.t. it will be seen from Fig. 2 that the input from the data register to the u.u.t. and the output from the u.u.t. to the logical comparator are passed through controllable level converters. The converter in the input line requires two programmable level references to set both the one and zero logic voltage levels. These can of course be programmed near to the limit values for the u.u.t. to check that the input switching threshold levels are satisfactory.

The converter in the output line from the u.u.t. requires only one programmable reference level, an

output voltage above this level giving a one to the comparator and below the reference level a zero. The adequacy of the output can be checked by programming this reference near to each of the limit values for the u.u.t. in turn.

### 2.8. Multiple Transition Stimuli

The machine as described so far is suitable for verifying the response to a single input pattern, even though the response may contain time dependent functions. In some cases this is not sufficient and changes of input must be made at defined intervals. When the required test rate is lower than the computer output rate, then software control is adequate. This is not usually the case. For example, if a u.u.t. can respond to both leading and trailing edges of an input pulse and it is required to verify both responses with the minimum pulse length, then two tests must be performed separated in time by a period equal to the pulse length. For a pair of tests the data must be stored in two buffer registers and in fact for a group of  $n$  tests there must be a total of  $n$  buffer registers. Each register includes both truth table data and DS and DT time data.

To perform a group of tests the buffers are loaded by the computer with the full test data for each test and the first data transfer is initiated; subsequent data transfers from the set of buffers follow at the end of the DT period for each test.

### 3. Acknowledgment

The author wishes to thank The Marconi Company for permission to publish this paper.

*Manuscript first received by the Institution on 20th February 1970 and in final form on 26th October 1970. (Paper No. 1367/Comp. 133.)*

© The Institution of Electronic and Radio Engineers 1971

# Efficiency of the Two-Frequency M.T.I. System

By

**J. KROSZCZYŃSKI,**

Dr.habil.Eng.†

Efficiency of the two-frequency moving target indication (m.t.i.) radar system is considered under the assumption that the echo and clutter signals are stochastic processes, and clutter spectrum is Doppler-shifted. Single and double cancellation circuits are investigated. The analysis indicates a fairly good tolerance of the system efficiency to clutter drift, especially when double cancellation is used.

## 1. Introduction

In many radar systems there is a need for effective cancelling of moving clutter. In such a case, the clutter spectrum is Doppler-shifted, which may seriously degrade the efficiency of m.t.i. operation,<sup>1</sup> unless some means for overcoming this effect are used.

Various methods have been devised in the past for this purpose, e.g. adding a correcting frequency to the coho output; the non-coherent method; 'clutter locking'; but as the result of the inherent limitations and drawbacks of these schemes, the problem still seems to remain not satisfactorily solved.<sup>2-4</sup>

As another approach, the two-frequency m.t.i. system has been proposed occasionally in the last few years. In this, the target is illuminated simultaneously at two radio frequencies and two coherent receivers are interconnected so as to produce an output dependent on the phase difference between the received signals at the two frequencies.<sup>3,4</sup> The two-frequency m.t.i. system is slightly less efficient than the optimum one in the case of stationary clutter,<sup>5</sup> but it is relatively immune to degradation from clutter motion. A basic theory of this method was published previously for the case of non-fluctuating echo and clutter signals.<sup>6</sup> In this paper, a more general consideration of the two frequency m.t.i. system is presented, based on the assumption that the echo and clutter signals may be represented by appropriate stochastic processes. As far as is known to the author, such an analysis has not as yet appeared in the available literature.

## 2. System Theory

Consider a radar transmitter, emitting coherent signals at two different carrier frequencies  $f_1$  and  $f_2$ . Signals appearing at the input of the first receiving channel may be written as:<sup>7</sup>

$$V_1 = U_{1c}(t) \cos(\alpha_e \omega_1 t + \varphi_{1t}) + U_{1s}(t) \sin(\alpha_e \omega_1 t + \varphi_{1t}) + Z_{1c}(t) \cos(\alpha_z \omega_1 t + \varphi_{1t}) + Z_{1s}(t) \sin(\alpha_z \omega_1 t + \varphi_{1t}) \quad \dots (1)$$

where  $U_{1c}(t)$ ,  $U_{1s}(t)$  are zero-mean Gaussian stochastic processes, representing signal echo fluctuations in the first channel;  $\alpha_e = 1 + v_e/c \approx 1 + 2v_e/c$ , where  $v_e$  is the radial target velocity and  $c$  is the velocity of wave propagation;  $\varphi_{1t}$  stands for the initial transmitter phase in channel 1;  $Z_{1c}(t)$ ,  $Z_{1s}(t)$  are zero-mean Gaussian stochastic processes representing clutter fluctuations in the first receiving channel;  $\alpha_z = 1 + v_z/c \approx 1 + 2v_z/c$ , where  $v_z$  is the radial clutter drift velocity;  $\omega_1 = 2\pi f_1$ ;  $\omega_2 = 2\pi f_2$ . Similarly, the signal received by the second channel is:

$$V_2 = U_{2c}(t) \cos(\alpha_e \omega_2 t + \varphi_{2t}) + U_{2s}(t) \sin(\alpha_e \omega_2 t + \varphi_{2t}) + Z_{2c}(t) \cos(\alpha_z \omega_2 t + \varphi_{2t}) + Z_{2s}(t) \sin(\alpha_z \omega_2 t + \varphi_{2t}) \quad \dots (2)$$

The beat signal, obtained at the output of a narrow-band multiplicative mixer‡ having  $V_1$  and  $V_2$  as the inputs, is given by:

$$V_b = \frac{1}{2} \{ [U_{1c}(t)U_{2c}(t) + U_{1s}(t)U_{2s}(t)] \cos[\alpha_e(\omega_1 - \omega_2)t + \varphi_t] + [U_{1s}(t)U_{2c}(t) - U_{1c}(t)U_{2s}(t)] \sin[\alpha_e(\omega_1 - \omega_2)t + \varphi_t] + [U_{1c}(t)Z_{2c}(t) + U_{1s}(t)Z_{2s}(t)] \cos[(\alpha_e \omega_1 - \alpha_z \omega_2)t + \varphi_t] + [U_{1s}(t)Z_{2c}(t) - U_{1c}(t)Z_{2s}(t)] \sin[(\alpha_e \omega_1 - \alpha_z \omega_2)t + \varphi_t] + [U_{2c}(t)Z_{1c}(t) + U_{2s}(t)Z_{1s}(t)] \cos[(\alpha_z \omega_1 - \alpha_e \omega_2)t + \varphi_t] + [U_{2c}(t)Z_{1s}(t) - U_{2s}(t)Z_{1c}(t)] \sin[(\alpha_z \omega_1 - \alpha_e \omega_2)t + \varphi_t] + [Z_{1c}(t)Z_{2c}(t) + Z_{1s}(t)Z_{2s}(t)] \cos[\alpha_z(\omega_1 - \omega_2)t + \varphi_t] + [Z_{1s}(t)Z_{2c}(t) - Z_{1c}(t)Z_{2s}(t)] \sin[\alpha_z(\omega_1 - \omega_2)t + \varphi_t] \} \quad \dots (3)$$

where  $\varphi_t = \varphi_{1t} - \varphi_{2t}$ . To obtain the autocorrelation function of  $V_b$ , which will be denoted  $R\{V_b\}$ , the following equations (resulting from the properties of narrow-band processes) are useful:

† Przemysłowy Instytut Telekomunikacji, Warsaw, Poland.

‡ The pass-band is centred around the difference frequency  $f_1 - f_2$ .

$$R\{U_{1c}\} = R\{U_{1s}\} = R\{U_1\} \quad \dots\dots(4a)$$

$$R\{U_{2c}\} = R\{U_{2s}\} = R\{U_2\} \quad \dots\dots(4b)$$

$$R\{Z_{1c}\} = R\{Z_{1s}\} = R\{Z_1\} \quad \dots\dots(4c)$$

$$R\{Z_{2c}\} = R\{Z_{2s}\} = R\{Z_2\} \quad \dots\dots(4d)$$

As a further result from the theory of narrow-band stochastic processes, it may be noted that  $U_{1c}$  and  $U_{1s}$  are uncorrelated; the same is valid for  $U_{2c}$  and  $U_{2s}$ ;  $Z_{1c}$  and  $Z_{1s}$ ;  $Z_{2c}$  and  $Z_{2s}$ .<sup>7</sup>

For determining the possibility of detecting the signal among the clutter, the ratio

$$g = \frac{\text{average power at the output when signal present}}{\text{average power at the output when signal absent}} \quad \dots\dots(11)$$

will be computed.

For the single-delay-line canceller, it follows from (10) that:

$$g_1 = \frac{[R_e(0) + R_z(0)]^2 - R_e^2(T) \cos \Delta\omega_e^D T - R_e(T)R_z(T)[\cos(\omega_{1e}^D - \omega_{2z}^D)T + \cos(\omega_{1z}^D - \omega_{2e}^D)T] - R_z^2(T) \cos \Delta\omega_z^D T}{R_z^2(0) - R_z^2(T) \cos \Delta\omega_z^D T} \quad (12)$$

In most practical applications, both channels are identical, and it can be assumed that:

$$R\{U_1\} = R\{U_2\} = R_e \quad \dots\dots(5a)$$

$$R\{Z_1\} = R\{Z_2\} = R_z \quad \dots\dots(5b)$$

As the target and clutter signals are statistically independent, their cross-correlation functions vanish. The difference  $f_1 - f_2$  is in most practical cases sufficiently great to allow the target echo signals in both channels to be regarded as virtually uncorrelated; the same applies for the clutter.<sup>4</sup>

For statistically independent stochastic processes, there is:<sup>8</sup>

$$R\{X(t) \cdot Y(t)\} = R\{X(t)\} \cdot R\{Y(t)\} \quad \dots\dots(6)$$

Taking into account eqns. (3)–(6), the autocorrelation function of  $V_b$  may be obtained:

$$R\{V_b\} = R_e^2(\tau) \cos[\alpha_e(\omega_1 - \omega_2)\tau] + R_e(\tau)R_z(\tau) \cos[(\alpha_e\omega_1 - \alpha_z\omega_2)\tau] + R_e(\tau)R_z(\tau) \cos[(\alpha_z\omega_1 - \alpha_e\omega_2)\tau] + R_z^2(\tau) \cos[\alpha_z(\omega_1 - \omega_2)\tau] \quad \dots\dots(7)$$

With the knowledge of the autocorrelation function  $R\{V_b\}$ , average power at the output of the periodic filter (which follows the mixer) can be easily derived. It can be shown<sup>9</sup> that average power at the output of a single-subtraction delay-line canceller is simply:

$$P_1 = 2[R_{in}(0) - R_{in}(T)] \quad \dots\dots(8)$$

where  $R_{in}$  denotes the autocorrelation function of the input signal and  $T$  is the delay time. For the double-subtraction circuit, we have:<sup>9</sup>

$$P_2 = 2[3R_{in}(0) - 4R_{in}(T) + R_{in}(2T)] \quad \dots\dots(9)$$

In our case,  $R_{in} = R\{V_b\}$ ; remembering that for the i.f. cancellation there must be  $(\omega_1 - \omega_2)T = n \cdot 2\pi$ , where  $n = \text{an integer}$ , we may write:

$$P_1 = 2\{R_e^2(0) - R_e^2(T) \cos[v_e(\omega_1 - \omega_2)T] + 2R_e(0)R_z(0) - R_e(T)R_z(T)[\cos(v_e\omega_1 - v_z\omega_2)T + \cos(v_z\omega_1 - v_e\omega_2)T] + R_z^2(0) - R_z^2(T) \cos[v_z(\omega_1 - \omega_2)T]\} \dots\dots(10)$$

where

$\Delta\omega_e^D = v_e(\omega_1 - \omega_2)$  differential Doppler frequency for the signal;

$\omega_{1e}^D = v_e\omega_1$  Doppler frequency for the signal in the first channel;

$\omega_{2e}^D = v_e\omega_2$  Doppler frequency for the signal in the second channel;

$\Delta\omega_z^D = v_z(\omega_1 - \omega_2)$  differential Doppler frequency for the clutter;

$\omega_{1z}^D = v_z\omega_1$  Doppler frequency for the clutter in the first channel;

$\omega_{2z}^D = v_z\omega_2$  Doppler frequency for the clutter in the second channel.

A similar expression for the double-delay canceller may be obtained, using eqns. (7) and (9):

$$g_2 = (3[R_e(0) + R_z(0)]^2 - 4\{R_e^2(T) \cos \Delta\omega_e^D + R_e(T)R_z(T)[\cos(\omega_{1e}^D - \omega_{2z}^D)T + \cos(\omega_{1z}^D - \omega_{2e}^D)T] + R_z^2(T) \cos \Delta\omega_z^D T\} + R_e^2(2T) \cos 2\Delta\omega_e^D T + R_e(2T)R_z(2T) \times [\cos 2(\omega_{1e}^D - \omega_{2z}^D)T + \cos 2(\omega_{1z}^D - \omega_{2e}^D)T] + R_z^2(2T) \cos 2\Delta\omega_z^D T) / [3R_z^2(0) - 4R_z^2(T) \cos \Delta\omega_z^D T + R_z^2(2T) \cos 2\Delta\omega_z^D T] \dots(13)$$

The above considerations were formulated as if a c.w. transmitter would be used, but it is easy to see that for coherent carrier waves similar results are obtained for a train of short pulses having the recurrence frequency equal to  $1/T$ .

### 3. System Characteristics

It seems appropriate to compare the equations obtained above with the results derived earlier for the simpler case of non-fluctuating signals.<sup>6</sup> Taking similar assumptions, it may be written:  $R(2T) = R(T) = R(0) = U^2$ . Using the equality  $2 \sin^2 x = 1 - \cos 2x$ , eqn. (12) can be in this special case written in the form:

$$G_1(\alpha; \beta; \gamma) = \frac{\sqrt{\sin^2 \alpha + \gamma^2 [\sin^2(\omega_{1e}^D - \omega_{2z}^D)T/2 + \sin^2(\omega_{1z}^D - \omega_{2e}^D)T/2]} + \gamma^4 \sin^2 \beta}{\gamma^2 \sin \beta} \quad \dots\dots(14)$$

where  $\alpha = \Delta\omega_c^D T/2$ ;  $\beta = \Delta\omega_z^D T/2$ ;  $\gamma = U_z/U_c$ . This equation is identical with its equivalent in ref. 6. A similar result may be obtained for the double subtraction canceller, using the equality  $8 \sin^4 x = 3 - 4 \cos 2x + \cos 4x$ :

$$G_2(\alpha; \beta; \gamma) = \frac{\sqrt{\sin^4 \alpha + \gamma^2 [\sin^4 (\omega_{1c}^D - \omega_{2c}^D)T/2 + \sin^4 (\omega_{1z}^D - \omega_{2z}^D)T/2]} + \gamma^4 \sin^4 \beta}{\gamma^2 \sin^2 \beta} \dots\dots(15)$$

This again is identical with its counterpart in ref. 6. Figure 1 shows  $G_2(\alpha; \beta; \gamma)$  for  $\gamma = 100$  and  $\beta = 1, 2, \dots, 5^\circ$ .

To evaluate system performance in the case of fluctuating signal and clutter, the averaged (over all possible and equiprobable radial velocities)  $g$  function will be determined first. An appropriate expression is easy to obtain, assuming an uniform echo spectrum (which corresponds to the assumption  $R_c/nT = 0$ , where  $n$  is an integer). For the single-subtraction canceller, then:

$$|g_1|_{av} = \frac{R_c^2(0) + 2R_c(0)R_z(0) + R_z^2(0) - R_z^2(T) \cos \Delta\omega_z^D T}{R_z^2(0) - R_z^2(T) \cos \Delta\omega_z^D T} \dots\dots(16)$$

It may be noted that  $2[R_z^2(0) - R_z^2(T) \cos \Delta\omega_z^D T]$  is the average power of the uncanceled clutter residue at the output of the subtraction circuit.<sup>1, 9</sup> In practice, in most cases  $R_z(0) \gg R_c(0)$ , and an approximate equation may be used:

$$|g_1|_{av} \simeq 4 \frac{R_c(0)}{R_z(0)} \cdot CA_{1D} + 1 = 4 \frac{CA_{1D}}{\bar{\gamma}^2} + 1 \dots(17)$$

where

$$CA_{1D} = \frac{0.5}{1 - \frac{R_z(T)}{R_z(0)} \cos \Delta\omega_z^D T} \dots\dots(18)$$

is the clutter attenuation in single-subtraction canceller for moving clutter, taken for a differential Doppler shift,<sup>1</sup> and

$$\bar{\gamma} = \sqrt{R_z(0)/R_c(0)} \dots\dots(19)$$

For the double-subtraction circuit, we have:

$$|g_2|_{av} = \frac{3[R_c(0) + R_z(0)]^2 - 4R_z^2(T) \cos \Delta\omega_z^D T + R_z^2(2T) \cos 2\Delta\omega_z^D T}{3R_z^D(0) - 4R_z^2(T) \cos \Delta\omega_z^D T + R_z^2(2T) \cos 2\Delta\omega_z^D T} \dots\dots(20)$$

and

$$|g_2|_{av} \simeq 12 \frac{R_c(0)}{R_z(0)} CA_{2D} + 1 = 12 \frac{CA_{2D}}{\bar{\gamma}^2} + 1 \dots(21)$$

Figure 2 shows  $|g_2|_{av}$  as the function of  $\beta = \Delta\omega_z^D T/2$ , for  $R_z(nT) = R_z(0) \exp(-sn^2)$  and  $R_z(0)/R_c(0) = 100$ .

Equations (17) and (21) convey a simple interpretation of the results obtained: to secure detection, the attenuation of moving clutter must be greater than the clutter-to-signal average power ratio at the system input. Because the clutter attenuation in a double-subtraction canceller is usually much greater than in a simple one, the double canceller gives theoretically much better results.

To illustrate better the characteristics of the two-frequency m.t.i. system, a following case was considered: the radar antenna has a Gaussian beam shape, with 10 pulses per beamwidth; target echo fluctuates from scan to scan, but may be considered as fully correlated during

each scan;  $R_z$  is Gaussian in shape, and the spectrum of clutter fluctuations has the same width as the spectrum resulting from antenna scanning alone. As it follows from the assumptions listed above (see ref. 10, Chapter 7

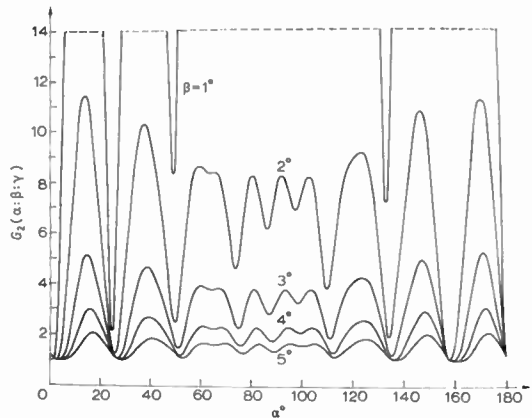


Fig. 1. The characteristics of a double-subtraction two-frequency m.t.i. system for non-fluctuating signal and clutter,  $\gamma = 100$ ,  $\omega_2/\omega_1 = 7/8$ .

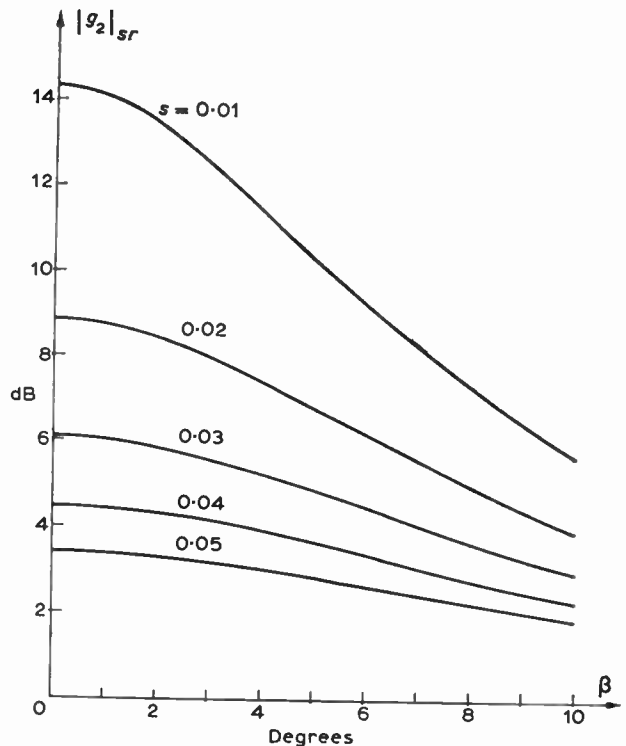


Fig. 2. The  $|g_2|_{av}$  function for  $R_z(nT) = R_z(0) \exp(-sn^2)$  and  $R_z(0)/R_c(0) = 100$ .

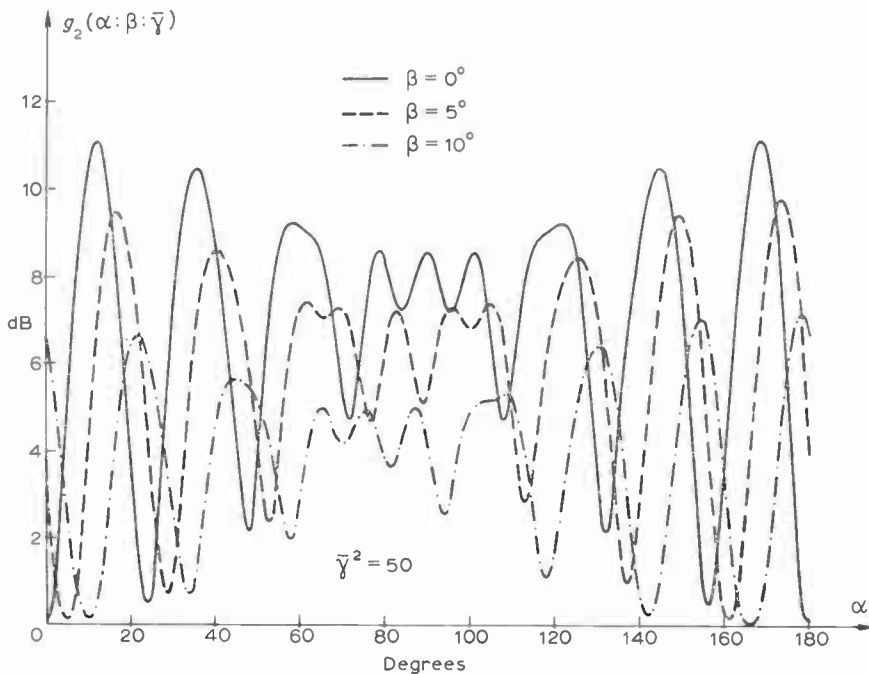


Fig. 3. The characteristics of a double-subtraction two-frequency m.t.i. system for fluctuating signal and clutter ( $R_c$  and  $R_z$  according to eqn. (20)),  $\bar{\gamma}^2 = 50$ ,  $\omega_2/\omega_1 = 7/8$ .

and Appendix 6), in this case:

$$R_c(nT) = R_c(0) \exp(-0.0171n^2) \dots\dots(22a)$$

$$R_z(nT) = R_z(0) \exp(-0.0342n^2) \dots\dots(22b)$$

Figure 3 gives the results of computations performed on the basis of eqn. (13), for  $\bar{\gamma}^2 = 50$  and  $\beta = 0^\circ; 5^\circ; 10^\circ$ . Figure 3 shows that for the two-frequency m.t.i. system described above, there is only a relatively small diminishing of the detection performance for  $\beta = 5^\circ$ , and even for  $\beta = 10^\circ$  signals could be fairly well detected in the clutter. These values of  $\beta$  would correspond—for a p.r.f. of 500 Hz and  $f_1 - f_2 = 100$  MHz—to clutter drift speeds of 80 and 160 km/h and 100 miles/h, respectively. It is evident<sup>1</sup> that such clutter drift speeds would render the single-channel uncompensated m.t.i. systems in the L, S, C or X bands completely useless.

**4. Conclusions**

The two-frequency m.t.i. system appears to be fairly tolerant to clutter drift effect; the analysis shows indeed that in the case of fluctuating clutter this system seems to be relatively more immune to Doppler shift of the clutter spectrum than in the case of non-fluctuating passive interference. This can be explained using Fig. 2, where relatively flat maxima may be observed. Comparing Fig. 1 and Fig. 3 leads to similar conclusions. A corollary from Figs. 1 and 3 is that targets cannot be detected in clutter having the same radial velocity as the target; this is in agreement with simple physical reasoning. Finally, it may be concluded that the double-subtraction canceller shows a distinct advantage over the single-subtraction one.

**5. Acknowledgments**

Acknowledgments are due to the Management of the P.I.T. for permission to publish this paper, and to Mrs. B. Mazurek, who programmed the computer.

**6. References**

1. Kroszczyński, J., 'Efficiency of attenuation of moving clutter', *The Radio and Electronic Engineer*, 34, No. 3, pp. 157-9, September 1967.
2. Skolnik, M. I., 'Introduction to Radar Systems', (McGraw-Hill, New York, 1962).
3. Bradsell, P., 'Moving Target Indication—A Survey of Developments since 1948', 8th AGARD Avionics Panel Symposium, September 1964. Published in: Blackband, W.T., 'Radar Techniques for Detection, Tracking and Navigation', (Gordon and Breach, New York and London, 1966).
4. Drushynin, W. W., *et al.*, 'Spravotchnik po Osnovam Radiolokatsyonnoy Tekhniki', (Handbook on the Fundamentals of Radiolocation Technique), (Moscow 1967).
5. Tartakowskij, G. P., *et al.*, 'Woprosy Statisticheskoy Teorii Radiolokatsyi', (Problems of the Statistical Radiolocation Theory), Vol. I, Chap. 4.11.6, (Moscow 1963).
6. Kroszczyński, J., 'The two-frequency m.t.i. system', *The Radio and Electronic Engineer*, 39, No. 3, pp. 172-6, March 1970.
7. Middleton, D., 'Statistical Communication Theory', (McGraw-Hill, New York, 1960).
8. Zadeh, L. A., 'Correlation functions and power spectra in variable networks', *Proc. Inst. Radio Engrs*, 38, No. 11, pp. 1342-5, November 1950.
9. Kroszczyński, J., 'Efficiency of attenuation of constant echoes in simple and double cancellation circuits', *Prace Przemyslowy Inst. Telekom.*, No. 24, pp. 41-6, 1958 (in Polish), (English translation available from the U.S. Dept. of Commerce, OTS, Order 59-16132).
10. Kroszczyński, J., 'Tłumienie ech stałych w radiolokacji', (Attenuation of constant echoes in radiolocation), (PWN, Warsaw, 1965).

Manuscript first received by the Institution on 14th July 1970 and in final form on 20th October 1970. (Paper No. 1368/AMMS 36.)

# The Relationships and Measurements of Cross-modulation and Intermodulation on Combined Signal Working C.C.I.R. System A V.H.F. Band III Relay Systems

By

J. W. MORRIS†

*Reprinted from the Proceedings of the Conference on Television Measuring Techniques held in London from 11th to 14th May 1970.*

In order to extend v.h.f. coverage in Great Britain to areas of relatively poor reception, the Independent Television Authority has recently commissioned a number of hybrid solid-state/valved combined signal working relay stations. Whilst this has led to a high level of performance and reliability, the use of combined signal working has introduced problems peculiar to this system in so far as the measurement of linearity is concerned.

The paper describes a typical relay system and the methods of expressing the linearity requirements in terms of intermodulation and cross modulation are defined, together with the empirical relationship between cross-modulation degradation and the standard subjective severity scale.

## Symbols and Abbreviations

$f_v$	vision carrier frequency
$f_s$	sound carrier frequency
$f_{sc}$	colour sub-carrier frequency
$f_i$	input frequency
$f_o$	output frequency
$f_p$	pump oscillator frequency
$f_{va}$	variable frequency
$f_{i.f.}$	intermediate frequency
c.m.p.	cross modulation product
$V_{vid.}$	video voltage (peak to peak)
$V_{c.m.p.}$	c.m.p. voltage (peak to peak)
i.p.	intermodulation product
$J_n(\Delta\theta)$	Bessel function of first kind and order $n$ .

## 1. Introduction

Combined signal working is at present used for u.h.f. C.C.I.R. system I television relay systems and a small number of v.h.f. C.C.I.R. system A television relay systems. In either case a non-linear transfer characteristic will give rise to the generation of intermodulation products and possibly cross-modulation products. However, the linearity measurements that may be made on these two systems must take into account the fundamental cause of picture degradation and the measurement should describe precisely the level of this effect against a specification.

In the case of u.h.f. colour systems,<sup>1</sup> the use of an amplitude modulated vision carrier with an amplitude modulated chroma subcarrier at a peak level of  $-17$  dB relative to peak sync, and a frequency modulated sound carrier at a level of  $-7$  dB relative to peak sync means that the effects of cross-modulation between carriers will be negligible compared with the subjective effect of the in-band intermodulation products generated and shown in Fig. 1.

† Independent Television Authority, Engineering Division, 70 Brompton Road, London S.W.3.

A simple specification of the amplitudes of carriers to be used, and the highest value of in-band intermodulation product that may be tolerated in a three-tone test adequately defines the amplitude linearity of the system, providing that no in-band spurious signals arise due to any mixing processes that may be involved.

C.C.I.R. system A involves the use of amplitude-modulated vision and sound carriers of the same peak amplitude. With combined working on this system, no in-band intermodulation products are normally generated and picture degradation is due to cross-modulation between the carriers. As will be shown, this cross-modulation product may be measured in defined terms but may not agree with the empirical values of cross-modulation levels given to a subjective appraisal of the picture degradation.

If the signal handling stages are operated well below their saturation levels it should be possible to predict fairly accurately the level of cross-modulation to be expected from a knowledge of the corresponding intermodulation products.

If, however, cross-modulation is due to effects other than non-linearity, or if the signal handling stages are working near their saturation levels, these predictions cannot be made and generally apply only to single stage amplifiers working well below their saturation levels whose amplitude/frequency responses can be accurately measured.

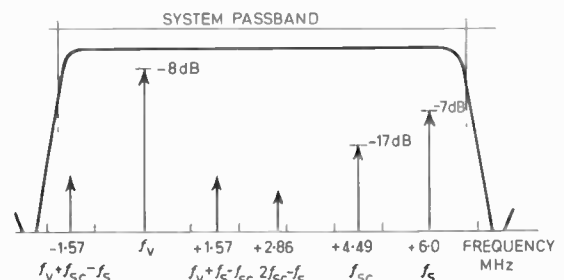


Fig. 1. Frequencies of carriers and intermodulation products relative to  $f_v$  MHz.

## 2. Description of the System

The requirement was for a v.h.f. solid-state transposer driving a valved linear amplifier. Two types of linear amplifier are used, the output powers being:

- (i) 10 W peak vision plus 2.5 W nominal sound carrier (10 W peak sound carrier).
- (ii) 100 W peak vision plus 25 W nominal sound carrier (100 W peak sound carrier).

The linear signal handling capacity in (i) is therefore 40 W and in case (ii) 400 W.

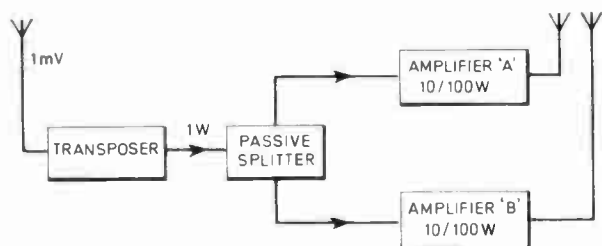


Fig. 2. Block diagram of basic equipment layout.

These amplifiers have been suitably de-rated to obtain the required linearity performance, the 10 W amplifier having a saturation power of 250 W and the 100 W amplifier a saturation power of 500 W.

The transposer output power is standardized at 1.0 W peak vision plus 0.25 W nominal sound carrier, this being a fairly high power level for solid-state devices, to reduce the number of valve stages in the linear amplifier to one for the 10 W requirement and three for the 100 W requirement.

The power requirements and de-rating factors are shown in Table 1.

Table 1. Power requirements and de-rating factors

Amplifier Power (C.W.)	Input Power	Output Power	De-rating Factor
250 W	0.25 W	10 W	25 : 1
500 W	0.1 W	100 W	5 : 1

The transposer, which may be divided into low- and high-power level stages, as in Fig. 3, is of conventional design, all the active stages being broad-band and the overall shaping being effected by the i.f. filter to the requirement shown in Fig. 4.

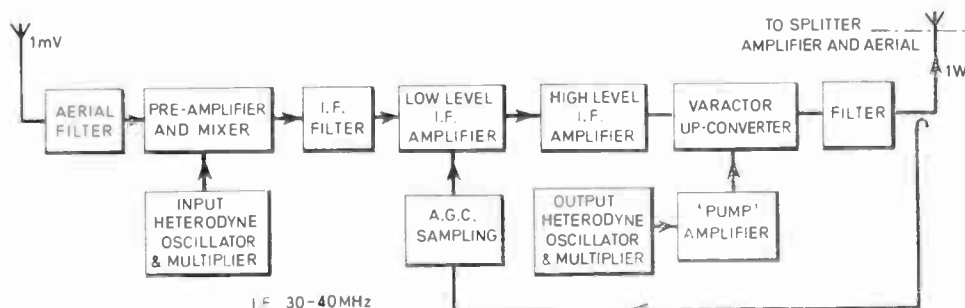


Fig. 3. Block schematic of the transposer.

The low-level transposer stages and the high-level i.f. amplifier are of conventional class A design but the necessity for a 4 W linear signal handling capacity together with a saturation power of some 12 W to realize the linearity requirements demands the use of a varactor upper sideband upconverter as the final mixer and output stage. A pump power of some 24 W is required to achieve the saturation power of 12 W as the pump to upper sideband conversion is far below the lossless maximum of  $f_o/f_p$  due to losses in the lumped constant matching circuit between the pump amplifier output stage and the varactor mount. It is necessary therefore to follow the upconverter with a bandpass filter with high out of band attenuation to prevent the pump frequency from being radiated at a level greater than -60 dB relative to peak vision power.

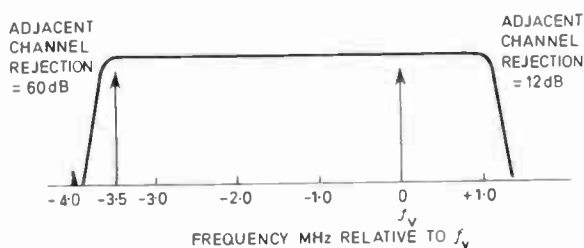


Fig. 4. Transposer overall response.

The high level i.f. amplifier is required to deliver a power output equal to the transposer power output less the upconverter gain, hence the lower Band III channels prove the most difficult in so far as non-linearity in this stage is concerned, as the upconverter gain is proportioned to the ratio of the output and input frequencies. Table 2 shows the typical high level i.f. power requirements for a transposer output of 1 W peak vision and i.f. of 30 MHz on the extreme channels 6 and 13.

Table 2. I.f. power requirements<sup>2</sup>

Channel	Gain (Power) $f_o/f_{i.f.}$ dB	Typical Power Gain dB	High Level I.F. Amplifier Output Watts
6	7.77	4.0	0.4
13	8.55	5.0	0.32

As we can expect to have no in-band intermodulation products, it is important to ensure that spurious mixing

products do not appear in-band. The upconverter is by its nature of use an efficient harmonic generator and mixer, therefore certain relationships between the intermediate and pump frequencies may cause in-band products to be generated, as follows:

$$f_p = f_o - f_{i.f.} \quad (i)$$

Let 
$$f_o = 2f_p - nf_{i.f.}$$

$$= 2f_o - 2f_{i.f.} - nf_{i.f.}$$

Therefore 
$$(2+n)f_{i.f.} = f_o \quad (ii)$$

If then 
$$n = 3$$

from (i) 
$$f_o = 2f_p - 3f_{i.f.}$$

and from (ii) 
$$f_{i.f.} = \frac{f_o}{5}$$

Similarly if 
$$n = 4$$

$$f_o = 2f_p - 4f_{i.f.}$$

and 
$$f_{i.f.} = \frac{f_o}{6}$$

It follows that if a spurious frequency  $2f_p - nf_{i.f.}$  is generated, a knowledge of  $n$  can be used to determine the i.f. that will not result in an in-band spurious frequency. For Band III output frequencies with an i.f. range of 30-40 MHz the integer  $n$  will be 3 or 4 and a table of prohibited i.f.s may be drawn up. Table 3 shows the restrictions for the extreme channels 6 and 13.

**Table 3.** Prohibited i.f. ranges for  $n = 3$  or 4 and Band III output frequencies (non-inverted i.f.)

Channel	Passband Frequencies MHz		Prohibited I.F. Ranges MHz			
	Lower	Upper	$n = 3[(2+n)=5]$		$n = 4[(2+n)=6]$	
6	176.0	181.0	35.8	36.8	29.84	30.66
13	211.0	216.0	42.8	43.8	35.67	36.49

Whilst the spurious components described are the result of non-linear additive mixing processes they cannot be used as indications of linearity as:

- (i) they are functions of pump drive level and i.f. drive level;
- (ii) the two components in (i) are fed into the up-converter via different ports;
- (iii) the pump level is far in excess of the vision and sound carrier levels produced by the high level i.f. amplifier.

As would be expected, the significant sources of non-linearity in the system are those working near their saturation figures:

- (a) The transposer high level i.f. amplifier, which is called upon to deliver output power at a level equal to the transposer output level less the conversion gain of the upconverter.
- (b) The upconverter and high level i.f. amplifier combination.
- (c) The valved linear amplifier.

**3. Linearity Specification**

There are two possible ways of expressing the linearity requirements:

- (i) In terms of the *cross modulation product ratio*, by specifying the ratio of peak-to-peak cross-modulation component to the peak-to-peak video signal with the interfering signal modulated to the maximum extent.
- (ii) In terms of the related *intermodulation product* levels relative to the maximum amplitude of the signal carriers, the latter being of equal amplitude.

The basic specification must be in terms of (i) above, as this defines the active troublesome component.

Table 4 shows the relationship between the cross modulation product ratio as in (i) and the standard subjective severity scale.

**Table 4.**

C.M.P. Ratio dB	Severity Scale
> -40	1. Imperceptible
-38	2. Just perceptible
-36	3. Definitely perceptible
-34	4. Somewhat objectionable
-32	5. Definitely objectionable
< -30	6. Signal unusable

From Table 4 it can be seen that the specification limit in terms of the c.m.p. ratio must then be -40 dB.

If the specification is to be in terms of i.p. ratio measurements as in (ii) above, the relationship between this measurement and the measurement of c.m.p. ratio must be established.

**4. Measurement of Intermodulation Products**

**4.1. Method of Measurement**

Two r.f. carriers, or tones, are combined and fed to the equipment under test, the levels of each of these tones being adjusted to represent the normal dynamic working levels. One tone is fixed at  $f_v$  and the other varied throughout the passband. The spectrum analyser will then show the intermodulation products generated and these may be measured with respect to the amplitude of the vision tone.

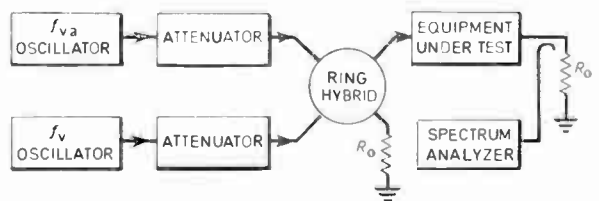


**Fig. 5.** Typical test set-up for a two-tone test.

It will be seen from Fig. 6 that the intermodulation products will only lie in-band if the variable oscillator frequency is < 2.0 MHz from vision frequency. As measurements of i.p.s with  $f_v - f_{va} > 2$  MHz are required, particularly  $f_v - f_{va} = 3.5$  MHz, the i.p.s will lie outside the system or stage passband and their measured value must be increased by the attenuation of the response at the i.p. frequency.

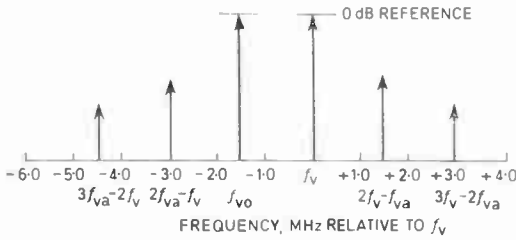


Fig. 6. Typical spectrum analyser display for a two-tone test.

4.2. Relationship of Intermodulation Products to Cross-modulation Products<sup>3</sup>

Let

$$e = E_a \sin \omega_a t + E_b \sin \omega_b t$$

second-order expansion

$$e^2 = \frac{E_a^2 + E_b^2}{2} - \frac{E_a^2}{2} \cos 2\omega_a t - \frac{E_b^2}{2} \cos 2\omega_b t + E_a E_b \cos (\omega_a + \omega_b)t \left. \begin{array}{l} \text{intermodulation} \\ \text{products} \end{array} \right\}$$

third-order expansion

$$e^3 = \left( \frac{3E_a^3}{4} + \frac{3E_a E_b^2}{2} \right) \sin \omega_a t + \left( \frac{3E_b^3}{4} + \frac{3E_a^2 E_b}{2} \right) \sin \omega_b t \left. \begin{array}{l} \text{cross-modulation} \\ \text{products} \end{array} \right\} - \frac{E_a^3}{4} \sin 3\omega_a t - \frac{E_b^3}{4} \sin 3\omega_b t \left. \begin{array}{l} \text{odd harmonics} \\ \text{intermodulation products} \end{array} \right\}$$

In the second-order expansion, the usual sum and difference frequencies exist but there is no cross-modulation component. In the third-order expansion, the cross-modulation components are shown with coefficients  $3E_a E_b^2/2$  and  $3E_a^2 E_b/2$  and the intermodulation products with coefficients  $3E_a E_b^2/4$  and  $3E_a^2 E_b/4$  at frequencies  $(2\omega_a - \omega_b)$  and  $(2\omega_b - \omega_a)$ . In the two-tone test ( $E_a$ ) and ( $E_b$ ) will have equal amplitudes and therefore the cross-modulation product level will be 6 dB above the measured and amplitude corrected i.p. level.

As the nominal sound carrier is symmetrically modulated, we can use the 6 dB conversion provided that we measure the peak-to-peak c.m.p. as defined in Section 3.

4.3. Measurements on the Equipment

The system may be divided into three parts for the purpose of these measurements:

- (i) the low-level transposer stages;

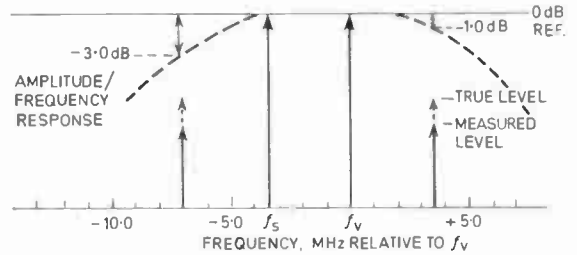


Fig. 7. Spectrum analyser display of the two carrier signals and corresponding intermodulation products.

- (ii) the high-level i.f. amplifier and upconverter combination;
- (iii) the valved linear amplifier.

4.3.1. The low-level transposer stages

Only the low-level transposer stages are operating sufficiently below their saturation power levels to have an assumed power transfer function represented by the series

$$e = av + bv^2 + cv^3$$

For this case then, these stages may be tested and aligned using the i.p. ratio as a guide to the c.m.p. ratio, the necessary conversion being simply that of subtracting 6 dB from the former to obtain the latter.

Table 5. Typical low-level unit parameters

Frequency	I.P. Ratio dB	Response Attenuation dB	Corrected I.P. Ratio dB	Predicted C.M.P. Ratio dB
$2f_v - f_s$	-55.0	1.0	-54.0	-48.0
$2f_s - f_v$	-57.0	3.0	-54.0	-48.0

4.3.2. The high-level i.f. amplifier and up-converter combination

Particular problems exist with the measurement of the i.p. ratio on the high level i.f. amplifier and upconverter combination due to mutual phase modulation caused by the passage of two carriers through a voltage dependent reactance such as a varactor diode. If we consider the phase modulation of the vision carrier by the sound carrier, we can write<sup>4</sup>

$$y = V \cos (\omega_v t + \Delta\theta \cos \omega_s t)$$

The sideband products, for small phase deviations are given by

$$y = V [ J_0(\Delta\theta) \cos \omega_v t - J_1(\Delta\theta) (\sin (\omega_v + \omega_s)t + \sin (\omega_v - \omega_s)t) - J_2(\Delta\theta) (\cos (\omega_v + 2\omega_s)t + \cos (\omega_v - 2\omega_s)t) + J_3(\Delta\theta) (\sin (\omega_v + 3\omega_s)t + \sin (\omega_v - 3\omega_s)t) ]$$

For phase modulation of the sound carrier by the vision carrier, we can merely interchange  $\omega_v$  and  $\omega_s$  in the above expansion. As this is so, the sidebands generated due to this mutual phase modulation will have equal amplitudes. From the above expansion it will be seen that there are terms with an amplitude  $J_2(\Delta\theta)$  at frequencies corresponding to  $2f_s - f_v$  and  $2f_v - f_s$ . For a deviation figure

$$\Delta\theta = 0.5 \text{ radian} \\ J_2(\Delta\theta) = 0.03$$

This then results in component frequencies  $2f_s - f_v$  and  $2f_v - f_s$  at a level of  $-30$  dB with respect to vision carrier peak amplitude. Although it is desirable to obtain i.p. levels at levels not greater than  $-46$  dB with respect to vision carrier peak amplitude, it will be seen that the true i.p. frequency components and the p.m. frequency components at the frequencies  $2f_s - f_v$  and  $2f_v - f_s$  will add in arbitrary phase, making the measurement of the true i.p. ratio impossible.

Whilst these components at  $2f_s - f_v$  and  $2f_v - f_s$  do not appear in-band, it is necessary to effect a high level of response attenuation in the valved amplifier following the transposer to ensure that these components are not radiated above a level of  $-60$  dB with respect to peak vision carrier amplitude.

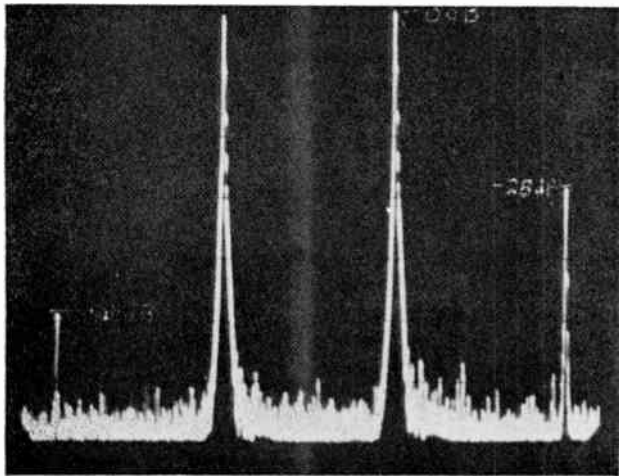


Fig. 8. Spectrum analyser display of the two r.f. carriers  $f_s$  and  $f_v$ , and the corresponding i.p. and p.m. sideband products, taken on a transposer where the c.m.p. ratio performance was better than  $-40$  dB.

The transposer output spectrum will normally contain only the two signal carriers and their associated amplitude modulation sideband components. As this is so, if mutual phase modulation of the sound and vision carriers is taking place, the only components shown in the Bessel function expansion that will exist at the output of the system will be those involving  $J_0(\Delta\theta)$ , i.e. the vision and sound carriers, the higher order terms being out of band. For a stated deviation

$$\Delta\theta = 0 \text{ to } 0.5 \text{ radian}$$

we get a deviated carrier amplitude variation from a normalized unity value 1.0 to 0.9385.

Considering the phase modulation of the vision carrier due to the sound carrier with 100% sinusoidal modulation, the vision carrier will vary in amplitude sinusoidally between 100% and 94% of its undeviated amplitude. We have then a phase modulation to amplitude modulation (p.m. to a.m.) conversion process taking place, and as the phase modulation deviation amplitude is proportional to the audio modulation of the sound carrier the practical effect is that of cross modulation. However, the c.m.p.s due to p.m./a.m. conversion and those due to amplitude

non-linearity will add in arbitrary phase, so that if they are near equality in amplitude the overall c.m.p. component may vary from an arbitrary maximum value to a minimum value which approaches complete cancellation. This latter effect is useful in practice where the circuit parameters, i.e. operating voltages and drive levels can be varied to achieve a cancellation effect.

From the foregoing, it can be seen that the c.m.p.s generated, whether due to amplitude non-linearity or p.m./a.m. conversion, are proportional to the signal carrier amplitudes. The third-order expansion above shows that the cross-modulation terms in the signal carrier coefficient are squared, i.e.

$$E_b^2 \text{ in the coefficient } \left( \frac{3E_a^3}{4} + \frac{3E_a E_b^2}{2} \right) \sin \omega_a t$$

so that a 1 dB increase in the amplitude of the signal carriers will result in a 2 dB increase in the c.m.p. amplitude. This is considering third-order terms only, but is well borne out in practice. The mutual phase deviation of the two signal carriers is proportional to their amplitudes so that the amplitude change in  $J_0(\Delta\theta)$  is proportional to them also, the law of the proportionality being  $J_0(N)$ , which shows that for deviation values  $< 2.4$  radians, the rate of increase in the p.m. to a.m. conversion product amplitude increases with increase in  $\Delta\theta$  and hence in the signal carrier amplitudes.

These non-linear proportionalities demand the maximum possible gain utilization from each stage, particularly those working near their power saturation capability. For this reason, the upconverter gain is kept as near the theoretical maximum shown in Table 2, commensurate with the requirements of the upconverter output filter and its associated insertion loss.

Table 6 shows the measured relationship between the i.f. input level and measured c.m.p. ratio at the output of an upconverter with a nominal gain of 4 dB.

Table 6.

Input	Nominal 0dB	+1.0dB	+2.0dB	+3.0dB	+4.0dB
C.M.P. Ratio	-48.0	-46.0	-43.5	-40.75	-37.5

A loss in gain of 1 dB necessitating an input level increase of 1 dB would result in an increase in the c.m.p. ratio of 2 dB and an increase in drive level of +2 dB to overcome a high output filter loss would result in a c.m.p. ratio increase of 4.5 dB.

#### 4.3.3. The valved linear amplifier

In the case of the 10 W amplifier, the derating is 25 : 1 and some consistency has been noticed between the measured i.p. and c.m.p. ratios; however, this is not so in the case of the 100 W amplifier and the use of i.p. ratio techniques as a guide to the c.m.p. ratio performance have been abandoned.

From the above, it will be seen that in practice, it is only possible to evaluate the c.m.p. ratio performance in terms of the associated i.p. ratio in the transposer stages operating well below their saturation levels. It has been

necessary in view of this to produce a method of measurement of the c.m.p. ratio directly and to use this method for evaluating the performance of the equipment as a whole. Although it is convenient to separate the transposer from the linear amplifier for purposes of alignment, the basic measurement of the c.m.p. ratio is made on the overall equipment and this figure taken as that which must meet the c.m.p. ratio specification.

**5. Measurement of the Cross-modulation Product Ratio**

The causes of cross-modulation so far established are:

- (i) A non-linear transfer characteristic involving third or higher order terms.
- (ii) P.m. to a.m. conversions.

A third cause should now be added:

- (iii) Crosstalk effects, where the transfer gain becomes inversely proportional to the signal carrier amplitudes. These effects in practice are confined to poor power supply regulation and pump supply saturation in the varactor upconverter.

Whatever the cause of the cross modulation component at the output of the system, the c.m.p. ratio may be established. A typical test set-up is shown in Fig. 9.

The test transmitter produces combined r.f. signals at  $f_s$  and  $f_v$ , the sound carrier modulated to 100% by an audio tone of 1 kHz, the vision carrier modulated to peak white by a composite line repetitive waveform consisting of any standard test waveform with an average picture content around mid-grey. A standard 2T pulse and 20  $\mu$ s bar plus 10-step staircase waveform or sawtooth waveform are suitable and are normally used. The r.f. levels are adjusted so that the peak sound voltage with 100% modulation is equal to the peak white voltage of the vision carrier. These two combined equal amplitude r.f. carriers are adjusted to the 1 mV peak required for the transposer input. As it is not possible to drive the amplifier directly from the test transmitter, the procedure is to produce good c.m.p. ratio performance from the transposer, and then adjust the amplifier for the best performance in conjunction with the transposer.

The transposer, or transposer plus amplifier, output is terminated in the normal working load and the levels adjusted to those required for normal operation.

A low-level probe sample is taken from the output of the system under test to a good quality receiver or v.s.b. demodulator with a sound carrier notch attenuation better than 55 dB. From this receiver then we shall get demodulated video plus any 1 kHz cross-modulation component. It remains now to measure c.m.p. ratio, this being defined as

$$-20 \log_{10} \frac{V_{vid}}{V_{c.m.p.}} \text{ dB}$$

This ratio may be measured directly, and Fig. 10 shows the block diagram of the c.m.p. ratio measuring unit.

The filter amplitude/frequency response is shown in Fig. 11.

This filter and amplifier passband presents zero insertion loss to the c.m.p. fundamental of 1 kHz and any harmonics of this fundamental up to the sixth. The presence of these harmonics is due to the fact that the final cross-modulation component is an integral function of components from individual stages in the system, these components adding in arbitrary phase and being themselves subject to any non-linearity in the system. As the subjective degradation of the picture is due to the peak value of the cross-modulation product component all the significant harmonics must be preserved if the c.m.p. ratio is to be meaningful.

Retention of the harmonic structure up to the sixth harmonic has been found to allow faithful transfer of the c.m.p. The video line frequency components and low-frequency hum components are heavily attenuated to avoid measurement errors. The method of measurement is simple and follows the following sequence:

- (a) In the 'calibrate' position, the video input is peak-to-peak detected, amplified and fed to the indicating meter, a variable gain adjustment being available to adjust the meter reading to full scale or 0 dB.
- (b) The filter/amplifier combination is switched into circuit in the 'measure' position and the 1 kHz component, plus harmonics, peak-to-peak detected. The amplifier gain is increased in 20 dB steps until an 'on-scale' meter reading is obtained.
- (c) By adding the increase in amplifier gain to the scale reading on the meter, the c.m.p. ratio is obtained.

This straightforward technique allows adjustments to be made to the transposer or transposer/amplifier combination with a continuous indication of the c.m.p. ratio, providing that the peak modulated vision r.f. signal is kept at a constant level by adjustment or by means of the existing a.g.c. system.

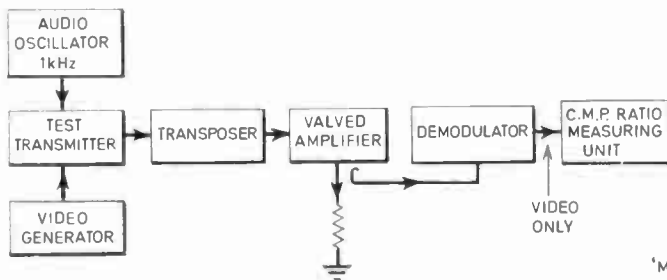
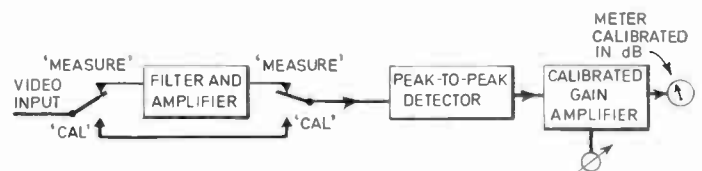


Fig. 9 (left). Test set-up for c.m.p. ratio measurements.

Fig. 10 (right). C.m.p. ratio measuring unit.



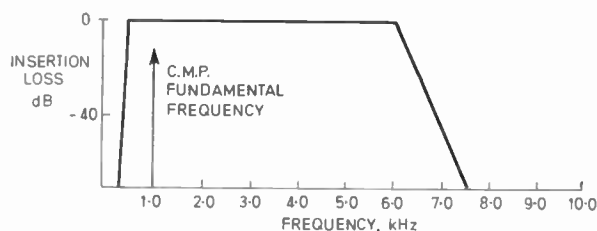


Fig. 11. Filter amplitude/frequency response.

Apart from the separation of the transposer and amplifier for this test, no other account need be taken of individual unit performance and each may be adjusted in turn for the optimum overall result.

However, it is necessary to ensure that there are no measurement errors due to the demodulation process and three simple checks may be effected during the course of equipment measurements to test the demodulator performance in the following aspects:

(i) *Demodulator cross-modulation*

With the demodulator fed from the equipment under test, its input level is varied  $\pm 1$  dB around the normal working level. If the demodulator is introducing no cross-modulation components, there will be a linear relationship between the demodulator input level and the indicated c.m.p. ratio on the measuring unit. A non-linear relationship of the form shown in Table 6 would indicate a cross modulation product contribution from the demodulator.

(ii) *Demodulator noise*

The demodulator is fed with modulated vision carrier only. The c.m.p. ratio measuring unit will then indicate an arbitrary noise level which will not invalidate c.m.p. ratio measurements if it is equal to or better than an indicated  $-55$  dB.

(iii) *Demodulator sound notch rejection performance*

With the demodulator fed with modulated sound carrier only, the c.m.p. ratio measuring unit will indicate the sound notch rejection performance which is required to be equal to or better than an indicated  $-55$  dB.

## 6. C.M.P. Ratio Measurement Errors

It has been found that the indicated c.m.p. ratio does not always correspond to the subjective assessment shown in Table 4, the indicated c.m.p. ratio often being rather better than subjective assessment would suggest. The reasons for this effect, assuming no test equipment anomalies, have been investigated and will now be described.

### 6.1. Cross-modulation Differential Phase

In any stage producing cross-modulation products, we have seen that the c.m.p. ratio is proportional to the signal carrier levels. Under certain conditions a variation of c.m.p. phase with signal level may be experienced.

An effect of this nature has been experienced particularly in the valved linear amplifier. There are two classes

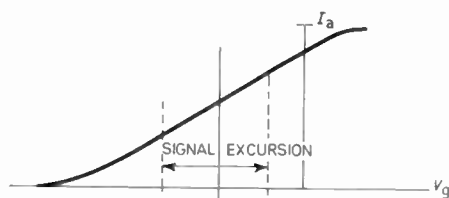


Fig. 12.  $I_a/V_g$  characteristics for class A operation with a nominal  $V_a/V_{g2}$  and load line.

of operation that may be employed with combined signal working.

(a) *Class A* (Fig. 12).

Providing that the stage is suitably derated, the advantages yielded by this class of operation are:

- (i) optimum linear transfer;
- (ii) high gain;

and the disadvantages:

- (i) very low efficiency, typically 15–20%;
- (ii) high anode dissipation, often near the rated maximum for the valve type in use.

This class of operation will then yield a transfer characteristic of the form shown in Fig. 13.

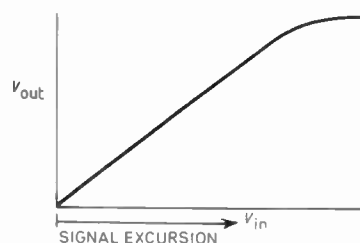


Fig. 13. Class A transfer characteristic.

(b) *Class B* (Fig. 14).

In this mode of operation, the r.f. cut-off (sync. tip) is arranged so that the picture excursion is over the linear part of the characteristic, and a small degree of non-linearity is tolerated in the sync. region. The advantages of this system are:

- (i) relatively high efficiency;
- (ii) low anode dissipation;

and the disadvantages:

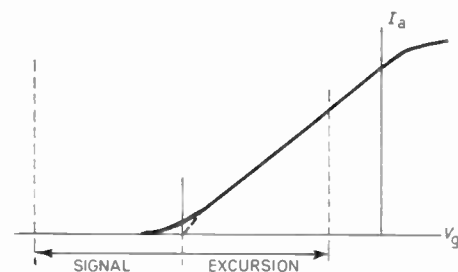


Fig. 14.  $I_a/V_g$  characteristics for class AB operation, with a nominal  $V_a/V_{g2}$  and load line.

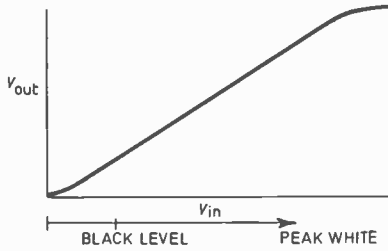


Fig. 15. Class B transfer characteristic.

- (i) relatively low gain, necessitating a correspondingly higher drive level;
- (ii) a not wholly linear transfer, sometimes resulting in c.m.p. differential phase.

This class of operation will yield a transfer characteristic of the form shown in Fig. 15.

To obtain longer valve life and performance stability, class B operation has been used with satisfactory results. However, care must be taken to optimize the circuit parameters, particularly  $V_a$ ,  $V_{g2}$  and the anode dynamic load if c.m.p. differential phase is to be avoided. Low  $V_{g2}$ ,  $V_a$  and incorrect anode loading often lead to a working condition in Fig. 16.

Under these conditions, the transfer characteristic inflects in the picture region and c.m.p.s are generated at vision carrier levels corresponding to black and white level with a phase change from black to white level of  $180^\circ$ . In this case c.m.p.s are generated with significant amplitudes at signal levels other than those corresponding to peak white, and it is necessary to have a test video waveform with a full excursion from black to white level. The standard test waveform including a 5, 7, or 10-step staircase is quite suitable. Figure 17 shows a full frame of line repetitive test waveform taken from a distortionless demodulator with the system set up as previously described for direct c.m.p. ratio measurement with a normal cross-modulation effect, and Fig. 18 shows the cross-modulation differential phase effect.

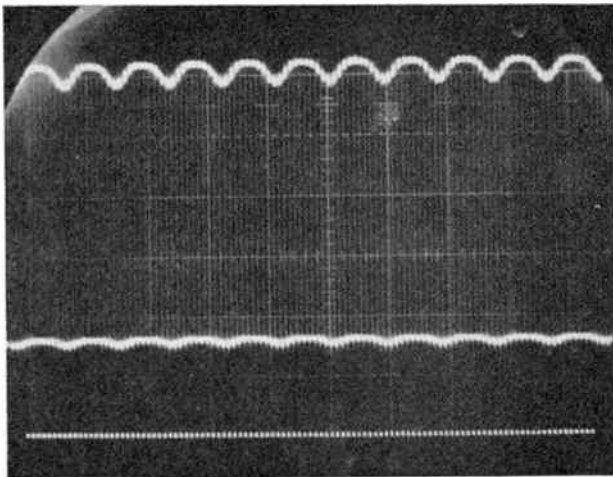


Fig. 17. Oscilloscope display of full frame with normal cross-modulation effect.

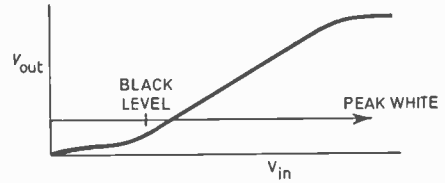


Fig. 16. Transfer characteristic to produce c.m.p. differential phase.

The top line represents peak white and the bottom line black level, the intermediate lines being the steps of a 5 step staircase. A  $180^\circ$  phase change of the c.m.p. can be seen between black and white levels. However, when the 1 kHz sound c.m.p. component is filtered off by the c.m.p. ratio measuring equipment, partial or total cancellation of the c.m.p. components between black and white levels takes place. As a result, the indicated c.m.p. ratio is at variance with the subjective assessment of the c.m.p. ratio on a picture monitor or video waveform display. It is quite possible to have an indicated c.m.p. ratio of  $-50$  dB when subjective assessment would indicate the ratio to be not better than  $-40$  dB.

It is necessary, therefore, to verify the test equipment indicated c.m.p. ratio by observation of a picture monitor or video display.

## 6.2. Crosstalk

Crosstalk effects due to poor power supply regulation are rare in equipment of low power levels requiring low voltage supplies which may be well controlled. An effect of this nature however has been observed in practice and investigation traced the cause to the varactor up-converter. It is essential that the pump supply to the upconverter is matched so that maximum pump power is delivered to the varactor diode. In the case of gross mismatch, the varactor saturation power drops with two significant effects:

- (i) non-linearity of the upconverter power transfer characteristic;

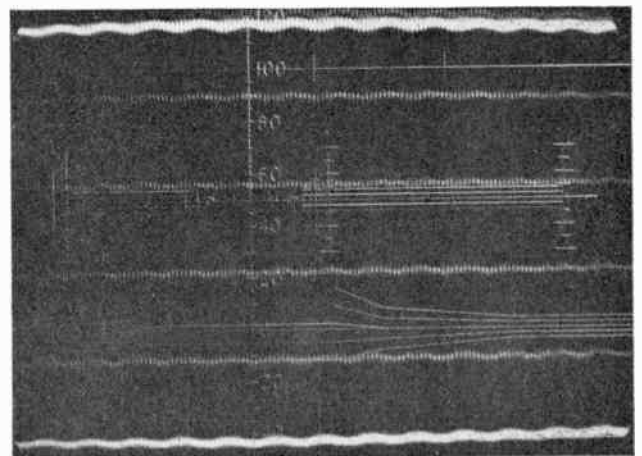


Fig. 18. Oscilloscope display of full frame with cross-modulation differential phase effect.

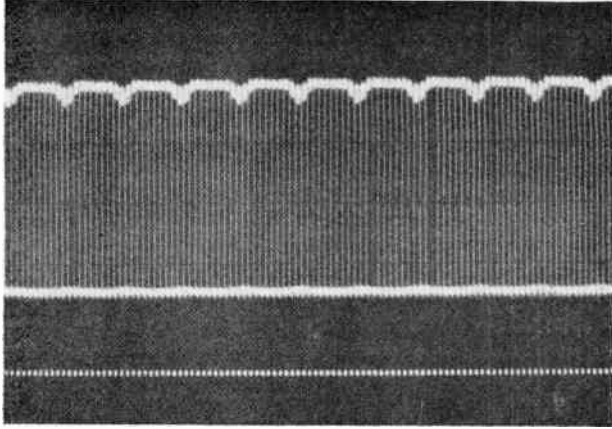


Fig. 19. Pump sag crosstalk effect.

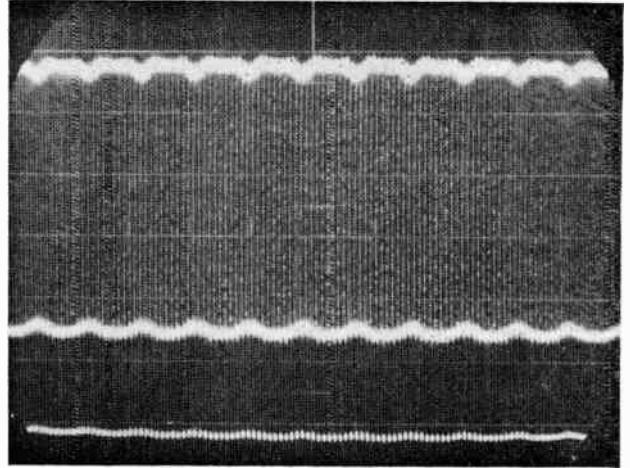


Fig. 20. Pump sag crosstalk with cross-modulation.

(ii) a sudden defined sag in the pump power availability at peaks of power, in this case corresponding to peaks of sound modulation, the drop in pump power across the varactor diode being due to excessive loading of the pump supply.

Figure 19 shows the effects, in exaggerated form, of this crosstalk effect on a full frame of line repetitive sawtooth waveform.

Figure 20 shows the crosstalk effect taking place with cross-modulation.

It can be seen that the c.m.p. at black level is in anti-phase with the sag corresponding to peaks of sound modulation at peak white. The fundamental component of this sag effect waveform is then 1 kHz and partial cancellation of these components takes place in the c.m.p. ratio measuring instrument. Again, this indicates the necessity for subjective verification of the indicated c.m.p. ratio.

6.3. Spurious Signals

It is shown in Section 3 that phase modulation sidebands exist due to the up-conversion process at peak levels of approximately -30 dB referred to peak white. These sidebands exist at frequencies corresponding to  $2f_v - f_s$  and  $2f_s - f_v$ , i.e. 3.5 MHz above vision carrier and 3.5 MHz below sound carrier. Whilst measures are taken in the shaping of the valved linear amplifier frequency response to reduce the amplitude of these p.m. sidebands

to  $> -60$  dB referred to peak white carrier level, they will exist at a significant level at the output of the transposer, where it is necessary to measure the c.m.p. ratio.

High quality v.s.b. demodulators for accurate measurement of transient responses generally have frequency responses extending well beyond the nominal system bandwidth to avoid group delay errors.

One or both of the p.m. sidebands may then be present at the detector of the demodulator and detected as vision carrier sidebands.

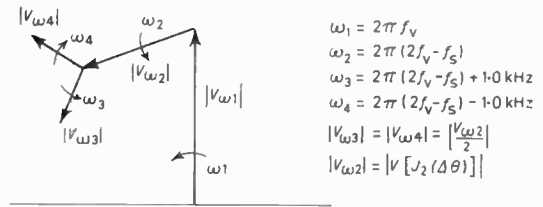


Fig. 22. Vector representation of carrier and spurious signal.

As the amplitude of the p.m. sidebands is proportional to the instantaneous amplitude of the sound carrier the p.m. sideband amplitudes will vary sinusoidally at a frequency of 1 kHz. The subjective effect on a picture monitor is of a dot pattern intensity modulated at 1k Hz which, when viewed under normal conditions, appears as cross-modulation. The effect on a waveform display is shown in Fig. 23.

The c.m.p. ratio measuring instrument 1 kHz filter will not of course accept this spurious signal and the indicated measurement will be that of the true c.m.p. ratio, whilst the picture monitor will indicate the presence of c.m.p.s.

In this case, it is necessary to observe the indicated c.m.p. ratio, the picture monitor and the video waveform display, before an indication of system performance can be made.

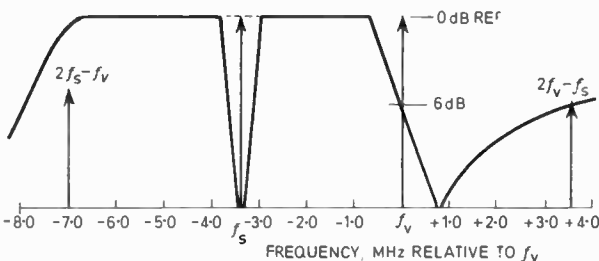


Fig. 21. Typical frequency response of a high quality v.s.b. demodulator with a switchable sound notch.

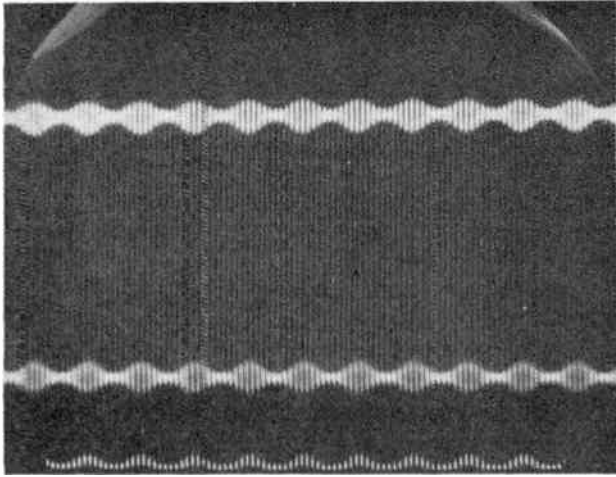


Fig. 23. Full frame waveform of line repetitive sawtooth showing a superimposed amplitude modulated 3.5 MHz spurious signal.

The discrepancy described does not have any 'off-air' implications as the p.m. sidebands are attenuated to -60 dB before radiation.

### 7. Conclusions

The measurement of the effects of non-linearity in a combined amplitude modulated signal working system are reasonably straightforward, provided that the effect causing subjective degradation is measured directly. It has been found impossible to correlate the intermodulation product and cross-modulation product ratios, so that the former may not be taken as an indication of the

latter in a multistage system involving stages working near their saturation levels or involving level dependent reactances.

The direct measurement of the c.m.p. ratio must be validated by subjective assessment of a picture monitor and video waveform display to eliminate the possibility of having a satisfactory but false indicated c.m.p. ratio performance due to cancellation or other extraneous effects.

### 8. Acknowledgments

The Author wishes to thank the Director of Engineering of the Independent Television Authority for his kind permission to publish this paper, and also his colleagues in the R.F. Section of the Experimental and Development Department, who were responsible for the design of the c.m.p. ratio measuring unit.

### 9. References

1. O'Loughlin, C. N., 'Intermodulation characteristics of high power klystrons used in frequency transposers for colour television', Proc. I.E.R.E. Conference on U.H.F. Television, London 1965.
2. Manley, J. M. and Rowe, H. E., 'Some general properties of non-linear elements—Part I, General energy relations', *Proc. Inst. Radio Engrs*, 44, No. 7, pp. 904-13, July 1956.
3. Terman, F. E., 'Electronic & Radio Engineering', Chap. 10, Sect. 10.3 (McGraw Hill, New York, 1955).
4. Standard Telephones & Cables Ltd., 'Reference Data for Radio Engineers', 4th Edn., Chap. 19, pp. 532-6.

*Manuscript received by the Institution on 21st January 1970. (Paper No. 1369/Com. 36.)*

© The Institution of Electronic and Radio Engineers, 1971

# Ultrasonic Imaging in Solids

By

**M. G. MAGINNESS,**  
B.E., Ph.D.†

and

**Professor L. KAY,**  
Ph.D., C.Eng., F.I.E.R.E.†

*Reprinted from the Proceedings of the Conference on Industrial Ultrasonics held at Loughborough from 23rd to 25th September 1969.*

An experiment is described in which a focused image of objects within a solid material was obtained from signals received at a transducer array on the material surface. Image construction from these data was done by digital computer. The results conform to the theoretical resolution obtainable under the prevailing physical constraints.

## 1. Introduction

The inspection of solids by ultrasonic imaging can be modelled as shown in Fig. 1.<sup>1</sup> Conventional pulse-echo non-destructive testing systems using probes restrict the information from the object space  $S$  and the transform space  $T$  to a very gross approximation at  $U$  which is directly displayed. The instantaneous signals from elements of the receiving aperture are simply added arithmetically by a common electrode. This produces a signal which is effectively the total back scattering from a thin shell normal to the direction of propagation of the energy. The amplitude and phase distribution of signals, generated from within the shell, is predetermined by the radiating and receiving apertures with the effect of discontinuities superimposed. Reconstruction of the reflexion characteristics of discontinuities in the object space is very coarse and requires movement of the probe. The dotted connexion in Fig. 1 shows the operations which are bypassed by these systems.

In this paper we describe the results obtained by processing signals from elements of the aperture (receiving transducer) before summation.

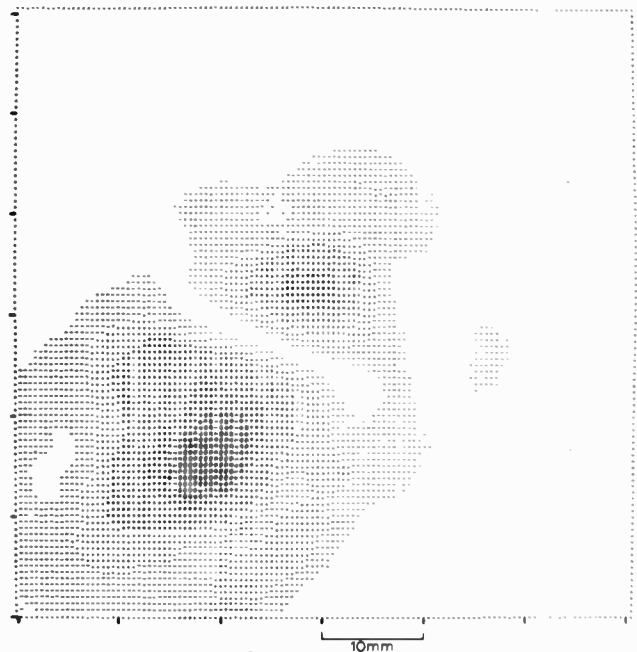


Fig. 2. Computer print-out.

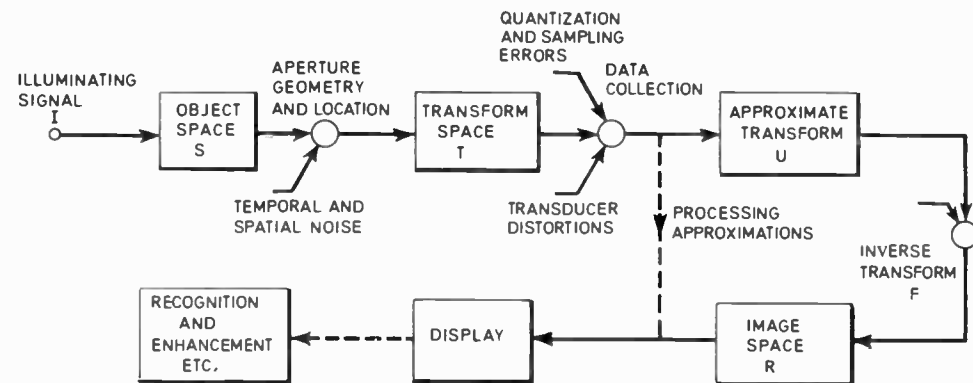


Fig. 1. Inspection system model.

## 2. Basic System

In essence, information from the object space is collected by a multi-electrode transducer (approximately  $12 \times 12$  elements) and the record from each element stored on paper tape. This is fed to a computer, programmed to process these data in such a way that the print-out is a plot of any chosen plane within the

object space, dark areas representing sections of the plane which contain discontinuities. Figure 2 shows an example which is discussed later.

## 3. General Principles

Consider the operation of a lens; this receives signals reflected from what we have called the object space  $S$ . According to the position on the lens where the signal is incident a time delay is introduced before re-radiation to a point on the image plane corresponding to the region

† Department of Electrical Engineering, University of Canterbury, Christchurch, New Zealand.

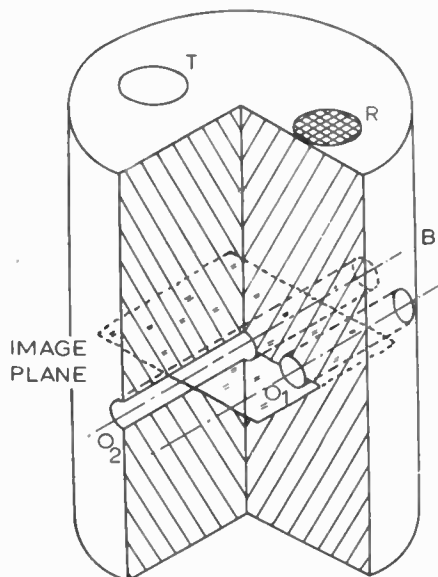


Fig. 3. Block with radiating and receiving transducers.

in the object space from which the signal originated. All signal components from a given point in the object space, on passing through the lens, experience varying degrees of delay such that on arrival at the image plane they bear the same time relationships as at the generating point. The sum of these components then represents the reflected signal. At the image plane an intensity is produced representing the reflectors—or scatterers—in so far as the illuminating signal is capable of revealing them. The distance into space over which the system operates depends upon the focal length of the lens.

In our system we effectively carry out a similar operation.

The simplest method of describing the actual operation is to consider each small receiving element at position  $(x_A, y_A)$  of an array in the  $z = 0$  plane as re-radiating energy received from the object space after introducing a delay depending upon the relative co-ordinates of the array elements and the object space. Consider the reflexions from any elemental volume A, located at co-ordinates  $(x, y, z)$  in S. Each array element will receive a signal of amplitude depending on the reflexion characteristics of the region being considered; but the time of arrival will vary according to the co-ordinates  $(x_A, y_A)$ . Let each signal now be given a delay and be re-radiated from the array element. This re-radiation will pass through the volume A. Since the re-radiating elements are small the radiation will be uniform (or can be easily corrected) in all directions. To make all re-radiations arrive simultaneously at A they must be given specifiably different delays depending on the distance,

$$[(x-x_A)^2 + (y-y_A)^2 + z^2]^{\frac{1}{2}}$$

prior to re-radiation. Signals received by elements furthest from A will receive little or no delay whereas those from elements geometrically closest to A will receive the greatest delay. The computer program simulates this process, introducing appropriate delays

by computation of the return path lengths so that all signals may be correctly added. The operation can be thought of as a convolution of the ensemble of received signals with a (spatial) 'impulse response' representing the delay characteristics of the aperture—object space. Alternatively the operation may be implemented via a Fourier transform representation of the aperture distribution and a multiplicative operation followed by an inverse transform.

These two viewpoints correspond to regarding the measured field distribution as formed from a superposition of spherical waves converging to 'sinks' on the array elements, or as formed from a superposition of plane waves, respectively.

By similarly considering reflexions from any thin surface made up of many elemental volumes such as A it will be seen that the re-radiated energy on passing through this shell will reconstruct the original reflexions—within of course the resolution limits imposed by the dimensions of the aperture.

The print-out of the computer is essentially this reconstruction on paper.

#### 4. Basic Equipment in the Experiment

The radiating and receiving transducers were bonded to an aluminium block as shown in Fig. 3. Two holes 3 mm diameter and 21 mm apart were drilled parallel to the upper surface at a depth of 77 mm. One hole was under the receiving transducer, the other was between the transmitter and the receiver (in plan). The transmitting transducers were crystals of initially 15 and later 5 mm diameter, resonant at 5 MHz. The receiving transducer was a single crystal 15 mm diameter resonant at 5 MHz also, but the free electrode was etched to form an array of elemental electrodes each approximately 1 mm square. There was a total of 156 active elements.

A thin disk such as this responds point by point with an electrical signal proportional to the acoustic signal of that point, there being very little transverse coupling. Hence, effectively, each electrode gives a signal proportional only to the acoustic field incident over that small area. At 5 MHz in aluminium 1 mm spacing corresponds to sampling the incident field at 0.78 wavelength intervals.

The radiated acoustic energy was in the form of very short pulses. Figure 4 is a trace of a signal received by

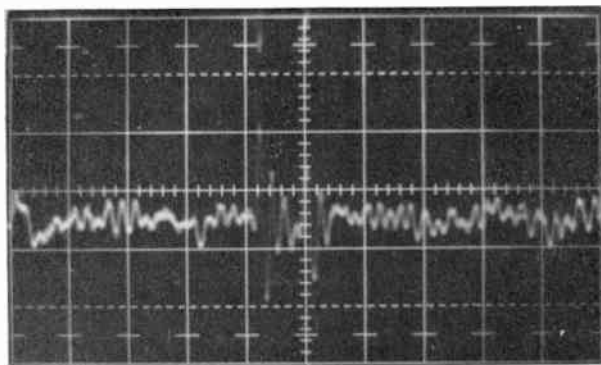


Fig. 4. Received signal. 1 large horizontal division = 1 μs.

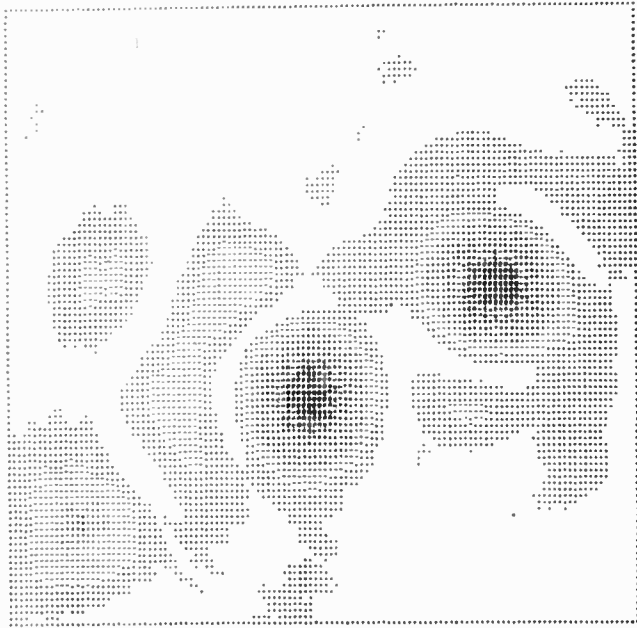


Fig. 5. Print-out from computer.

one receiver element, from which it will be seen that the acoustic pulses consist of approximately 2 cycles of a 5 MHz wave.

To facilitate connexion to the electrode grid a perspex jig drilled with 156 holes was mounted over the transducer. The holes acted as guides for a spring-loaded contact pin which was manually moved from electrode to electrode for each recording. Each element record was taken automatically by a programmed analogue-digital converter specially designed for the purpose. A method similar to that described in ref. 2 was used to sample the received signal at a sufficient rate (24 MHz) to accommodate the highest received frequencies. This data was quantized to 2 bits, then recorded on paper tape together with the coordinates ( $x_A, y_A$ ) of the transducer element.

An IBM 360/44 computer was programmed to perform all subsequent operations to obtain the output shown in Fig. 5.

## 5. Discussion

The recording shown in Fig. 2 was obtained by a laborious manual process using 5 MHz ultrasonic pulses of 50 cycles duration. Each value of phase and amplitude was measured on a c.r.o. By comparison the recording of Fig. 5 was obtained almost automatically using pulses of approximately 2 cycles duration. The range resolution capability of the wideband signal is potentially high and this factor is probably the most significant difference between the present method and conventional acoustic holography using monochromatic insonification as described in recent publications.<sup>3-6</sup> The record of Fig. 5 contains the 5 MHz components because of computer speed limitations when using the straight-forward convolution formulation. There is, however, no basic reason why the display cannot be a summation over all frequency components given adequate computer capacity and suitable programming using the Fourier

transform approach implemented with the 'fast' algorithm.<sup>7</sup> Preliminary work indicates that by this method pictures containing frequency components spanning at least two octaves can be computed in approximately the same time as for a single frequency picture computed by straight convolution. This makes it possible to observe, from one record, variations in the reflexion characteristics of scatterers in a metal block over a wide frequency band.

## 5.1. Picture Interpretation

The holes were approximately 2.2 wavelengths in diameter at 5 MHz and this factor combined with poor insonification to produce only 'highlights' of reflexion. The scattered field was viewed by an aperture with a focal spot diameter of about 5 wavelengths at the depth of 77 mm. Quite clearly then one could not expect to obtain a record showing two parallel lines. In fact the record very closely resembles what should theoretically be obtained, showing few deficiencies in the system at this stage. Even so, the resolution of the two holes 21 mm apart is encouraging and is significantly superior to that obtained using commercial probes.

We are now proceeding with the use of a larger aperture and investigating means of insonifying the medium more uniformly. Together with fuller use of the wide frequency band signal this should produce a 10-20 fold increase in resolution, providing more practically useful pictures. Operation in materials of much coarser grain structure than aluminium (steel brass, zinc and aluminium-silicon alloys) is currently being investigated to assess the ultimate limitations of the system.

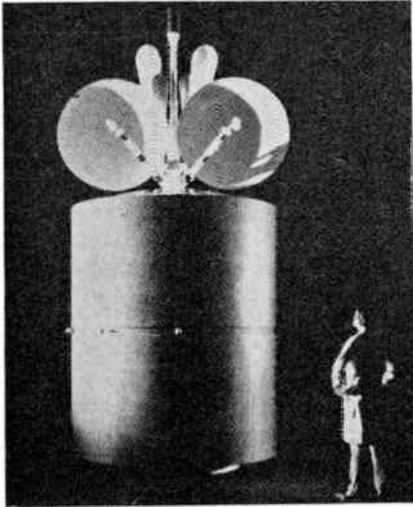
## 6. Acknowledgments

The authors wish to thank the New Zealand University Grants Committee and the National Research Development Corporation (U.K.) for their generous financial support of this work.

## 7. References

1. Maginness, M. G. and Kay, L., 'Signal processing for acoustic imaging systems', Paper K-5-3, 6th International Congress on Acoustics, Tokyo, August 21st to 28th, 1968.
2. Cashin, P. M. and Johnson, D. A. H., 'A novel method of analysing singly occurring pulses with nanosecond resolution', *The Radio and Electronic Engineer*, **38**, pp. 1-4, July 1969.
3. Metherell, A. F. *et al.*, 'Introduction to acoustic holography', *J. Acoust. Soc. Amer.*, **42**, pp. 733-42, October 1967.
4. Kreuzer, J. L., 'Ultrasonic three dimensional imaging using holographic techniques'. Symposium on Modern Optics, Polytecnic Inst. Brooklyn, March 22nd to 24th, 1967.
5. Marom, E. *et al.*, 'Ultrasonic holography by electronic scanning of a piezoelectric crystal', *Appl. Phys. Lett.*, **12**, pp. 26-28, 15th January 1968.
6. Thurston, F. L., 'Holographic imaging with ultrasound', *J. Acoust. Soc. Amer.*, **45**, pp. 895-9, April 1969.
7. Cooley, J. W. and Tukey, J. W., 'An algorithm for the machine calculation of complex Fourier series', *Math. of Computation*, **19**, pp. 297-301, April 1965.

Manuscript first received by the Institution on 2nd September 1969 and in final form on 19th October 1970. (Paper No. 1370/CC98.)



taking detailed design and manufacture of ground handling equipment and special jigs and tools for the entire programme. Thomson-CSF is assisting the Hughes Project Group in Los Angeles for the overall design of the satellite as well as the design of telemetry and telecommand sub-systems. The company also is in charge of manufacturing the complete telemetry and telecommand sub-systems operating at microwave, including

## *Intelsat IV Satellite —* EUROPEAN PARTICIPATION

The new *Intelsat IV* communications satellites are currently under construction by Hughes Aircraft Company for the International Telecommunications Satellite Consortium. The programme is directed by the Communications Satellite Corporation, acting in its role as manager for the Consortium which is comprised of 68 member-nations. Companies from 10 nations are participating as sub-contractors to Hughes in this programme.

Designed to meet the increased global communications needs of the 1970s, *Intelsat IV* has substantially greater capability than previous communications satellites. Each satellite will have 12 broadband communications channels each having a bandwidth approaching 40 MHz providing capacity for about 500 communications circuits. Thus each satellite can relay 6000 two-way telephone calls or 12 colour television programmes or any combination of such communication transmissions. The satellites are 5.33 m high and have a diameter of 2.5 m.

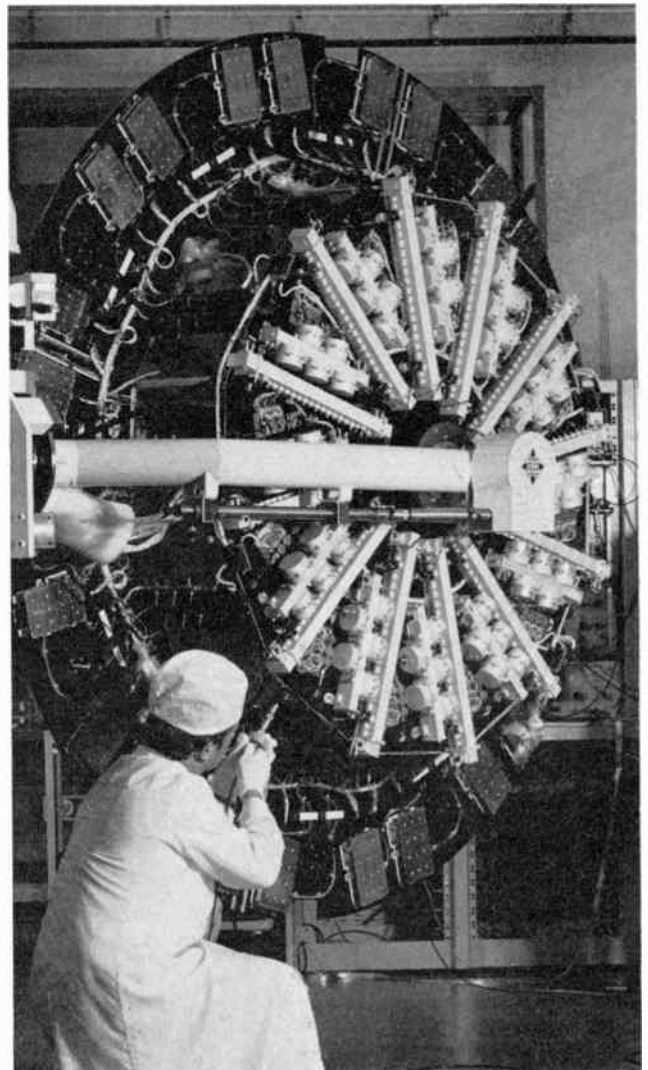
During its expected seven-year operational lifetime, two 'spotlight' antennae can be beamed at heavily populated areas, such as western Europe and the eastern United States. In addition two Earth coverage antennae can serve areas not covered by the spot beams. Ground controllers can remotely select the desired spot or global coverage.

The first flight model and its sub-systems will be built and tested at the Hughes space facilities in El Segundo, California, with the member-nation sub-contractors directly participating. The second and third spacecraft will be assembled and tested at Hughes, but most of the sub-systems of the third and even more of the fourth spacecraft will be built by the participating sub-contractors. The fourth flight spacecraft will be assembled at British Aircraft Corporation, Bristol, England, using sub-systems furnished by sub-contractors. Integration and tests will be carried out by a European team formed by BAC, Thomson-CSF and AEG-Telefunken. The roles of these three companies are as follows:

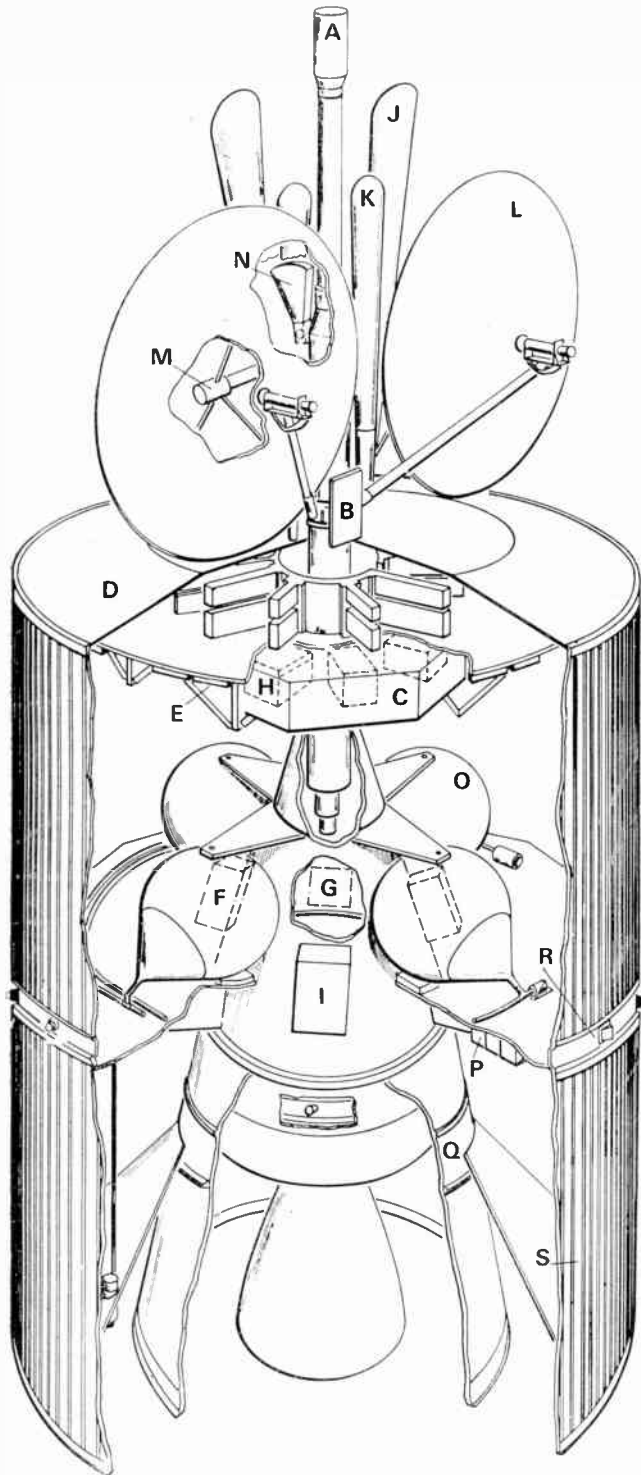
British Aircraft Corporation is assisting the Hughes team designing *Intelsat IV* in U.S.A. In addition to co-ordinating the activities of the European integration team for all the flight spacecraft BAC will be responsible for manufacture of the following hardware on three of the four satellites: Structures, attitude and position control system and power supply system including cable harness and solar panels. BAC is also under-

taking detailed design and manufacture of ground handling equipment and special jigs and tools for the entire programme. Thomson-CSF, in addition, is a member of the tripartite European team responsible for the integration and test flight models No. 3 and 4 of *Intelsat IV* programme.

AEG-Telefunken will supply the complete communications system comprising 12 broadband communications channels for



The communications section, which incorporates power supply, transmitter and receiver, undergoing final testing in the AEG-Telefunken factory at Backnang prior to being flown to America.



Cut-away view of the *Intelsat IV* satellite showing the disposition of the various sub-systems.

### Participants in the *Intelsat IV* satellite programme

Hughes Aircraft Company  
 British Aircraft Corporation  
 Thomson-CSF  
 AEG-Telefunken  
 Nippon Electric Company  
 Contraves AG (Switzerland)  
 Selenia SpA (Italy)  
 Etudes Techniques et Constructions Aérospatiales (ETCA) (Belgium)  
 Société Anonyme de Télécommunication (SAT) (France)  
 Ferranti Limited (United Kingdom)  
 Northern Electric Company (Canada)  
 Svenska Radio AB (Sweden)  
 Kolster-Iberica SA (Spain)

one of the four satellites and 100,000 solar cells including the test and classification shop for two satellites. Furthermore, AEG-Telefunken engineers will directly participate in the realization of the project at the space facilities of Hughes Aircraft Company in the U.S.A. Likewise, the integration of two satellites will be accomplished with the substantial assistance of AEG-Telefunken engineers.

- A Telemetry and Command Antennas (Thomson-CSF)
- B Planar Array Antenna (Thomson-CSF)
- C Telemetry and Command Equipment (Thomson-CSF)
- D Repeater F-2 (Nippon)
- D Repeater F-3 (AEG-Telefunken)
- D Repeater F-4 (Northern Electric)
- E T.W.T. Power Supply Converters for Drivers (Kolster-Iberica)
- F Battery Controller and Relay (ETCA)
- G Solenoid and Squib Drivers (Svenska Radio)
- H Antenna Positioning Electronics (Contraves)
- I De-spin Control Electronics (Contraves)
- JK Earth Coverage—Transmit and Receive Antennas (Selenia)
- L Spot Beam Communication Antennas (Selenia)
- M Antenna Positioner Mechanism (Selenia)
- N Nutation Damper (BAC)
- O Positioning and Orientation Sub-system (BAC)
- P Battery Pack (BAC)
- Q Structure and Harness (BAC)
- R Sun Sensor (BAC)
- S Solar Panel (BAC)  
 Solar Cells (SAT, Ferranti, AEG-Telefunken)

Associated Ground Equipment (not shown):

Digital Portion of Systems Test Equipment and Ground Control Equipment (ETCA)

R.F. Portion of Systems Test Equipment (Svenska Radio)  
 Handling Equipment (BAC)

## Contributors to this issue



**Dr. M. G. Maginness** received the degree of B.E. from the University of Canterbury, Christchurch, New Zealand, in 1966. From 1966 to 1969 he pursued research into ultrasonic imaging systems at Canterbury University and obtained his Ph.D. in 1970. He now holds a research fellowship and is engaged in further work in this field.

**Professor D. R. Towill** (F. 1970) occupies the Chair of Engineering Production in the Department of Mechanical Engineering and Engineering Production in the University of Wales Institute of Science and Technology to which he was appointed just over a year ago. A fuller note on his career appeared in the *Journal* in October 1969.

**Mr. P. A. Payne** (G. 1965) is currently completing the requirements for a Ph.D. at the University of Wales Institute of Science and Technology. (See *The Radio and Electronic Engineer* for December 1970.)

**Professor Leslie Kay** (F. 1965) has occupied the Chair in Electrical Engineering at the University of Canterbury, Christchurch, New Zealand, since 1966. He is currently visiting universities and research organizations in the U.S.A. in connection with work on ultrasonic blind guidance aids. (See *The Radio and Electronic Engineer* for December 1970.)

**Dr. Jan Kroszczyński** is with the Institute of Telecommunications (P.I.T.), Warsaw. (See *The Radio and Electronic Engineer* for March 1970.)



**Mr. J. W. Morris** received his technical education at Leeds College of Technology. After initial technical experience with the Post Office, he joined the Independent Television Authority in 1961 and from 1968-1970 was Senior Engineer in the Transmitter Section of the Station Design and Construction Department. Mr. Morris is now Senior Engineer (North Region) in the Station Operation and Maintenance De-

partment of I.T.A. and he is responsible for the installation, commissioning and subsequent maintenance of u.h.f. main and relay stations.

**Dr. G. G. Bloodworth** (F. 1969, M. 1960) is a senior lecturer in the Electronics Department at the University of Southampton. (See *The Radio and Electronic Engineer* for July 1969.)

**Dr. R. J. Hawkins** is continuing research on low frequency noise phenomena in the Department of Electronics at the University of Southampton following the acceptance of his thesis on current noise in field-effect transistors in July 1970. (See *The Radio and Electronic Engineer* for July 1969.)



**Squadron Leader N. R. S. Nesbitt** graduated in 1958 from University College, Durham University, with a B.Sc. degree in physics. He joined the Education Branch of the Royal Air Force in 1959 and for the next few years he was mainly concerned with technician and engineer training. In 1966 he completed the M.Sc. course in electronics at Southampton University receiving his degree in 1967. Squadron Leader Nesbitt

at present holds a research post at the Royal Air Force College, Cranwell, and is responsible for the post-graduate training of engineer officers.

---

## Short Contributions and Letters

Short contributions, not longer than 2000 words in length and with no more than two illustrations, are welcomed for consideration for publication in the *Journal*. These may describe circuit techniques, device technology, novel experimental methods for research in electronics or other disciplines, and computer programs for electronic engineering design calculations. These communications will be given priority in publication. General requirements for manuscript preparation etc., are similar to those for full-length papers, details of which are given in the leaflet 'Guidance for Authors', obtainable on application to the Institution.

Letters commenting on papers already published are also invited for inclusion in *The Radio and Electronic Engineer*. Similar contributions dealing with non-technical matters will normally be published in the *Supplement*.